UNIVERSITÀ DEGLI STUDI DI PAVIA
DOTTORATO DI RICERCA IN FISICA - XXIII CICLO

MCSTHAR++, a Statistical Hadronization code for Monte Carlo Event Generators

Christopher Bignamini

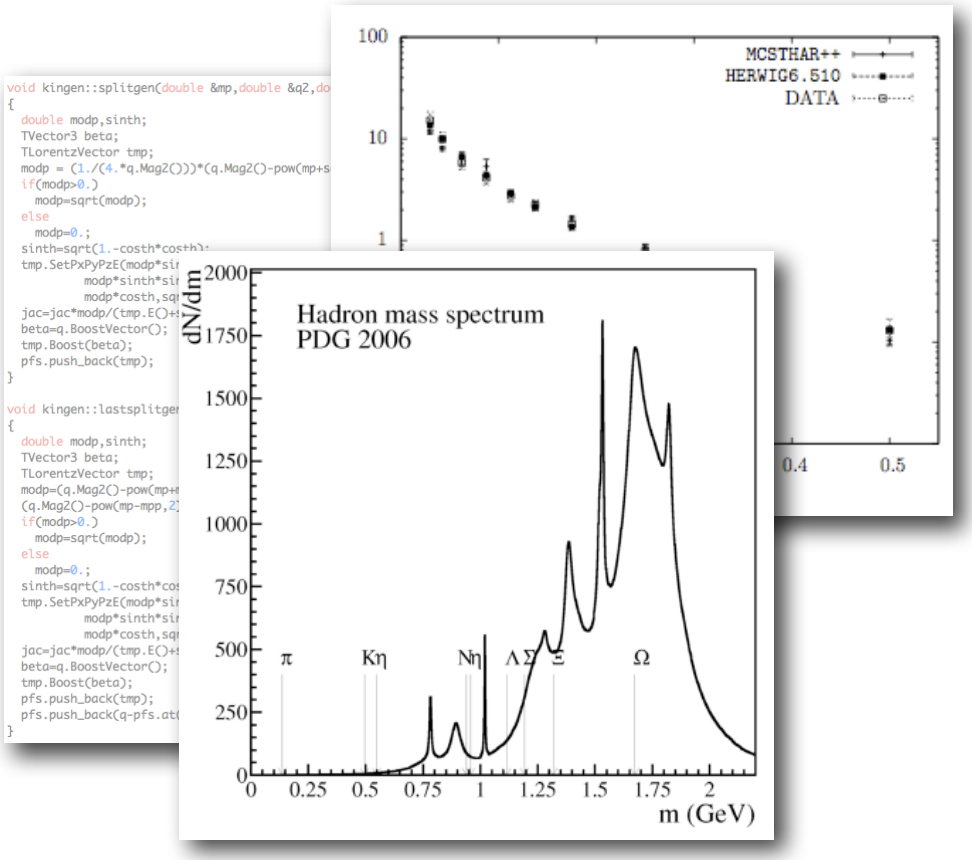

Tesi per il conseguimento del titolo

Università degli Studi di Pavia

Dipartimento di Fisica Nucleare e Teorica

Istituto Nazionale di Fisica Nucleare

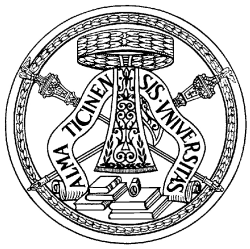

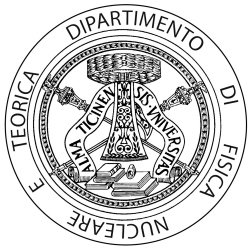

DOTTORATO DI RICERCA IN FISICA – XXIII CICLO

MCSTHAR++, a Statistical Hadronization code for Monte Carlo Event Generators

dissertation submitted by

Christopher Bignamini

to obtain the degree of

DOTTORE DI RICERCA IN FISICA

Supervisor: Dr. Fulvio Piccinini (INFN - Sezione di Pavia)

Referee: Dr. Antonio Davide Polosa (INFN - Sezione di Roma)

Cover: The hadron mass spectrum, from PDG 2006.

The scaled energy distribution of the ω meson at LEP at 91.2 GeV center of mass energy: comparison among MCSTHAR++ predictions, HERWIG6.510 results and experimental data.

MCSTHAR++ code fragment for the generation of phase space configuration.

MCSTHAR++, a Statistical Hadronization code for Monte Carlo Event Generators.
Christopher Bignamini
PhD thesis - University of Pavia
Printed in Pavia, Italy, December 2010
ISBN 987-88-95767-35-2

Contents

Note

The advancements of the research project discussed in the present thesis have been presented in the following talks:

- *MCSTHAR++, implementation of the Statistical Hadronization Model in Herwig - Preliminary results.*
  Talk given at the workshop "Modeling of the Parto-Hadron Phase Transition", 23-24 September 2010, Villasimius, Italy.
  `http://th.physik.uni-frankfurt.de/~huovinen/hadronization.html`

- *MCSTHAR++, implementation of the Statistical (Microcanonical) Hadronization Model in Herwig.*
  Talk given at the workshop "Statistical particle production: beyond the first moment", 25-28 April 2010, Bad Liebenzell, Germany.

- *Adronizzazione Microcanonica in Herwig.*
  Talk given at the conference "IFAE 2010", 7-9 April 2010, Roma, Italy.
  `http://ifae2010.roma1.infn.it/`

- *Statistical hadronization in HERWIG - Preliminary results.*
  Talk given at the workshop "INFN RM31 national meeting", 3-4 March 2010, Firenze, Italy.

- *MCSTHAR++, a statistical hadronization code for MC event generators.*
  Talk given at the school "MCnet School 09",1-4 July 2009, Lund, Sweden.
  `http://conference.ippp.dur.ac.uk/conferenceDisplay.py?confId=264`

- *The statistical hadronization model.*
  Forgschungsseminar, 25 June 2009, Karlsruhe, Germany.
  `http://www-itp.particle.uni-karlsruhe.de/~gieseke/Forschungsseminar.ss09/`

- *MCSTHAR++, a statistical hadronization code for MC event generators.*
  Talk given at the workshop "INFN RM31 national meeting", 18-19 June 2009, Torino, Italy.

The present work has been performed thanks to the support of the INFN "Iniziativa specifica" RM31 and of the University of Pavia. Moreover, the development of `MCSTHAR++` and its implementation in `Herwig++` have been partially supported by the european network MCnet, thanks to a collaboration with the Karlsruhe team of `Herwig++`.

Introduction

The *hadronization* or *fragmentation* process is the process describing the transition from a partonic system, namely a physical system composed only of quarks and gluons, to a system composed of hadrons, namely mesons and baryons. Considering the color degree of freedom, this transition corresponds to the confinement of the color inside the hadrons, starting from a system of colored objects. The hadronization process is driven by the QCD dynamics in a low energy regime, a condition in which not many theoretical tools useful to make prediction from theory are available. In particular perturbation theory, which is the general framework used to obtain theoretical predictions from the QCD in high energy Physics, is not available in this situation because of the behavior of the strong coupling constant as a function of the energy: as will be described in the first chapter of the present thesis, the lower the energy/virtuality of the process and the higher the value of the QCD coupling constant, with the consequence that, at the hadronization energy regime, a power series expansion of the QCD transition probability in the coupling constant itself is not possible. Other theoretical approaches, for example Lattice Field Theory, are more suited for the analysis of static proprieties of the QCD, like the calculation of the hadron mass spectra.

Because of the above reason, the description of the QCD dynamics for the hadronization energy range is based, at present, on the usage of various phenomenological models which try to explain the hadronization process starting from different hypothesis and including different features of the fundamental theory of reference, like the QCD preconfinement or the behavior of the color field. One of these approaches, which is also the first one historically developed, preceding the introduction of the QCD itself, is strongly based on a statistical formulation of the hadronization problem: these phenomenological models are globally known as *Statistical Hadronization Models* and have been introduced originally by Fermi and Hagedorn, who formulated the hypothesis that in a high energy collision a set of extended objects, called clusters, are being created. In this set of models the hadrons come from the hadronization of these objects, which are considered as equivalent to a set of statistical ensembles whose particular states correspond to the possible hadronization channels. Dif-

ferent approaches are possible within this class of models, depending on which kind of statistical ensemble is associated to the clusters, namely the microcanonical, canonical or grandcanonical one. These formulations give different levels of conservation of the quantities involved in the hadronization process, like energy-momentum and electric charge. In particular, as will be discussed, the microcanonical formulation is the one which assures the exact conservation of the considered physical quantities and therefore is the most suited for the description of the hadronization process in a high energy collision. Nevertheless, this is also the most demanding approach from a computational point of view, with respect to the other formulations, and for this reason the largest part of the data analysis based on the Statistical Hadronization Model has been done using the (grand)canonical approach. This is one of the general motivations of the present work, namely to begin an extensive analysis to evaluate the power of the microcanonical model to reproduce the experimental data.

One of the most effective ways to verify the validity of a hadronization model is based on its implementation in a Monte Carlo event generator, which gives the opportunity to check the predictions of the hadronization model via a comparison of the results obtained by the numerical simulation with the corresponding experimental data. A large set of hadronization models have been implemented in the available Monte Carlo event generators, in particular in the ones focused on High Energy Physics. Nevertheless no one of these codes gives the possibility to use the statistical model for the simulation of the hadronization step: this is the main motivation of the present work, which is focused on the development of a Monte Carlo code, `MCSTHAR++`, implementing the Statistical Hadronization Model (in particular in the microcanonical formulation) and on the inclusion of this hadronization module in the available event generators, with the final goal of checking the reliability of this model and of building a statistical hadronization "plug-in" which could be used alternatively to the standard hadronization codes.

The present thesis will describe the above research work, starting from the description of the hadronization problem and a discussion on the available hadronization models contained in the first chapter. The second chapter is focused on the microcanonical formulation of the statistical model, the one on which `MCSTHAR++` is based, and gives a description of the model itself beginning from an overview of the original Fermi and Hagedorn models to arrive to the modern formulation of the Statistical Hadronization Model. In particular, starting from the fundamental hypotheses of the model, the microcanonical transition probability, which represents the probability to produce a particular channel, is derived, describing the inclusion of the quantum statistics, related to the presence of identical particles in the final state, and of the interactions among the produced hadrons. Finally a discussion on the free parameters needed by the model is presented.

The details of the developed code, of the various algorithms used and of the interfacing of `MCSTHAR++` to the external event generators `HERWIG6.510` and

Herwig++ will be discussed in the third chapter. More in detail, after a description of the general structure of the code, the single steps performed during the hadronization process are discussed giving the details of the algorithms used to choose the hadronization channels, the corresponding kinematical configurations, the initial merging procedure on the input clusters and of the procedure used to get the information about the microcanonical partition functions of the clusters appearing during the simulation, an information needed to correctly normalize the event weight. The last part of the chapter is focused on the particular strategy adopted to obtain this information in a fast way and on the description of the interfacing of MCSTHAR++ to HERWIG6.510 and Herwig++.

Finally, in the fourth and last chapter the numerical results obtained for LEP experimental setup, for a center of mass energy of 91.2 GeV, will be presented, together with a discussion on a preliminary tuning of the hadronization model and a comparison with the predictions of HERWIG6.510 and its standard hadronization model: after a description of the considered observables, whose definitions are reported in the appendix of the present thesis, the results obtained for the hadronization of light quarks only and the ones for the full hadronization process are shown, with a comparison against the corresponding LEP data and HERWIG6.510 results, for a large set of particle multiplicities, event shape and single particle distributions. The search for a preliminary best fit configuration of the MCSTHAR++'s parameters is also discussed, in view of the final tuning of the code.

Chapter 1

Event generator structure and hadronization models

In the present chapter a description of the hadronization problem, together with an overview of the hadronization phenomenological models implemented in the available Monte Carlo event generators for High Energy Physics, will be given setting the general framework of the present work. The main features of each model are discussed in order to better understand the differences and advantages characterizing the Statistical Hadronization Model, which will be presented in the next chapter.

1.1 Event evolution and the hadronization process

The description of the evolution of an high energy collision, in a Monte Carlo event generator, is based on the separation of the whole event in a set of steps, which can be summarized in the following list:

1. Considering for example a hadron-hadron collision, the first step is the choice of the interacting partons and of their momentum, which is done using the parton distribution functions.

2. The description of the parton evolution, due to the emission of colour radiation. This step is performed using a parton shower algorithm.

3. The hard-scattering between the evolved partons: this step is associated to the calculation of a matrix element describing the transition probability for the elementary processes involved in the main collision.

4. The description of the radiation emission by the hard scattering final state partons, obtained as in item 2.

5. The inclusion of the interactions among the partons not involved in the hard scattering (Underlying events).

6. *The transition from the partonic state, composed only of quarks and gluons, to the hadronic state, in which the QCD parton colors are confined within the hadrons (mesons and baryons).*

7. The processing of the produced unstable hadrons, whose decay gives the final state particles.

The above separation is strongly related to the factorization theorem [1], which allows to compute/simulate each step separately by factorizing the long-distance contributions to the collision cross section from the short-distant one. The emphasized step is known as *hadronization* (or *fragmentation*) process and, as it has been said in the introduction, it is the general topic of this thesis. The possiblity to describe the previous steps within the QCD perturbative framework, as can be done for example for the hard-scattering and the radiative correction calculations, is related to the behaviour of the QCD coupling constant α_s as a function of the process energy/virtuality. As can be seen in Fig. (1.1), the α_S constant behaviour is such that at energies smaller than about 1 GeV the perturbative calculations are not possible anymore. This range of energy is the one characterizing the parton-hadron transition point of a collision evolution, so that a fundamental description of the confinement process is not possible and the introduction of phenomenological models describing the hadronization process is mandatory. Actually, even though a description of this process based on the QCD perturbative framework is unavailable, it is important to remember that within this framework some "hints" of the above transition are present. In particular, these hints are related to the QCD preconfinement property [2], which in its turn is related to the angular ordering in the parton emission of the QCD shower. Thanks to this ordering condition, the partons producing a colour singlet appear close to each other in the event phase space and the production of these colourless pairs can be seen as the first step towards the production of physical hadrons.

As will be described in the next section, different approaches can be used in the development of a phenomenological model describing the hadronization process. In particular at present two different classes of models are available in the Monte Carlo codes: the cluster models, which are strongly inspired by the above mentioned QCD preconfinement property, and the string models, which describe the hadronization process as a fragmentation of a string connecting the partons, which in its turns represents the color field describing the interactions among the partons themselves. Moreover a completely independent class of hadronization models, inspired by statistical mechanics and describing the hadronization as a termodynamical process, exists even if at present no one of these models is available in a Monte Carlo event generator. This last class is the main subject of this thesis and will be introduced in the next chapter.

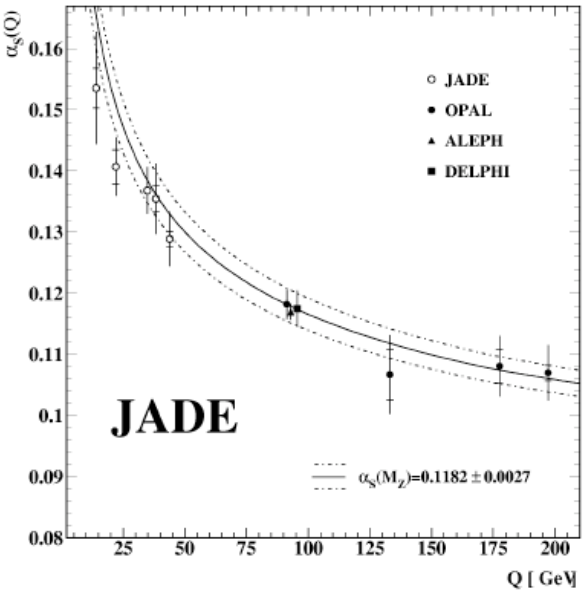

Figure 1.1: α_s value measured by JADE experiment in 4-jet production events, together with the corresponding results from OPAL, ALEPH and DELPHI experiments at LEP. The lines indicate the QCD prediction for the running of α_s with $\alpha_s(M_{Z^0}) = 0.1182 \pm 0.0027$ [20].

1.2 Overview of the available hadronization models

Many different hadronization models have been developed and implemented in the Monte Carlo event generators for High Energy Physics. In the following lines a short description of these models and of the corresponding free parameters will be given while more detailed information can be found in the cited event generator manuals.

The first model presented is the *Independent fragmentation model* [3], studied by Field and Feynman and available as alternative fragmentation model in `Pythia` [10, 11]. In this model the confined states are produced by an iterative algorithm which works on each single parton present at the end of the QCD shower, so that the hadronization of a set of quarks is obtained as a set of *independent* fragmentation processes. More in detail, the algorithm produces the hadrons starting from a quark q, for example, picking from the vacuum a $q_1\bar{q}_1$ pair and coupling the anti-quark $\bar{q}_1$ to the quark q to produce a meson $q\bar{q}_1$ and similarly for the involved antiparticles. The flavor of the quark q_1 is randomly chosen with probability given by $u : d : s = 1 : 1 : \lambda_S$ with $\lambda_S = 0.3$. When a gluon appears at the end of the shower one of the following two alternative strategies is followed, before starting again the previous algorithm: the first consists in splitting the gluon into a $q\bar{q}$ pair according to the Altarelli-Parisi splitting function [12] . The alternative one is based again on

the split of the gluon into a $q\bar{q}$ pair, but in this case the gluon's momentum is entirely assigned to one of the two new partons with equal probability, so that the gluon behaves as a quark (or antiquark). In each case the quark flavor is again randomly extracted among u,d and s with relative probability given by the proportion $1 : 1 : \lambda_S$. An important drawback of this model, which is common also to other models which will be described here, is that the fragmentation algorithm gives information only about the flavor composition of the produced mesons and baryons, but it does not choose a particular hadron. This problem is solved, for this model, considering as possible hadrons only the set of particles included in the light multiplets and introducing a set of free parameters to choose the spin of the produced hadrons.

While this model is available in `Pythia` as alternative hadronization model, the main model of this event generator is the *String fragmentation model* (or *Lund model*) [5]. In this model a color string is supposed to connect the final state partons trying to keep them close to each other with an attractive linear potential. Considering for simplicity a string connecting a quark q to an antiquark $\bar{q}$, the hadron production is obtained in the following way: as the quarks move apart the string length increases and because of the color potential also the amount of potential energy carried by the string increases, so that at some point it becomes energetically more convenient to break the string into shorter fragments with a smaller overall potential energy, using the energy excess to pick parton-antiparton pairs from the vacuum which, together with the already present partons, represent the extremes of the new string fragments. This process is then repeated iteratively on the new string fragments, until the energy carried by the new strings is large enough to allow a convenient energy balance in the fragmentation algorithm, otherwise the parton pairs connected by a string fragment are considered as final hadrons. The transverse momentum of the new partons picked from the vacuum is obtained by two independent samplings of a gaussian distribution, this transverse momentum being transferred to the newly created hadron. The longitudinal momentum p_z and the energy E of the new hadron are defined as a fraction $1 - z$ of the same quantities belonging to the original pair using a fragmentation function $f(z)$, while the remaining fraction z is assigned to the unpaired parton. Actually, only one of the two previous quantities can be fixed, since a constraint on the transverse momentum is already present. Therefore, to obtain the longitudinal boost invariance in a iteration from the quark end, the quantity considered is the combination $E+p_z$ (and $E-p_z$). In particular the energy-momentum transfer is given by

$$(E + p_z)_{\text{new}} = (1 - z)\,(E + p_z)_{\text{old}} \tag{1.1}$$

$$(E - p_z)_{\text{new}} = (E - p_z)_{\text{old}} - \frac{m_t^2}{z\,(E + p_z)_{\text{old}}}, \tag{1.2}$$

where $m_t^2 = m^2 + p_x^2 + p_y^2$. In this formulation the fragmentation function

$f(z)$, which determines the distribution of z, can be chosen almost arbitrarily. However, assuming for simplicity a 2-jet event, if a symmetry condition on the result of the fragmentation process with respect to the quark taken as starting parton for the fragmentation algorithm is required, the choice being between the quark and the antiquark coming from the hard scattering, the definition of the fragmentation function is almost unique and represented by the *Lund symmetric fragmentation function*:

$$f(z) \propto \frac{1}{z}(1-z)^a \exp\left(-bm_t^2/z\right), \tag{1.3}$$

where a and b are two free parameters and where m_t is the transverse mass of the created hadron.

The baryon production can not be included in this hadronization algorithm in a unique way and two different procedures have been introduced to solve this problem: the diquark picture [10] and the popcorn picture [6]. In the first case the baryon production is obtained by simply assuming that also diquarks could be picked from the vacuum during the string breaking and then using the same machinery described above. In the second framework a different procedure, which does not involve diquarks, is used: normally the quark pair picked from the vacuum ($q_1\bar{q_1}$) is a color singlet carrying the same color of the quark and antiquark pair ($q\bar{q}$) whose connecting string has been broken to create the new pair. In this case the new quark (antiquark) q_1 ($\bar{q_1}$) is pulled, by the color field, toward the old preexisting antiquark (quark) $\bar{q}$ (q) creating a new color singlet $q_1\bar{q}$ ($q\bar{q_1}$). Occasionally the new pair can have a different color, a condition with no net color field acting among the old and new partons, the only field being between the new quark and antiquark. In this field an additional pair $q_1\bar{q}_2$ can be created, where now q_2 ($\bar{q}_2$) is pulled toward the pair qq_1 ($\bar{q}\bar{q_1}$). In these conditions a baryon (antibaryon) made up of q_1, q_2 and an additional quark q_4 produced between q and q_1 ($\bar{q_1}$, $\bar{q}_2$ and an additional quark $\bar{q_5}$ produced between $\bar{q}$ and $\bar{q_1}$) would be created. Also this model gives only the information about the flavor composition of the new hadrons but says nothing about the particular mesons and baryons produced during the hadronization process. Again, this problem is solved by the introduction of a set of free parameters which are used to choose a particular hadron given its flavor composition.

The list of free parameters characterizing the String model is quite long and partially dependent on the user choices for the particular algorithms adopted during the fragmentation process. The full set of parameter can be found in the code's manual, while a shorter list of the parameters involved in the last tuning of the generator is the following [13][1]:

[1]In the lists of free parameters, only the parameters strictly belonging to the hadronization model have been included: the QCD shower cutoffs and energy scale for example, which are parameters common to all the generators presented here, are therefore excluded from the list even if they are fundamental in the determination of the hadronization results.

- `PARJ(1)`: this parameter determines the suppression of diquark-antidiquark pair production in the colour field compared with quark-antiquark production.
- `PARJ(2)`: same as above but for the suppression of s quark pair production compared with u or d pair production.
- `PARJ(3)`: same as above but for the extra suppression of strange diquark production compared with the normal suppression of strange quarks.
- `PARJ(4)`: same as above but for the suppression of spin 1 diquarks compared with spin 0 ones (excluding the factor 3 coming from spin counting).
- `PARJ(11)`: this parameter fixes the probability that a light meson (containing u and d quarks only) has spin 1.
- `PARJ(12)`: same as above but for the probability that a strange meson has spin 1.
- `PARJ(13)`: same as above but for the probability that a charm or heavier meson has spin 1.
- `PARJ(21)`: this parameter corresponds to the width σ in the Gaussian p_x and p_y transverse momentum distributions for primary hadrons.
- `PARJ(41)`: this parameter gives the a parameters of the symmetric Lund fragmentation function (1.3).
- `PARJ(42)`: same as above but for the b parameter.
- `PARJ(47)`: this parameter allows the modification of the Lund symmetric fragmentation for heavy endpoint quarks, in this case for b quark.
- `PARJ(25)`: this parameter sets the extra suppression factor for η production in fragmentation.
- `PARJ(26)`: same as above but for η'.

A completely independent hadronization model is represented by the *Cluster hadronization model* [4], the fragmentation model used by the event generator `Herwig` [8, 9]. This model is based on the QCD preconfinement property which has been described in the previous section: after the QCD shower and the non perurbative split of the potentially present gluons, the final partons, which thanks to the preconfinement are disposed in the phase space in such a way to form colorless pairs, are coupled to build colorless objects called *clusters*. These objects, composed of a quark-antiquark, diquark-antidiquark or quark-antidiquark (and vice versa) pair, are characterized by a mass spectrum independent of the main process energy and collision type (e^+e^-, $p\bar{p}$ or pp).

For this reason they can be considered as pseudo resonances and decayed into hadrons as it would be for real particles, following the procedure described in the following lines. In the general case a two-body decay is considered, with the cluster decaying into a hadron pair in which the particles, whose flavor is determined as described in what follows, are chosen with probability proportional to phase space availability and spin multiplicity. However, to be the two body decay a reasonable hypothesis, the cluster mass has to be not too high. In particular it must be under a maximum limit fixed by the formula:

$$M^{\texttt{CLPOW}} = \texttt{CLMAX}^{\texttt{CLPOW}} + (m1 + m2)^{\texttt{CLPOW}}, \tag{1.4}$$

where M is the maximum mass limit, m_1 and m_2 the mass of the partons composing the cluster and `CLMAX` and `CLPOW` two phenomenological parameters of the model which need to be fixed by the tuning of the model predictions on the experimental data. All the too heavy clusters, with mass larger than the limit fixed by the previous equation, are fissioned into two lighter clusters, picking from the vacuum a $q\bar{q}$ pair chosen among the light quarks only, which is used together with the partons composing the original cluster to build the two new clusters, in a way similar to the one which will be described for the hadron production step. This fission procedure is repeated iteratively on all the clusters to be hadronized until all their masses are under the mass limit. Moreover it is also possible, for a cluster, to be too light for a two body decay: in this case the cluster itself is considered to be a hadron, in particular the lightest one with the same flavor content, shifting the mass of the light cluster to the correct value by a momentum exchange with a neighbouring cluster. This procedure would fail for a light diquark-antidiquark cluster: in this case the momentum exchange among the clusters is used to put the mass of the cluster above the two body decay threshold. At this point the remaining clusters are ready to be hadronized in the standard way: for each one of them a flavor-antiflavor $f\bar{f}$ is chosen randomly with f among u, d, s, their six combinationsin a diquark and c. These new partons are used to build the two primary hadrons into which the cluster will decay isotropically with the following recipe: supposing to start from a $f_1\bar{f}_2$ cluster, the primary hadrons will have flavor compositions $f_1\bar{f}$ and $f\bar{f}_2$. Also in this case, of course, the flavor composition is not enough to fix a particular hadron: within this framework, once the hadron flavors have been determined, the decay products are randomly chosen among the particles with appropriate flavor composition, according to the phase space availability and spin degeneracy of each possible channel.

The list of the free parameters of the model involved in the tuning of the model itself on the experimental data [14] is given by:

- `CLMAX`: as can be seen in Eq. (1.4), this is one of the two parameters which determine the maximum allowed cluster mass value. Above this limit the cluster split process is called.

- `CLPOW`: this is the second parameter which defines the maximum cluster mass.
- `CLMSR(1)`: in the decay of a cluster, this parameter controls the gaussian smearing of the hadron direction with respect to the direction of the constituent quark, for light and charm quarks.
- `CLMSR(2)`: similarly to the previous parameter, this one controls the gaussian smearing for the bottom quark.
- `PSPLT(1)`: this parameter determines the mass distribution in a cluster splitting, for u, d, s and c quarks only.
- `PSPLT(2)`: this parameter has the same role of the previous one but for b quark.
- `DECWT`: this parameter gives the relative weight for the production of decuplet baryons compared to octect baryons.

The last hadronization model presented in this short overview is the *Modified cluster hadronization model* [7], which has been implemented in the event generator `Sherpa` [15]. This model is quite similar to the previous one, since also in this case the partons present at the end of the QCD shower and after the non perturbative gluon splitting are paired to build colorless clusters, which are decayed with a procedure very similar to the previously discussed one. Nevertheless some interesting new features are present here, with respect to the standard cluster model, starting from the cluster building, since in this new model also non planar diagrams (and therefore parton pairings) are taken into account and chosen according to the suppression factor $1/N_c^2$, where N_c is the number of colors. Another fundamental difference with respect to the original cluster model is given by the diquark spin, which in this new model is explicitly taken into account. As a consequence, diquarks with the same flavour can appear, during the hadronization process, with different spin configurations: a diquark state like ud, for example, can appear both as ud_0 and ud_1.

In this case the list of free parameters involved in the hadronization process is [16]:

- `STRANGE_FRACTION`: this parameter defines the rate of strange quark produced from the vacuum during the cluster decay.
- `BARYON_FRACTION`: same as above but for the diquark production.
- `P_{QQ_1}/P_{QQ_0}`: this parameter determines the relative ratio of production of spin-1 diquarks with respect to spin-0 ones.
- `P_{QS}/P_{QQ}`: same as above but for the diquarks containing a strange quark with respect to lighter diquarks.

- P_{SS}/P_{QQ}: same as above but for ss diquarks.
- TRANSITION_OFFSET: this parameter sets the maximum mass value for a cluster decaying in 1 hadron.
- DECAY_OFFSET: same as above, but for 2-body decay.
- C->H_TRANSITION_FACTOR: this parameter is used to change the relative probability ratio between the cluster transition into one hadron and its decay in a hadron pair.
- C->HH_DECAY_EXPONENT: this parameter is used to tune the 2-body decay probability, allowing to increase the production of heavy hadrons.
- SINGLET_SUPPRESSION: this parameter reduces the transition probability to single-octet mixed states in the meson sector.
- MULTI_WEIGHT_L0R0_PSEUDOSCALARS: this parameter is used to change the pseudoscalar hadron multiplet production probability. The following parameters have the same role for different hadron multiplets.
- MULTI_WEIGHT_L0R0_VECTORS
- MULTI_WEIGHT_L0R0_TENSORS2
- MULTI_WEIGHT_L1R0_SCALARS
- MULTI_WEIGHT_L1R0_AXIALVECTORS
- MULTI_WEIGHT_L1R0_TENSORS2
- MULTI_WEIGHT_L2R0_VECTORS:
- MULTI_WEIGHT_L0R0_N_1/2
- MULTI_WEIGHT_L0R0_N*_1/2
- MULTI_WEIGHT_L0R0_DELTA_3/2
- C->HH_DECAY_THETA_EXPONENT: this parameter characterizes the transverse momentum distribution of the hadrons produced in the cluster hadronization.

1.3 The Statistical Hadronization Model and Heavy Ion Physics

As will be discussed in the next chapters, a completely different approach for the description of the hadronization process based on a statistical formulation is possible. The hadronization models built within this framework are known as Statistical Hadronization Models: even though these models are not available in the Monte Carlo event generators for High Energy Physics, they are widely used by the Heavy Ion Physics simulation codes, like `SHARE` [17], `THERMUS` [18] and `THERMINATOR` [19]. The first two codes are focused on the statistical-thermal analysis of the heavy ion collision data, allowing the calculation, in the statistical framework, of hadron abundances starting from the set of free parameters needed by the model used for the analysis, with the possibility to choose among different formulations of the statistical model itself. The third code, `THERMINATOR`, is to some extent an extension of the previous ones: including a description of the fireball evolution and dynamics, it is able to give the full space-time and momentum information of the produced particles, allowing the calculation of a set of interesting distributions like the transverse momentum of the identified particles. With the described features, each one of the above codes gives the possibility to test the physical hypothesis adopted, both for the theoretical model used and for the corresponding free parameters, thanks to a best fit of the theoretical predictions on the available experimental data of heavy ion collisions.

A similar public tool, which could be used to study the performances of the statistical model in High Energy Physics is still missing: in the next chapters the development of a prototype of such a kind of code will be described, with a particular emphasis on the microcanonical framework. Moreover, the developed code allows for an analysis of the Statistical Hadronization Model performances within a full event simulation including all the steps of a high energy collision, a missing feature of the codes listed above.

Chapter 2

The Statistical Hadronization Model

The Statistical Hadronization Model can be built starting from different statistical hypothesis, leading to different formulations of the model itself. The present work however is focused on the microcanonical formulation of the model itself which, as will be discussed, is the most suited for the high energy collisions considered here. In the next sections, after a brief overview of the historical evolution of this model, its microcanonical formulation will be derived and its most relevant features discussed, giving the information needed for the development of the Monte Carlo code which will be described in the next chapter.

2.1 General features of the model

As it has been discussed, a completely independent set of hadronization models, based on a statistical interpretation of this process, exists. The history of these models begun with a work by Fermi [21] who, trying to explain the multiparticle production in *pp* collisions, hypothesized that the particles produced in such a kind of collisions originate from an excited region with an uniform occupation of the available phase space states. However, the isotropical particle emission in the center of mass frame of the reaction, which is one of the consequences of the hypothesis of Fermi's model, disagrees with the experimental data.

This problem has been addressed some years later by Hagedorn [22], who refined the model introduced by Fermi postulating the existence of two excited regions emitting the hadrons and moving apart longitudinally in the collision center of mass. In its model, which is known as *Statistical Bootstrap Model*, Hagedorn hypothesized also a full equivalence between these excited objects, which he called *clusters* or *fireballs*, and a thermodynamical ensemble of hadrons at equilibrium. Because of this condition it follows that the mass

spectrum of the resonances can be derived from the calculation of the multi-hadronic state density, obtained considering all the hadrons and clusters with mass smaller than the mass value at which the spectrum is calculated. To understand the above general consideration it is useful to consider a particular case, for example the one of the nuclear matter: considering a set of b nucleons, the total number of possible "clusterizations" of these particles (from the state given by $b/2$ two-particle clusters to the one given by two $(b/2)$-nucleon clusters), which can be viewed as the possible states of the ensemble, are described by a function $\rho(b)$ obeying the equation

$$\rho(b) = \rho(1)\delta(b-1) + \sum_{j=2}^{b} \frac{1}{j!} \sum_{\{b_i\}_j} \delta(\sum_{i=1}^{j} b_i - b) \prod_{i=1}^{j} \rho(b_i), \tag{2.1}$$

where the sum is over all the sets with j elements (clusters) with $b_i \in \{1, ..., b-1\}$ and where the conservation of the baryonic number is imposed by the Kronecker delta function. Switching to a continuos variable m, which can be seen as the mass of the system, the above equation becomes

$$d(m) = d_0(m) + \sum_{j=2}^{\infty} \frac{1}{j!} \int_0^\infty dm_1 \int_0^\infty dm_2 \cdots \int_0^\infty dm_j \delta(m - \sum_{i=1}^{j} m_i) \prod_{i=1}^{j} d(m_i). \tag{2.2}$$

The previous equation reflects the fact that a cluster described by $d(m)$ consists of an arbitrary number of clusters of smaller mass, each of which is in its turn made of an arbitrary number of lighter clusters as can be obtained iterating the equation itself. The above equation is the simplest and most generic *bootstrap equation*, whose solution is given by the exponential function

$$d\,(m) \propto m^a \exp\,(m/T_0), \tag{2.3}$$

where m is the resonance mass and where a and T_0 are two free phenomenological parameters. It is important to note that the same exponential behavior is present also in the experimental data, as can be seen in Fig. (2.1), in particular in the small mass range, where the resonance spectrum is better known.

The interest in this phenomenological model of strong interactions has been reduced by the introduction of the QCD and its fundamental approach, while the Statistical Hadronization Model has conserved its importance in the study of ultrarelativistic heavy ion collisions [23], in particular thanks to the hypothesis that an equilibrated hadron source gas in this kind of collisions could be a signature of the formation of a transient *Quark Gluon Plasma*. Indeed the production of an almost equilibrated hadron gas in ultrarelativistic heavy ion collisions has been confirmed [24] and, at the same time, the interest in the Statistical Model has been also revived thanks to its capacity to reproduce with very good agreement the particle multiplicities observed in different elementary collisions [29, 30, 31] together with their transverse momentum distribution [32].

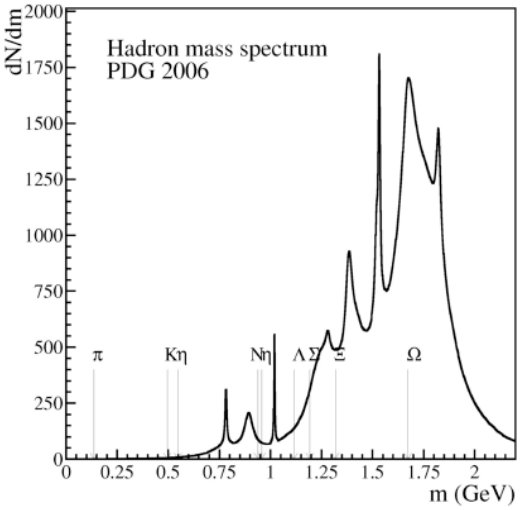

Figure 2.1: Hadronic experimental mass spectrum [25]

Various formulations of the Statistical Hadronization Model are possible, assuming a different statistical ensemble for the multi-hadronic system: microcanonical, canonical, grandcanonical and so on, each of which corresponds to a different level of conservation of the physical quantities of interest for the considered system. Even if the microcanonical formulation, which corresponds to the exact conservation of all the quantum numbers of a cluster in the hadronization of the cluster itself, is the correct one as it is described in [27], the largest part of the data analysis based on the statistical framework has been done using the canonical and grandcanonical formulations: within this frameworks the quantum numbers are conserved only on average, with the advantage of dealing with more easier calculations compared to the microcanonical case, while the (grand)canonical model is a good approximation of the microcanonical one for heavy clusters. However it is worth to face the computational problems involved in using the last formulation to obtain a more precise check of the reliability of the Statistical Hadronization Model, in particular for high energy collisions since, in this case, the clusters are on average light enough to exclude the above approximation [26].

For the same reason it must be also taken into account that some observables, which could be used to check the theoretical predictions of the model, are determined not only by the hadronization process but also by the previous steps of the event evolution, like the QCD parton shower. Therefore it would be useful to have at disposal a full event generation using the Statistical Hadronization Model for the hadronization process, to make a comparison between theoretical predictions and experimental data on a large set of observables.

2.2 The microcanonical formulation of the statistical model

The next chapters will describe the implementation of the Statistical Hadronization Model in its microcanonical formulation in a Monte Carlo code and the comparison between the experimental data and the theoretical predictions obtained using that code to simulate high energy collisions, therefore it is now mandatory to give a rigorous formulation of the model. As it is described in [27] and [28], the fundamental assumptions of the Statistical Hadronization Model are the following:

- In a high energy collision a set of extended objects made of pre-hadronic matter, called clusters or fireballs, are being created.
- Each of these clusters is a colorless object with well defined physical quantities, like energy-momentum and electric charge, which hadronizes according to a specific statistical law.
- In the present case, which refers to the *microcanonical* formulation of the model, *in the hadronization of each cluster all the multi-hadronic states confined within the cluster itself and conserving all its physical quantities are equally likely.*

Various sets of conservation laws can be used, with reference to the the last item: in the present work, in particular, the conservation is imposed on energy-momentum (P) and on the set of abelian charges composed of electric charge (Q), strangeness (S), baryonic number (B), charm (C) and beauty (Bt).

Starting from the fundamental assumptions of the model, the transition probability for the cluster hadronization will be now derived. The first step is the calculation of the microcanonical partition function Ω, which is defined as

$$\Omega = \sum_{h_V} \langle h_V \mid \hat{P}_i \mid h_V \rangle, \tag{2.4}$$

where the sum is over all the multi-hadronic states $\mid h_V \rangle$ confined inside the cluster of volume V and $\hat{P}_i$ is the projector on the conserved quantities, which in the present case are the energy-momentum and the abelian charges. However, to be useful in the event generation, it is necessary to obtain the probability to produce, in the hadronization of a cluster, an asymptotic state $\mid f \rangle$: in most cases the difference between confined and asymptotic states is neglected, working in the so called large volume approximation in which the two kind of states are identical. Nevertheless, the finite volume condition leads to important effects which are among the most notable features of the model, namely the Bose-Einstein and Fermi-Dirac statistics effects due to the presence of identical particles in the final states. For this reason in the present work the large volume approximation will not be adopted, taking into account the

difference between confined and asymptotic states and deriving the transition probabilities as described in the following lines.

Using the identity spectralization on the final state set, the previous equation can be written as

$$\begin{aligned}\Omega &= \sum_{h_V} \langle h_V \mid \hat{P}_i \mid h_V \rangle \\ &= \sum_{h_V, f} \langle h_V \mid \hat{P}_i \mid f \rangle \langle f \mid h_V \rangle \\ &= \sum_{f} \langle f \mid \hat{P_V} \hat{P}_i \mid f \rangle,\end{aligned} \tag{2.5}$$

where

$$\hat{P_V} = \sum_{h_V} \mid h_V \rangle \langle h_V \mid$$

is the projector on the confined states. The previous equation can be slightly modified adding another projector on the conserved quantity $\hat{P}_i$, obtaining the following modified partition function:

$$\Omega' = \sum_{f} \langle f \mid \hat{P}_i \hat{P_V} \hat{P}_i \mid f \rangle. \tag{2.6}$$

The modification introduced gives a sum over positive defined quantities whose value is proportional to the real microcanonical partition function (2.4):

$$\begin{aligned}\Omega' &= \sum_{f} \langle f \mid \hat{P}_i \hat{P_V} \hat{P}_i \mid f \rangle \\ &= \sum_{h_V, f} \langle f \mid \hat{P}_i \mid h_V \rangle \langle h_V \mid \hat{P}_i \mid f \rangle \\ &= \sum_{h_V, f} \langle h_V \mid \hat{P}_i \mid f \rangle \langle f \mid \hat{P}_i \mid h_V \rangle \\ &= \sum_{h_V} \langle h_V \mid \hat{P_i}^2 \mid h_V \rangle \\ &= a \sum_{h_V} \langle h_V \mid \hat{P_i}^2 \mid h_V \rangle = a\Omega,\end{aligned} \tag{2.7}$$

where a is a positive and divergent constant which takes into account the "normalization" of the projector on continuous quantities like energy-momentum. At this point the transition probability for the hadronization of a cluster into a final asymptotic state $\mid f \rangle$ can be defined as

$$p_f = \frac{\langle f \mid \hat{P}_i \hat{P_V} \hat{P}_i \mid f \rangle}{\Omega}. \tag{2.8}$$

As it has been discussed, in the present work the conservation laws to which the projector $\hat{P}_i$ refers are energy-momentum conservation and abelian charge conservation, therefore the explicit definition of that operator is given by

$$\hat{P}_i = \delta^4(P - \hat{P})\delta_{\mathbf{Q},\hat{\mathbf{Q}}}, \tag{2.9}$$

where $\hat{P}$ is the energy-momentum operator, $\hat{\mathbf{Q}}$ the vector operator collecting the abelian charges, P is the cluster energy-momentum and $\mathbf{Q}$ the vector of its abelian charges.

Considering now explicitly the energy-momentum and charge configurations of the final state $\mid f\rangle$, given by P_f and $\mathbf{Q}_f$ respectively, the transition probability (2.8) can be written as

$$p_f = \frac{\delta^4(P - P_f)\delta_{\mathbf{Q},\mathbf{Q}_f}}{\Omega} \sum_{h_V} |\langle f \mid h_V\rangle|^2 . \tag{2.10}$$

More in detail, to perform the calculation of the scalar products contained in the previous equation, the multi-hadronic states can be represented in the Fock space as follows:

$$\begin{aligned} \mid f\rangle &= \mid \{N_1^f, N_2^f, ..., N_K^f\}, p_f\rangle = \mid \{N_j^f\}, p_f\rangle \\ \mid h_V\rangle &= \mid \{N_1^V, N_2^V, ..., N_K^V\}, p_V\rangle = \mid \{N_j^V\}, p_V\rangle, \end{aligned} \tag{2.11}$$

where $\{N_1^f, N_2^f, ..., N_K^f\}$ ($\{N_1^V, N_2^V, ..., N_K^V\}$) is the asymptotic (confined) multiplicity K-tupla describing a state composed of N_j particles of species j (with $j = 1, 2, ..., K$), K is the total number of hadronic species included and where p_f (p_V) represents the kinematical configuration corresponding to the asymptotic (confined) multiparticle K-tupla.

To obtain the final result it is useful to introduce the following condition of orthogonality:

$$\langle \{N_j^f\}, p_f \mid \{N_j^V\}, p_V\rangle = 0 \text{ if } N_j^f \neq N_j^V \text{ for at least one } j. \tag{2.12}$$

The previous equation holds only in non relativistic quantum mechanics, while in relativistic field theory the number of particles confined inside a volume, in the present case the cluster volume, is not a good quantum number. However the above condition can still be used, at least approximatively, when the linear dimensions of the confining volume are larger than the Compton wavelength λ_C of the lightest particle considered, which in this case is the pion with $\lambda_C = 1.4\ fm$. Considering for simplicity to have at maximum one particle for each one of the included hadronic species (the generalization to multiple identical particles will be shown in the following section), and assuming to have the same multiplicity configuration in the confined and asymptotic state, the previous scalar product can be rewritten as

$$\langle \{N_j^f\}, p_f \mid \{N_j^V\}, p_V \rangle = \prod_{i=1}^{N} \langle \mathbf{p}_f^i, \sigma_f^i \mid \mathbf{p}_V^i, \sigma_V^i \rangle \tag{2.13}$$

by splitting the scalar product into N single particle products to be performed in the corresponding single particle Hilbert spaces and where the product is over the N particles of the considered states and the particle spins σ_f^i and σ_V^i have been considered explicitly. Assuming the set of states $\mid \mathbf{p}_V^i, \sigma_V^i \rangle$ to be a complete one-particle set of states in the cluster region A, which is supposed to be a spherical region of volume V, and given the spatial representation for these states

$$\langle \mathbf{r}, \tau \mid \mathbf{p}_V, \sigma_V \rangle = \begin{cases} \psi_{\mathbf{p}_V}(\mathbf{r})\, U_{\sigma_V,\tau} & \mathbf{r} \in A \\ 0 & \text{otherwise} \end{cases}, \tag{2.14}$$

where $U_{\sigma_V,\tau}$ is an element of an unitary operator $\hat{U}$, it follows that

$$\begin{aligned} &\sum_{\mathbf{p}_V,\sigma_V} |\langle \mathbf{p}, \sigma \mid \mathbf{p}_V, \sigma_V \rangle|^2 = \sum_{\mathbf{p}_V,\sigma_V} \langle \mathbf{p}, \sigma \mid p_V, \sigma_V \rangle \langle p_V, \sigma_V \mid p, \sigma \rangle \\ &= \sum_{\mathbf{p}_V,\sigma_V} \int_A d^3r \int_A d^3r' \langle \mathbf{p}, \sigma \mid \mathbf{r}, \sigma \rangle \langle \mathbf{r}, \sigma \mid \mathbf{p}_V, \sigma_V \rangle \langle \mathbf{p}_V, \sigma_V \mid \mathbf{r}', \sigma \rangle \langle \mathbf{r}', \sigma \mid \mathbf{p}, \sigma \rangle \\ &= \sum_{\mathbf{p}_V,\sigma_V} \int_A d^3r \int_A d^3r' \frac{e^{i\mathbf{p}\cdot\mathbf{r}' - i\mathbf{p}\cdot\mathbf{r}}}{(2\pi)^3} \psi_{\mathbf{p}_V}(\mathbf{r})\, U_{\sigma_V,\sigma} \psi^*_{\mathbf{p}_V}(\mathbf{r}')\, U^*_{\sigma,\sigma_V} \\ &= \sum_{\mathbf{p}_V,\sigma_V} \int_A d^3r \int_A d^3r' \frac{e^{i\mathbf{p}\cdot(\mathbf{r}'-\mathbf{r})}}{(2\pi)^3} \psi_{\mathbf{p}_V}(\mathbf{r})\, \psi^*_{\mathbf{p}_V}(\mathbf{r}')\, |U_{\sigma_V,\sigma}|^2 \end{aligned} \tag{2.15}$$

Since the $\psi_{\mathbf{p}}$ functions are a complete set of eigenfunctions in A the following condition holds:

$$\sum_{\mathbf{p}} \psi_{\mathbf{p}}(\mathbf{r})\, \psi_{\mathbf{p}}(\mathbf{r}')^* = \sum_{\mathbf{p}} \langle \mathbf{r} \mid \mathbf{p} \rangle \langle \mathbf{p} \mid \mathbf{r}' \rangle = \delta^3(\mathbf{r} - \mathbf{r}')\,. \tag{2.16}$$

Using the previous condition and the unitarity of the operator $\hat{U}$, the (2.15) becomes

$$\sum_{\mathbf{p}_V,\sigma_V} |\langle \mathbf{p}, \sigma \mid \mathbf{p}_V, \sigma_V \rangle|^2 = \int_A d^3r \int_A d^3r' \frac{e^{i\mathbf{p}\cdot(\mathbf{r}'-\mathbf{r})}}{(2\pi)^3} \delta^3(\mathbf{r} - \mathbf{r}') = \frac{V}{(2\pi)^3}, \tag{2.17}$$

which leads to the following formula for the transition probability (2.10):

$$p_f = \frac{\delta^4(P - P_f)\delta_{\mathbf{Q},\mathbf{Q}_f}}{\Omega} \frac{V^N}{(2\pi)^N} \prod_{i=1}^{N} (2J_i + 1)\,, \tag{2.18}$$

where J_i is the spin module of the i-th particle and where a sum over the particle spins has been performed.

At this point it is also possible to obtain an explicit formula for the micro-canonical partition function, using the results previously derived and considering the correspondence

$$\sum_f \to \sum_{\{N_j\}} \prod_{i=1}^{N} \left(\sum_{\sigma_i} \int d^3 p_i \right). \tag{2.19}$$

Therefore the partition function Ω is given by

$$\begin{aligned} \Omega &= \sum_{\{N_j\}} \prod_{j=1}^{K} \left[\frac{(2J_i + 1)\, V}{(2\pi)^3} \right]^{N_j} \int \prod_{i=1}^{N} d^3 p_i \delta^4(P - P_f) \delta_{\mathbf{Q},\sum_{i=1}^{N} \mathbf{Q}_i} \\ &= \sum_{\{N_j\}} \Omega_{\{N_j\}} \delta_{\mathbf{Q},\sum_{i=1}^{N} \mathbf{Q}_i}, \end{aligned} \tag{2.20}$$

where the quantity $\Omega_{\{N_j\}}$ is the baryonic phase space for the hadronization channel $\{N_1, N_2, ..., N_K\}$ and N the number of particles contained in the channel itself.

2.3 Identical particles

In the more general case it is possible to have more than one particle of the same kind in the confined and asymptotic states, condition which leads to some modifications to the previous equation. Assuming to have only one kind of hadron and considering a channel composed of N particles of that kind, taking into account the spin-statistics theorem the multi-particle states of Eq. (2.15) becomes

$$\begin{aligned} \mid N, p_f \rangle &= \sum_{\pi} \frac{\chi(\pi)^b}{\sqrt{N!}} \prod_{i=1}^{N} \mid \mathbf{p}_{f\pi(i)}, \sigma_{f\pi(i)} \rangle \\ \mid N, p_V \rangle &= \sum_{\pi} \frac{\chi(\pi)^b}{\sqrt{N! n_1! n_2! \cdots n_M!}} \prod_{i=1}^{N} \mid \mathbf{p}_{V\pi(i)}, \sigma_{V\pi(i)} \rangle, \end{aligned} \tag{2.21}$$

where π is a permutation of the integers $1, 2, ..., N$ and $\chi(\pi)$ the parity of the permutation itself. The n_i integers count the number of particles composing the confined state which are in the same momentum-spin state and b is the symmetry factor of the considered particle ($b = 0$ fo bosons and $b = 1$ for

fermions). It must be noted that, in the asymptotic state, the last set of integers is not present because of the continuous nature of the momentum variable in infinite systems. With these new states the hadronic phase space becomes

$$\Omega_N = \prod_{i=1}^{N} \sum_{\sigma_i} \int d^3 p_i \delta^4 \left(P - P_f\right) \\ \sum_{p_V} \left| \sum_{\pi} \chi(\pi)^b \frac{1}{\sqrt{N! n_1! n_2! \cdots n_M!}} \prod_{i=1}^{N} \langle \mathbf{p}_{fi}, \sigma_{fi} \mid \mathbf{p}_{V\pi(i)}.\sigma_{V\pi(i)} \rangle \right|^2 , \tag{2.22}$$

Expanding the square modulus, the sum over the localized states can be written as

$$\sum_{p_V} \left| \sum_{\pi} \chi(\pi)^b \frac{1}{\sqrt{N! n_1! n_2! \cdots n_M!}} \prod_{i=1}^{N} \langle \mathbf{p}_{fi}, \sigma_{fi} \mid \mathbf{p}_{V\pi(i)}, \sigma_{V\pi(i)} \rangle \right|^2 = \\ \sum_{p_V} \sum_{\pi\pi'} \chi(\pi)^b \chi(\pi')^b \frac{1}{N! n_1! n_2! \cdots n_M!} \times \\ \prod_{i=1}^{N} \langle \mathbf{p}_{fi}, \sigma_{fi} \mid \mathbf{p}_{V\pi(i)}, \sigma_{V\pi(i)} \rangle \langle \mathbf{p}_{V\pi'(i)}, \sigma_{V\pi'(i)} \mid \mathbf{p}_{fi}, \sigma_{fi} \rangle = \\ \frac{1}{N!^2} \sum_{\pi\pi'} \chi(\pi\pi')^b \prod_{i=1}^{N} \sum_{\mathbf{p}_{Vi}, \sigma_{Vi}} \langle \mathbf{p}_{f\pi(i)}, \sigma_{f\pi(i)} \mid \mathbf{p}_{Vi}, \sigma_{Vi} \rangle \langle \mathbf{p}_{Vi}, \sigma_{Vi} \mid \mathbf{p}_{f\pi'(i)}, \sigma_{f\pi'(i)} \rangle \tag{2.23}$$

Summing over the permutations π', the previous quantity becomes

$$\frac{1}{N!} \sum_{\pi} \chi(\pi)^b \prod_{i=1}^{N} \sum_{\mathbf{p}_{Vi}, \sigma_{Vi}} \langle \mathbf{p}_{f\pi(i)}, \sigma_{f\pi(i)} \mid \mathbf{p}_{Vi}, \sigma_{Vi} \rangle \langle \mathbf{p}_{Vi}, \sigma_{Vi} \mid \mathbf{p}_{fi}, \sigma_{fi} \rangle, \tag{2.24}$$

and summing over the confined states by inserting two identity spectralizations on the position eigenstates it becomes

$$\begin{aligned}
&\frac{1}{N!}\sum_{\pi}\chi(\pi)^b\prod_{i=1}^{N}\sum_{\mathbf{p}_{Vi},\sigma_{Vi}}\langle\mathbf{p}_{f\pi(i)},\sigma_{f\pi(i)}\mid\mathbf{p}_{Vi},\sigma_{Vi}\rangle\langle\mathbf{p}_{Vi},\sigma_{Vi}\mid\mathbf{p}_{fi},\sigma_{fi}\rangle=\\
&\frac{1}{N!(2\pi)^{3N}}\sum_{\pi}\chi(\pi)^b\prod_{i=1}^{N}\int d^3xd^3x'e^{-i\left(\mathbf{p}_{fi}-\mathbf{p}_{f\pi(i)}\right)\cdot\mathbf{x}}\times\\
&\sum_{\mathbf{p}_{Vi},\sigma_{Vi}}\psi^*_{\mathbf{p}_{Vi}}(\mathbf{x}')\psi_{\mathbf{p}_{Vi}}(\mathbf{x})U_{\sigma_{fi},\sigma_{Vi}}U^*_{\sigma_{f\pi(i)},\sigma_{Vi}}=\\
&\frac{1}{N!(2\pi)^{3N}}\sum_{\pi}\chi(\pi)^b\prod_{i=1}^{N}\delta_{\sigma_{fi},\sigma_{f\pi(i)}}\int d^3xe^{i\left(\mathbf{p}_{f\pi(i)}-\mathbf{p}_{fi}\right)\cdot\mathbf{x}}.
\end{aligned}\tag{2.25}$$

Finally the hadronic phase space is given by

$$\begin{aligned}
\Omega_{\{N_j\}}=\Omega_N=\sum_{\pi}\frac{\chi(\pi)^b}{N!}\sum_{\sigma_1,\ldots,\sigma_{N_j}}\int\prod_{i=1}^{N}d^3p_i\times\\
\prod_{i=1}^{N}\delta_{\sigma_i,\sigma_{\pi(i)}}\frac{1}{(2\pi)^3}\int_V d^3xe^{i\mathbf{x}\cdot(\mathbf{p}_{\pi(i)}-\mathbf{p}_i)}\delta^4(P-P_f).
\end{aligned}\tag{2.26}$$

It is worth noting that, in case of identical particles, the hadronic phase space is given by the sum of $N!$ phase spaces, as it can be seen in the previous equation. Roughly speaking, the effect of the presence of identical particles in the considered channel, which is represented by the integral of the exponential function in Eq. (2.26), leads to a modulation of the microcanonical weight as a function of the phase space configuration: the effect of this modulation is the enhancement (suppression) of the microcanonical weight for the phase space configurations characterized by identical bosons (fermions) with similar momenta. These effects are known as Bose-Einstein and Fermi-Dirac quantum statistics and are one of the most important features of the Statistical Hadronization Model. A similar condition is obviously present also in the more general case of K hadronic species: the derivation of the formula for the hadronic phase space is analogous to the previous case and leads to the equation

$$\begin{aligned}
\Omega_{\{N_j\}}=\prod_{j=1}^{k}\Bigg[\sum_{\pi_j}\frac{\chi(\pi_j)^{b_j}}{N_j!}\sum_{\sigma_1,\ldots,\sigma_{N_j}}\int\prod_{i=1}^{N}d^3p_i\times\\
\prod_{i_j=1}^{N_j}\frac{\delta_{\sigma_{i_j},\sigma_{\pi_j(i_j)}}}{(2\pi)^3}\int_V d^3xe^{i\mathbf{x}\cdot(\mathbf{p}_{\pi_j(i_j)}-\mathbf{p}_{i_j})}\Bigg]\delta^4(P-P_f).
\end{aligned}\tag{2.27}$$

2.4 Strangeness suppression

The previously derived equations for the hadronic phase space require now a modification, which is common also to the canonical and grandcanonical formulations of the model, related to the production during the hadronization process of hadrons containing strange quarks and involving the introduction of a phenomenological parameter, which is known as *strangeness suppression parameter* (γ_S). This parameter is needed to implement a phenomenological extra suppression of the production of hadrons containing strange quarks to reproduce the experimental data, modifying the hadronic phase space in the following way:

$$\Omega_{\{N_j\}} \rightarrow \Omega_{\{N_j\}} \gamma_S^{\sum_{j=1}^{K} N_j s_j}, \tag{2.28}$$

where N_j is the number of hadrons of kind j contained into the channel $\{N_j\}$ and s_j the total number of valence strange and antistrange quarks contained in the j-th hadron. The strangeness suppression is needed also for the set of light unflavoured mesons, like the η meson, which are supposed to be characterized by a superposition of states possibly containing strange quarks, with a wave function with the general form

$$C_u u\bar{u} + C_d d\bar{d} + C_s s\bar{s} \quad \text{with } |C_u|^2 + |C_d|^2 + |C_s|^2 = 1. \tag{2.29}$$

For this kind of hadrons it is supposed to be suppressed only the $s\bar{s}$ part of the wave function or, equivalently, the $|C_s|^2$ fraction of the observed particles, with a suppression factor given by

$$1 - |C_s|^2 + |C_s|^2 \gamma_S^2, \tag{2.30}$$

so that, with the strangeness suppression, the hadronic phase space is given by

$$\Omega_{\{N_j\}} \rightarrow \Omega_{\{N_j\}} \prod_{j=1}^{K} f_j^{N_j}, \tag{2.31}$$

where

$$f_j = \begin{cases} 1 - |C_s|^2 + |C_s|^2 \gamma_S^2 & \text{Unflavored mesons} \\ \gamma_S^{s_j} & \text{Otherwise} \end{cases} \tag{2.32}$$

2.5 Interactions

Until now the hadrons produced in the hadronization process have been considered as free particles, since no interactions among them has been introduced. However it exists a relatively easy way to include, at least approximatively, the effects coming from the strong interactions, which is based on the Dashen-Ma-Bernstein hadron-resonance gas model [33]: one of the most important

results of the previous work is related to the interactions among the particles composing the hadron gas, since it is shown that it is possible to take into account with good approximation these effects by switching from the gas of free hadrons to a gas of free hadrons and resonances, considering the mass of the unstable particles as distributed with a Breit-Wigner distribution:

$$p_{BW}(m) = \frac{1}{\pi} \frac{m_0 \Gamma}{\left(m^2 - m_0^2\right)^2 + m_0^2 \Gamma^2}, \tag{2.33}$$

where m is the mass of the resonance, m_0 its central value and Γ its width. This condition, which corresponds to the assumption of dominance of resonant scattering among the interactions, leads to the following modification of the microcanonical partition function (2.20):

$$\Omega = \sum_{\{N_j\}} \prod_{j=1}^{K} \left[\frac{(2J_i + 1)\, V}{(2\pi)^3} \right]^{N_j} \int \prod_{i=1}^{N_R} dm_i \, p_{BW}(m_i) \int \prod_{i=1}^{N} d^3 p_i \, \delta^4(P - P_f) \delta_{\mathbf{Q}, \sum_{i=1}^{N} \mathbf{Q}_i}, \tag{2.34}$$

where N_R is the number of resonances contained in the channel $\{N_j\}$. The previous equation refers for simplicity to the easiest case, which neglects the quantum statistics effects described in the previous section, however the same modifications hold also for the more general and complex case.

2.6 Free parameters

One of the most important features of the Statistical Hadronization Model presented in the previous sections, besides its ability to include the effects of the quantum statistics (Sec. (2.3)) and of the interactions among the hadrons (Sec. (2.5)), is the number of free parameters which characterizes the model itself, limited to 2. These parameters are the strangeness suppression parameter γ_S, introduced in Sec. (2.4), and the cluster energy density ρ. This second parameter has not been described explicitly in the previous sections but, nevertheless, it is present in the equations derived in this chapter for the transition probabilities and for the microcanonical partition function: in these equations the cluster volume V, originated by the wave function integration over the cluster spatial extension, appears but, since the input information about these objects is limited to their momentum and flavor composition, a conversion factor which could be used to obtain the cluster volume from its mass is needed. This factor is represented by the energy density parameter ρ.

These two quantities, which are not predicted by the model itself, need to be tuned by a comparison between the theoretical predictions of the implemented model and the corresponding experimental data, with particular attention, as will be discussed in the last chapter, to the possible interplay between the above parameters belonging to `MCSTHAR++` alone and the set of

phenomenological parameters used by the main event generator: some "quantities" of fundamental importance for the hadronization procedure, in particular the cluster composition and phase space distribution, strongly depend on the QCD shower process preceding the hadronization itself. For this reason, a study of the impact of the changes in the setup of the QCD showering algorithm on the hadronization results is mandatory, to obtain a fine tuning of the statistical model on the experimental data.

However, it must be noted that the above condition holds also for the other hadronization models previously described, with a fundamental difference in the number of free parameters needed by each of them, as can be seen from the discussion of Chapter 1. Obviously, the small number of phenomenological parameters needed by the Statistical Hadronization Model is a measure of the predictivity of the model itself.

More details on the tuning procedures and on the main generator free parameters involved will be given in the last chapter presenting the results obtained with `MCSTHAR++`.

Chapter 3

MCSTHAR++

As it has been described in the introduction, the main objective of the present work is the development of a Monte Carlo code implementing the hadronization process in the statistical framework, in particular in the microcanonical formulation described in the previous chapter. In the following sections the development of a prototype of such a kind of code, MCSTHAR++ (**M**onte **C**arlo **ST**atistical **HA**dronization in high energy **R**eactions), the details of the implementation of the algorithms used for the event generation as well as the interfacing of this code to HERWIG6.510 [8] and Herwig++ [9] will be discussed.

3.1 General structure of MCSTHAR++

MCSTHAR++ is a Monte Carlo code, written in Object Oriented C++, performing the hadronization process as described in the microcanonical formulation of the Statistical Hadronization Model. It is built to take as input a set of clusters and to give in output a set of hadrons, both stable and unstable, coming from the microcanonical hadronization, with exact conservation of energy-momentum and abelian charges, of each single cluster.

A set of C++ classes and functions has been developed in order to describe the hadronization process: the following lines will go through the whole event generation describing, when they occur, the above elements. The first step to run MCSTHAR++ is a call to the `hadrsetup` function: this function fixes some parameters needed at runtime that will be described in the next chapter, calls the `iosetup` function which allows the user to modify the free parameters of the model and other generation parameters, and loads the hadron set to be used in the hadronization of the clusters, using the `fs_set` class. These operations are performed only once in a run and before the event generation cicle. After these preliminary steps, the generation begins following the standard procedures of the external event generator, from the QED/QCD (depending on the kind of colliding beams) initial state radiation emission to the cluster creation.

At this point the MCSTHAR++ function `hadronization` is called, perform-

ing the hadronization process and producing the primary hadrons. The first operation inside this function is the load of the incoming external clusters, described by the `cluster` class: this loading operation is performed by the `clustering` class, which is used to manage the clusters and the fusion process which can be called in case of too light clusters, as will be described in the next section. The clusters to be hadronized are then passed to the `cl_to_hadro` function, which represent the "kernel" function of the hadronization process: the first step performed here is, starting from the mass of the cluster, its abelian charges and the values of the free parameters of the hadronization model, to find the value of the microcanonical partition function of the cluster itself. This operation is performed by the `Z_interpolator` class using an interpolation method described in the next section: if the value is zero it means that no hadronization channels are available for the particular combination of mass and abelian charges of the cluster and therefore the current event is rejected, otherwise the hadronization algorithm continues towards the sampling of the hadronization channel. To perform this operation, for some reasons that will be explained later, the hadron set is broken into some subsets classified in function of particle abelian charges and the single particle mean production rates are calculated, actions managed by the `hadrongr` and `multsampl` classes. The second of the previous classes plays also the fundamental role of hadronization channel generator, using the algorithms discussed in the next section. The next and final step of the hadronization process of a cluster, when the hadronization channel has been produced, is the generation of the corresponding kinematical configuration, operation performed by the `kingen` class. The output coming from this last step is described by the `hadro` class, which contains the information about the particles, represented by the `particle` class, produced in the hadronization of a cluster, the weight of the event produced and the kinematical configuration. Finally, these information are loaded in a global event record, containing the complete output coming from the hadronization of all the clusters, and represented by the `cluevt` class.

At this point the hadronization process is closed adding to the external event record, belonging to the main generator, the new clusters which could have been produced during the initial fusion process and the primary hadrons coming from the hadronization of the clusters and updating the event weight using the microcanonical weight.

3.2 Algorithms

Some of the actions performed by the classes described in the previous section need to be discussed in detail, playing a fundamental role in the event generation. The following sections will give a deep explanation of these operations.

3.2.1 Cluster fusion

The first of the above actions is about the set of clusters taken as input for the hadronization process: since the predictions of the microcanonical hadronization model are in a better agreement with experimental data when it is used on sets of relatively heavy clusters, it has been introduced in `MCSTHAR++` an optional merging procedure working on the set of external "primary" clusters in order to obtain an heavier set of these objects, which could then be hadronized with better results. The above merging procedure is performed by the `clustering` class, which analyzes the set of incoming clusters and finds the too light ones, with respect to a mass cut value which has to be set by the user. If one or more light clusters are found an iterative fusion process is activated, which merges the cluster pairs containing at least one light object into heavier clusters, repeating this procedure until no light clusters remain. When more than one combination for a light cluster is possible, a condition which occurs when more than two primary clusters are present, the pair which will be merged is the one with the smallest invariant mass, therefore a higher priority is given to the merging of clusters close to each other in the collision phase space.

This procedure can be understood considering a particular case: supposing to have a set of four primary clusters coming from the external event generator, numbered from 1 to 4, two of which, for example the clusters 2 and 4, lighter than the imposed low cut mass, the first operation performed by the `clustering` class is to check the presence of light clusters. If no one of them is found the simulation continues with the hadronization of the primary clusters, otherwise, like in the considered case, the merging procedure is called: the merging algorithm begins considering all the possible pairings of the four clusters containing at least one light object, namely the pairs (1,2), (1,4), (2,3), (2,4) and (3,4), and calculating for each of them the invariant mass

$$m(i,j) = \sqrt{(p_i + p_j)^2}, \tag{3.1}$$

where i and j are the cluster indexes and p_i and p_j the corresponding 4-momenta. As can be seen, different pair configuration are possible, for example referring to the present example the possible combinations would be (1,2) and (3,4), (1,4) and (2,3) or 1, 3 and (2,4) (the clusters 1 ad 3 are not paired in this case): the choice among these possibilities is performed ordering the invariant masses and selecting the lighter ones avoiding any repetition of the cluster indexes. Supposing, for the present example, the pair (3,4) to be the lighter one, the other pair to be considered would be necessarily the pair (1,2): two new clusters, numbered 5 and 6, will be produced assigning to these objects a 4-momentum and a charge configuration given by the sum of the 4-momenta and charge configurations of the clusters composing the considered pairs. At this point two new clusters are present, while the old ones involved in the merging procedure are being deleted, and the algorithm restarts on these new

objects by checking their mass: if they are heavier than the mass cut the simulation continues with the hadronization of these two clusters, otherwise a merging process is performed on them. These operations are iteratively repeated on the new clusters appearing after every merging process until all the clusters have a mass above the cut or only one cluster remains after the fusion procedure.

The drawback of this fusion procedure is given by the mass cut value, which needs to be tuned on the experimental data as it must be done for the energy density and strangeness suppression paramenter, adding a phenomenological parameter to the model.

3.2.2 Partition function interpolation

The second step to be analyzed is relative to the microcanonical partition function of the clusters subject to the hadronization procedure: as it has been described in the previous chapter, a transition probability given by eq. (2.10),

$$p_f = \frac{\delta^4(P - P_f)\delta_{\mathbf{Q},\mathbf{Q}_f}}{\Omega} \sum_{h_V} |\langle f \mid h_V \rangle|^2 ,$$

corresponds to the hadronization of a cluster into a state $\mid f\rangle$. In this equation the microcanonical partition function of the cluster Ω appears in the denominator and it is needed to correctly normalize the transition probability. The problem here is that Ω is a function of the mass and abelian charges of the cluster and of the free parameters γ_S and ρ, and therefore it should be computed at runtime for each cluster to be hadronized. However, this is a quite CPU intensive quantity to be calculated and to make such a calculation during the event generation would be impossible. In the present work the problem to get the information about the partition function at runtime has been solved using the following approximate approach: after a preliminary study of the cluster abelian charge configurations and mass spectrum appearing during the event simulation, a grid of partition functions for each one of the possible charge configurations has been built, where the grid points correspond to different sets of values for γ_S, ρ and for the cluster mass. During the simulation this set of grids is loaded by the `Z_interpolator` class and the values of the needed partition functions are obtained using a method of the above class which finds the values by a linear interpolation among the grid points. The studies performed in order to estimate the error associated to this interpolation procedure show, on average, a maximum discrepancy of about 10% between the exactly calculated values and the interpolated ones.

The need for a normalization of the transition probability is strictly related, in the present work, to the use of the importance sampling method for the hadronization event generation, as it will be described in the next section. Other sampling and channel generation techniques could be used, for example the Metropolis algorithm [34] which would not need the knowledge of the

normalization factor. However, in order to obtain a generator which could be used for an intensive comparison with experimental data and for the study of the hadronization model, this sampling method is not convenient because of its slowness compared to the adopted importance sampling algorithm.

The need of the microcanonical partition function, moreover, introduces the problem of calculating the function itself to build the described grids, a quite expensive task from a computational point of view: in Sec. (3.4) a detailed description of the techniques adopted to make the above calculation can be found, even if it must be noted that the computation of the set of grids of partition functions has to be performed only once or in case of changes in the set of hadrons used.

3.2.3 Hadronization channel generation

The next fundamental issue to be discussed, which is strongly related to the partition function calculation, is about the algorithm used to generate the decay channel during the hadronization process. For a given charge configuration the number of allowed hadronization channels increases almost exponentially with the mass of the cluster itself. For this reason a random choice of the channel proportional to its microcanonical weight would be computationally too expensive, also because for each channel the calculation of the hadronic phase space would be needed. Therefore, discarding the Metropolis algorithm for the described reasons, the solution that has been adopted is represented by the importance sampling method. To apply this technique in the most effective way it is of fundamental importance to find a sampling function which could be, in its turn, sampled efficiently and which at the same time could reproduce with good accuracy the behavior of the phase space as a function of the hadronization channel. A possible sampling function with the above features is given by a product of poissonian distributions, one for each of the included hadronic species, as described in [28]. In this case the sampling function $\Pi_{\{N_j\}}$ would be given by:

$$\Pi_{\{N_j\}} = \prod_{j=1}^{K} \exp\left(-\nu_j\right) \frac{\nu_j^{N_j}}{N_j!}, \tag{3.2}$$

where ν_j is the mean number of particles of kind j, K the number of hadronic species included and N_j the number of particles of kind j contained in the channel $\{N_j\}$. The choice of this particular function is related to the fact that it represents the multi-species multiplicity distribution in the grandcanonical ensemble, when the corrections due to the quantum statistics discussed in Sec. (2.3) are not included. The mean multiplicities ν_j, cited in Sec. (3.1) describing the operations performed by the `hadrongr` and `multsampl` classes, are free parameters which should be fixed with the objective to reach the most efficient sampling function: the recipe presented in [28] and adopted in the present case is to set each mean multiplicity equal to its grandcanonical value

for a cluster with volume and average energy given by the volume and mass of the cluster whose hadronization channel will be sampled using the above function, using the grandcanonical equation

$$\nu_j = \frac{(2J_j+1)\,V}{2\pi^2} m_j^2 T K_2\left(\frac{m_j}{T}\right) \prod_i \lambda_i^{q_{ji}}, \tag{3.3}$$

where V is the cluster volume, T is the ensemble temperature, J_j the j-th hadron spin and m_j its mass and K_2 the modified Bessel function of the second kind. Moreover, the product is over the abelian charges and λ_i is the fugacity corresponding to the i-th charge Q_i. Temperature and fugacity can then be fixed by setting the grandcanonical mean energy and charges equal to the mass M and charges $\mathbf{Q}$ of the cluster, using the grandcanonical equations

$$M = T^2 \frac{\partial}{\partial T} \sum_{j=1}^{K} z_j\,(T) \prod_i \lambda_i^{q_{ji}} \tag{3.4}$$

$$\mathbf{Q} = \sum_{j=1}^{K} \mathbf{q}_j z_j\,(T) \prod_i \lambda_i^{q_{ji}} \tag{3.5}$$

with

$$z_j\,(T) = \frac{(2J_j+1)\,V}{2\pi^2} m_j^2 T\ K_2\left(\frac{m_j}{T}\right), \tag{3.6}$$

where $\mathbf{Q}$ and $\mathbf{q}_j$ are the vectors of the abelian charges of the cluster and j-th hadron respectively.

The sampling performances related to the use of the function (3.2) can be improved, reducing the rejection rate due to charge conservation, using a multi-step extraction algorithm which works on the hadron groups previously cited and managed by the `hadrongr` class, instead of extract independently the number of each hadron kind as would be done using the sampling function in the presented form. More in detail, the whole set of hadrons is broken into the following 11 groups: (anti)bottomed hadrons, (anti)charmed hadrons, light (anti)baryons, light strange (anti)mesons, light charged (anti)mesons with zero strangeness and neutral light mesons. Moreover, the following feature of the multi-poissonian function is used: excluding for simplicity the first 4 groups and the relative charge conservations, the original sampling function with an extra Kronecker delta added to impose the conservation of the abelian charges can be written as

$$\begin{aligned}\prod_{j=1}^{K} \exp\left(-\nu_j\right) \frac{\nu_j^{N_j}}{N_j!}\ \delta_{\sum_i N_i \mathbf{q}_i, \mathbf{Q}} &= \prod_{j=1}^{K} \pi_j\left(N_j\right)\ \delta_{\sum_i N_i \mathbf{q}_i, \mathbf{Q}} \\ &= \prod_{bar} \pi_j^b\left(N_j\right) \prod_{antibar} \pi_j^{\bar{b}}\left(N_j\right) \prod_{mes} \pi_j^m\left(N_j\right)\ \delta_{\sum_i N_i \mathbf{q}_i, \mathbf{Q}} \\ &= \Pi_{bar}\left(N_b\right) \Pi_{antibar}\left(N_{\bar{b}}\right) \times \\ &\quad P(N_1^b, N_2^b, ... \mid N_b) P(N_1^{\bar{b}}, N_2^{\bar{b}}, ... \mid N_{\bar{b}}) \times \\ &\quad \prod_{mes} \pi_j^m\left(N_j\right)\ \delta_{\sum_i N_i \mathbf{q}_i, \mathbf{Q}},\end{aligned} \tag{3.7}$$

where

$$\Pi_x\left(N_x\right) = \exp\left(-\nu_x\right) \frac{\nu_x^{N_x}}{N_x!}, \tag{3.8}$$

is the poissonian distribution of the total number of baryons ($x = b$) and antibaryons ($x = \bar{b}$) and where the corresponding mean multiplicity ν_x is given by the sum of the mean multiplicities of the single baryons or antibaryons, while the functions P are the conditioned multinomial distribution of the single hadronic species, namely

$$P\left(N_1^x, N_1^x, ... \mid N_x\right) \propto N_x! \prod \frac{\nu_j^{N_j^x}}{N_j^x}, \tag{3.9}$$

with, again, $x = b$ for baryons and $x = \bar{b}$ for antibaryons.

The above decomposition of the original multipoissonian, restricted to a smaller subset of particles, corresponds to a change in the channel generation algorithm: the original function would lead to an independent sampling of the number of each hadron kind, with a subsequent check of abelian charge conservations and an eventual rejection of the sampled channel. With the presented decomposition the sampling algorithm is instead the following:

1. Extract the number of baryons and antibaryons with the distributions $\Pi_b\left(N_b\right)$ and $\Pi_{\bar{b}}\left(N_{\bar{b}}\right)$.

2. Check if the baryonic number is conserved. If not reject the sampling and go to point 1, otherwise extract the single baryons and antibaryons using the multinomial distribution (3.9).

3. Extract the single mesons using the initial multipoisson distributions.

4. Check the conservation of the remaining abelian charges, taking into account the already extracted baryons and antibaryons. If the check is not passed start again with point 1, otherwise the sampled channel is momentarily accepted and the corresponding phase space availability can be verified.

The above sampling algorithm is equivalent to the first one from the point of view of the sampled channel distribution, while it is more efficient because of the smaller number of random extractions in case of rejected attempts. It must be noted that the described sampling method is a simplified version of the one actually implemented in MCSTHAR++, which works in a very similar way on the larger set of hadron groups previously cited, with a special treatment for heavy flavored hadrons and clusters: the clusters containing only light partons are supposed to hadronize into channels composed only of light baryons and mesons since, because of charm and beauty conservation, the heavy flavored hadrons would be produced in this case only in pairs, a condition strongly suppressed because of phase space availability reasons. Therefore the standard algorithm, based on the decomposed multipoissonian, is used in this case. Heavy clusters are instead supposed to hadronize into channels containing one heavy hadron and a set of light particles, again because of the phase space availability conditions: the particular heavy hadron is sampled with probability P_h given by

$$P_h \propto e^{-m_h/T}, \tag{3.10}$$

where m_h is the mass of the hadron and T the temperature parameter, while the remaining part of the channel is randomly chosen using the same algorithm applied for the hadronization of light clusters. This modification of the sampling function makes the sampling procedure even more efficient, since the use of the standard algorithm also for charmed and bottomed hadrons would result in a low multiplicity sampling of these particles because of their large mass which, in its turn, leads to very small mean multiplicities in Eq. (3.2)

3.2.4 Phase space configuration

The last item to be discussed, which refers to the kingen class, is the sampling of the multi-particle phase space configuration: when a hadronization channel of a cluster has been generated with the methods described in the previous section, a check on the phase space availability is performed and then a kinematical configuration for the produced particles needs to be sampled. In the present work a strategy inspired by the multi-particle decay phase space integration described in [35] has been followed.

The starting point to obtain the kinematical configuration and the corresponding weight for a channel containing N particles with masses $m_1, m_2, ..., m_N$ and for a cluster of mass M is the phase space integral of Eq. (2.20):

$$PS(M, m_1, m_2, ..., m_N) = \int \prod_{i=1}^{N} d^3p_i \delta^4 \left(P - \sum_{i=1}^{N} p_i \right), \tag{3.11}$$

the needed quantity will follow from the numerical solution of the above integral. As discussed in [35], the following condition holds for the relativistic N-body phase space element:

$$\begin{aligned} d\Phi_N(P;p_1,p_2,...,p_N) =& d\Phi_{N-J+1}(P;Q,p_{J+1},...,p_N)\times \\ & d\Phi_J(Q;p_1,p_2,...,p_J)(2\pi)^3 dQ^2 \end{aligned} \tag{3.12}$$

for $J < N$, where

$$d\Phi_N(P;p_1,p_2,...,p_N) = \delta^4\left(P - \sum_{i=1}^{N} p_i\right)\prod_{i=1}^{N}\frac{d^3p_i}{(2\pi)^3 2E_i} \tag{3.13}$$

and

$$Q^2 = \left(\sum_{i=1}^{J} E_i\right)^2 - \left|\sum_{i=1}^{J}\mathbf{p}_i\right|^2 .$$

The initial integral can be trasformed in order to deal with a relativistic phase space volume instead of the non relativistic one, with the result

$$\begin{aligned} PS(M,m_1,m_2,...,m_N) &= \int\prod_{i=1}^{N}\frac{d^3p_i}{(2\pi)^3 2E_i}\delta^4\left(P-\sum_{i=1}^{N}p_i\right)\prod_{i=1}^{N}(2\pi)^3 2E_i \\ &= \int d\Phi_N\left(P;p_1,p_2,...,p_N\right)\prod_{i=1}^{N}(2\pi)^3 2E_i. \end{aligned} \tag{3.14}$$

The integration procedure adopted is based on the split feature of Eq. (3.12), represented in Fig. (3.1) for a 4-body decay: splitting recursively the phase space elements in order to deal only with 2-body decays, the above integral becomes

$$\begin{aligned} PS(M,m_1,m_2,...,m_N) = \int\prod_{i=0}^{N-3} & d\Phi_2\left(q_i;p_{i+1},q_{i+1}\right)(2\pi)^3 dq_{i+1}^2\times \\ & d\Phi_2\left(q_{N-2};p_{N-1},p_N\right)\prod_{i=1}^{N}(2\pi)^3 2E_i, \end{aligned} \tag{3.15}$$

with $q_0 = (M,\mathbf{0})$. The integral of a 2-body phase space gives

$$\begin{aligned} \int d\Phi_2\left(k_1;k_2,k_3\right) &= \int\frac{d^3k_2}{(2\pi)^3 2k_2^0}\frac{d^3k_3}{(2\pi)^3 2k_3^0}\delta^4\left(k_1-k_2-k_3\right) \\ &= \int d\Omega_{k_2}\frac{1}{(2\pi)^3 2k_2^0}\frac{1}{(2\pi)^3 2k_3^0}\mid\mathbf{k_2}\mid^2, \end{aligned} \tag{3.16}$$

with

$$
\begin{aligned}
\mid \mathbf{k_2} \mid^2 &= \frac{\left((k_1)^2 - \left(\sqrt{(k_2)^2} + \sqrt{(k_3)^2}\right)^2\right)\left((k_1)^2 - \left(\sqrt{(k_2)^2} - \sqrt{(k_3)^2}\right)^2\right)}{4\,(k_1)^2} \\
&= \frac{\lambda\left((k_1)^2, (k_2)^2, (k_3)^2\right)}{4\,(k_1)^2},
\end{aligned}
\tag{3.17}
$$

as can be seen imposing the energy-momentum conservation condition and where

$$\lambda\,(x, y, z) = x^2 + y^2 + z^2 - 2xy - 2xz - 2yz$$

is the Kallen lambda function. Therefore, solving the 2-body integration, Eq. (3.15) becomes

$$
\begin{aligned}
PS(M, m_1, m_2, ..., m_N) = &\int \prod_{i=0}^{N-3} dq_i^2 d\Omega_{q_i} \frac{\mid \mathbf{q_i} \mid^2}{(2\pi)^3 4 q_i^0 E_i^0} \times \\
&d\Omega_{p_{N-1}} \frac{\mid \mathbf{p_{N-1}} \mid^2}{(2\pi)^6 4 p_{N-1}^0 p_N^0} \prod_{i=1}^{N} (2\pi)^3 2 E_i^{\mathrm{CM}} \\
= &\prod_{i=0}^{N-3} \int_{q_i^{2\ min}}^{q_i^{2\ max}} \int_{4\pi} dq_i^2 d\Omega_{q_i} \frac{\mid \mathbf{q_i} \mid^2}{(2\pi)^3 4 q_i^0 E_i^0} \times \\
&\int_{4\pi} d\Omega_{p_{N-1}} \frac{\mid \mathbf{p_{N-1}} \mid^2}{(2\pi)^6 4 p_{N-1}^0 p_N^0} \prod_{i=1}^{N} (2\pi)^3 2 E_i^{\mathrm{CM}},
\end{aligned}
\tag{3.18}
$$

where the q_i^2 integral limits, for $i = 1, ..., N-2$, are given by

$$
\begin{aligned}
q_i^{2\ min} &= \left(\sum_{j=i+1}^{N} m_j\right)^2 \\
q_i^{2\ max} &= \left(\sqrt{(q_{i-1})^2} - m_i\right)^2
\end{aligned}
$$

and where E_i^{CM} is the energy of the i-th particle in the cluster rest frame. It must be noted that each one of the above 2-body integrals in dq_i^2 is a relativistic invariant solved in the rest frame of the 4-momentum q_{i-1}, in which the condition $\mathbf{p}_i = \mathbf{q}_i$ holds, while the energies contained in the last product of Eq. (3.18) and added to obtain the relativistic phase space, refer to the initial reference frame, namely the cluster rest frame. Therefore it is necessary to perform a number of relativistic boosts during the integration, as will be clear from the integration algorithm described in the following lines and based on a Monte Carlo flat sampling of q^2s an Ωs variables. Assuming to have a number of particles $N > 3$, the integration/generation algorithm is the following:

1. Sample the value of q_1^2 in $[q_1^{2\ min}, q_1^{2\ max}]$ and the direction of $\mathbf{q_1}$, in q_0 rest frame, in 4π. Build the 4-vector p_1, which is already in the correct reference frame, and calculate the integrand function

$$W_{i=1} = \frac{\mid \mathbf{q_i} \mid^2}{(2\pi)^3 4 q_i^0 E_i^0}. \tag{3.19}$$

2. Sample the value of q_2^2 in $[q_2^{2\ min}, q_2^{2\ max}]$ and the direction of $\mathbf{q_2}$, in q_1 rest frame, in 4π. Build the 4-vector p_2, calculate the integrand function W_2 defined in Eq. (3.19) for $i = 2$ and boost p_2 in the cluster rest frame using the q_1 4-vector. Boost the q_2 4-vector in the cluster reference frame redefining it as $q_2 = q_1 - p_2$.

3. Repeat the previous steps on q_i and p_i for $i = 3, ..., N-2$.

4. Sample the direction of p_{N-1} and calculate its module in q_{N-2} rest frame. Calculate the integrand function

$$W_{N-1} = \frac{\mid \mathbf{p_{N-1}} \mid^2}{(2\pi)^6 4 p_{N-1}^0 p_N^0}, \tag{3.20}$$

   boost p_{N-1} in the cluster rest frame and calculate p_N, which will be already in the right reference frame, as $p_N = q_{N-2} - p_{N-1}$.

5. Calculate the energy product and the sampling weight W_S as

$$W_S(q_1, q_2, ..., q_N) = (4\pi)^{N-1} \prod_{i=1}^{N-2} \left[q_i^{2max} - q_i^{2min} \right]. \tag{3.21}$$

In case of $N = 3$ after the step 1 the algorithm continues skipping the step 2 and 3. In case of $N = 2$ the situation is even easier, since only the direction of one of the two particle momenta has to be sampled, everything else being fixed by energy-momentum conservation: in this case the sampling weight W_S is equal to 4π. Finally, the total weight W_K corresponding to the sampled kinematical configuration is given by

$$W_K = \frac{W_{N-1}}{W_S} \prod_{j=1}^{2} (2\pi)^3 2 E_j^{\mathrm{CM}} \tag{3.22}$$

for $N = 2$ and

$$W_K = \frac{\prod_{i=1}^{N-2} W_i \prod_{j=1}^{N} (2\pi)^3 2 E_j^{\mathrm{CM}}}{W_S(q_1, q_2, ..., q_N)} \tag{3.23}$$

for $N > 2$.

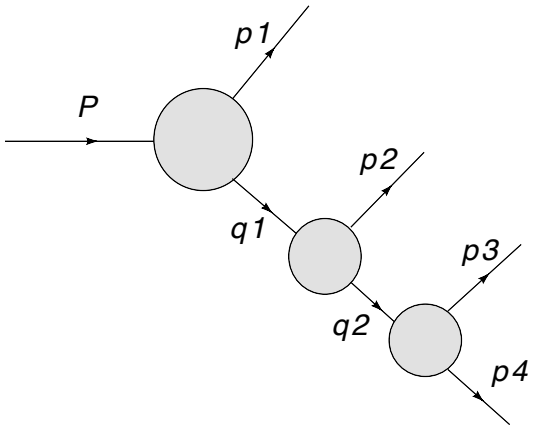

Figure 3.1: Graphical representation of the splitting procedure used by the multibody phase space generators for a 4-body decay.

3.3 Implementation in HERWIG6.510 and Herwig++

As it has been discussed in the introduction, the research project to which the present work refers has been focused not only on the development of the hadronization module MCSTHAR++ but also on its interface to a "general purpose" Monte Carlo event generator, with the aim of replacing the standard hadronization code block, in order to check the accuracy of the statistical model by a comparison against the experimental data of the model's theoretical prediction coming from full event generation. At present MCSTHAR++ has been interfaced to HERWIG6.510 and Herwig++ for simplicity reasons: as discussed in Chapter 1, these two event generators implement the cluster hadronization model and therefore the algorithms which build the clusters that can be used by MCSTHAR++ as primary input clusters are already implemented in the main generator. In the following lines the details of the interface of the developed code to HERWIG6.510 and Herwig++ will be given.

- HERWIG6.510

  This is a FORTRAN77 Monte Carlo code which works by setting the needed parameters in the available common blocks, to choose for example the beam particles, the hard scattering process and the beam energy, and by calling a sequence of subroutines to generate an event. To the standard version of the Monte Carlo code used in the present work, the only modification introduced is about the non-perturbative splitting of the gluons at the end of the QCD shower: the release setup of the code would let the gluons to produce only quark-antiquark pairs. This leads to the production of clusters with zero baryonic number only, which can be sources of baryon production using the standard hadronization model while they strongly suppress the production of this kind of particles using MCSTHAR++: because of the features of the statistical model, in

the hadronization of these "mesonic" clusters baryons can be produced only as baryon-antibaryon pairs, a condition which is suppressed in a large number of cases because of the corresponding small phase space availability. However, it is possible to obtain from HERWIG also baryonic clusters without any changes in the source code, just modifying the value of the QDIQK variable belonging to the HWPRAM common block. This variable represents the scale at which the gluons can split into diquarks, therefore setting it to $2m_s$, where m_s is the mass of the strange quark, will let the gluons to split not only in quark-antiquark pair but also in diquark-antidiquark pairs with flavor content u, d or s.

With respect to the classes and functions belonging to MCSTHAR++ and previously described, few FORTRAN functions have been added to the source code to realize the interface of the new hadronization module to the main code, in particular to load HERWIG's clusters in MCSTHAR++: these functions are used to find the original clusters inside the HEPEVT common block of HERWIG, which contains the information about the particles and clusters involved in the current event and to calculate the cluster charges. Because of the language used to build the new hadronization module, a translation from FORTRAN77 to C++ data structures and back is mandatory: the solution adopted here is a wrapper header file containing the C++ structures corresponding to the F77 common blocks. This wrapper file is also used to allow MCSTHAR++ to access the HEPEVT common block to update the list of particles and clusters of the current event, in particular including the objects produced during the hadronization process. Other F77 and C++ source codes containing the definition of the routines, functions and classes used to perform the analysis and to build the corresponding distributions and histograms have been added: the set of analysis included and their definitions will be described in the next chapter.

- Herwig++

  As discussed in [9], Herwig++ is a general purpose Monte Carlo event generator with many similarities with its FORTRAN77 version but with a completely new structure. In particular it has been written in C++ using the building blocks offered by ThePEG [36], a framework for the implementation of Monte Carlo event generators: this is a C++ class library providing all parts of an event generator structure which do not depend on the particular physics models implemented in the generator itself. More in detail, each part of Herwig++ is a C++ class representing the implementation of a theoretical model used by Herwig++ itself and each one of the above classes inherits from an abstract base class of ThePEG. Among these classes, a central role is played by the "handler" classes, which are used to manage the various steps of the simulation as, for example, the CascadeHandler, which generates the parton shower,

the DecayHandler, which manages the decay of the unstable hadrons and elementary particles, and the HadronizationHandler, which performs the hadronization step.

In this case MCSTHAR++ has been implemented in the main generator following the general structure of the generator itself, making use of a set of handler classes to interface the new hadronization module to the external code. More in detail, the above HadronizationHandler class uses a number of "helper" classes to perform the actions required by the implemented cluster hadronization model as, for example, the ClusterFinder class, responsible for building the clusters starting from the partons, the ClusterFissioner class, which splits the large mass clusters into lighter ones, and the ClusterDecayer class which decays the clusters into hadron pairs as described by the hadronization model. The implementation of MCSTHAR++ in Herwig++ is based on a set of classes similar to the previous handlers and helpers, which realize the required interfacing operations from cluster building to the final update of the event record with the particles coming from the hadronization process, while the "kernel" operations performing the hadronization of the incoming clusters are realized using the same set of classes and functions which characterizes the implementation of MCSTHAR++ in HERWIG6.510 described in the previous item.

3.4 Microcanonical partition function calculation

As it has been discussed in Sec. (3.2.2), the knowledge of the partition function, at least in an approximated way, of a cluster to be hadronized is of fundamental importance in order to correctly normalize the weight associated to the hadronization process. Nevertheless the calculation of the microcanonical partition function is a quite expensive task from a computational point of view, because it involves a sum over all the available channels, which are expensive to be found, and because for each channel a phase space integral is required. In the next lines the adopted calculation techniques will be discussed.

Given a cluster with mass M, energy density ρ and abelian charges $\mathbf{Q}$ and given a strangeness suppression parameter γ_S, the microcanonical partition function is defined as

$$\Omega\left(M, \mathbf{Q}, \rho, \gamma_S\right) = \Omega = \sum_{\{N_j\}} \Omega_{\{N_j\}} \delta_{\mathbf{Q},\mathbf{Q}_{\{N_j\}}}, \tag{3.24}$$

where $\Omega_{\{N_j\}}$ is the hadronic phase space for the channel $\{N_j\}$. As it has been said, the number of available channels which respecting the abelian charges conservation have to be included in the above sum increases exponentially with the mass of the cluster itself, while at the same time a large number of these channels have a relatively small corresponding hadronic phase space

which, therefore, could be neglected in the sum over the channels. For these reasons it is not always worth the computational cost of taking into account all the channels to perform the above sum, especially for the heavy clusters.

For the present work two strategies have been adopted to perform the partition function calculation: for small mass values an algorithm which builds all the possible hadronization channels is used, therefore making the above sum in an exact way, without discarding any of the possible channels. For a given configuration of the abelian charges, however, to build all the available channels becomes very CPU time demanding increasing the cluster mass. Above a particular mass value, an importance sampling method identical to the one described in Sec. (3.2.3) is more convenient and therefore adopted instead of the exact method previously described.

The second computational task to be performed to obtain the microcanonical partition function of a cluster is, for each considered channel, the calculation of the hadronic phase space. As will be discussed in the next chapter, in the present work and for this first round of tests of the developed code, the quantum statistics and the interactions among the hadrons, which modify the following equations, are not included for simplicity reasons. Therefore, with these conditions, the hadronic phase space $\Omega_{\{N_j\}}$ for a channel $\{N_j\}$ is given by

$$\Omega_{\{N_j\}} = \prod_{j=1}^{K} \frac{(2J_i+1)^{N_j} V^{N_j}}{(2\pi)^{3N_j} N_j!} \int \prod_{i=1}^{N} d^3p_i \delta^4(P - P_f), \tag{3.25}$$

where N is the total number of particles contained in the considered channel. Following the method proposed by Cerulus and Hagedorn [37] and later adopted by Werner and Aichelin [38], the above equation can be rewritten as

$$\Omega_{\{N_j\}} = \frac{V^N T^{3N-4}}{(2\pi)^{3N}} \prod_{j=1}^{K} \frac{(2J_i+1)^{N_j}}{N_j!} \Phi\left(M, m_1, m_2, ..., m_N\right), \tag{3.26}$$

where m_i is the mass of the i-th particle of the channel,

$$T = M - \sum_{i=1}^{N} m_i$$

is the available kinetic energy and $\Phi\left(M, m_1, m_2, ..., m_N\right)$ is the adimensional integral

$$\Phi\left(M, m_1, m_2, ..., m_N\right) = \frac{1}{T^{3N-4}} \int d^3p_1 d^3p_2 \cdots d^3p_N \delta^4(P - P_f). \tag{3.27}$$

For two particles the above integral can be easily solved with the result

$$\Phi\left(M, m_1, m_2\right) = \frac{4\pi p}{T^2} \frac{E_1 E_2}{M}, \tag{3.28}$$

where $E_i = \sqrt{p^2 + m_i^2}$ and

$$p = \frac{1}{2}\left[M^2 - 2\left(m_1^2 + m_2^2\right) + \frac{\left(m_1^2 - m_2^2\right)^2}{M^2}\right]^{\frac{1}{2}}.$$

For $N > 2$ the integral of Eq. (3.27) can be written in the following way, by a separation of the angular variables from the other integration variables:

$$\Phi\left(M, m_1, m_2, ..., m_N\right) = \frac{(4\pi)^N}{T^{3N-4}} \int dp_1 p_1 dp_2 p_2 \cdots dp_N p_N \times \delta\left(M - \sum_{i=1}^{N} E_i\right) W\left(p_1, p_2, ..., p_N\right), \tag{3.29}$$

with

$$W\left(p_1, p_2, ..., p_N\right) = \frac{1}{(4\pi)^N} \int d\Omega_1 d\Omega_2 \cdots d\Omega_N \delta^3\left(\sum_{i=1}^{N} p_i \hat{\mathbf{p}}_i\right), \tag{3.30}$$

where $\hat{\mathbf{p}}_i = \mathbf{p}_i / \mid \mathbf{p}_i \mid$. As it is shown in [38], the previous integral can be solved explicitly, with the result

$$W\left(p_1, p_2, ..., p_N\right) = -\frac{1}{2^{N+1}\pi\left(N-3\right)! p_1 ... p_N} \sum_{\{\sigma_1 ... \sigma_N\}}^{\sum \sigma_j p_j \geq 0} \sigma_1 ... \sigma_N \left(\sum_{i=1}^{N} \sigma_i p_i\right)^{N-3}, \tag{3.31}$$

where $\sigma_i = \pm 1$ and where the external sum is over all the $\{\sigma_1 ... \sigma_N\}$ configurations which give $\sum \sigma_j p_j \geq 0$.

Since the above sum involves a large number of terms, which moreover increases quickly with the number of particles involved, an alternative calculation method is used when N increases to values such that the previous techniques become too slow: since the equation

$$\delta^3\left(\sum_{i=1}^{N} p_i \hat{\mathbf{p}}_i\right) = \frac{1}{(2\pi)^3} \int d^3u \exp\left(-i \sum_{i=1}^{N} p_i \hat{\mathbf{p}}_i \cdot \mathbf{u}\right) \tag{3.32}$$

holds, the W function can also be written as

$$W\left(p_1, p_2, ..., p_N\right) = \frac{1}{2\pi^2} \int_0^\infty du u^2 \prod_{i=1}^{N} \frac{\sin\left(p_i u\right)}{p_i u}. \tag{3.33}$$

Setting now $u = x/\left(1 - x\right)$, the above integral becomes

$$W\left(p_1, p_2, ..., p_N\right) = \frac{1}{2\pi^2}\int_0^1 dx \frac{(1-x)^{N-4}}{x^{N-2}} \prod_{i=1}^{N} \frac{\sin\left(\frac{p_i x}{1-x}\right)}{p_i}. \tag{3.34}$$

This integral can be solved numerically with a condition on the number of particles involved, since the integrand function shows a strongly oscillating behavior for small values of N which makes hard to obtain a stable result.

Finally, the external integral of Eq. (3.29) can be solved by means of Monte Carlo techniques: after the following sequence of variable transformation,

$$\begin{aligned}
p_i &= \sqrt{t_i\left(t_i + 2m_i\right)} \quad i = 1, 2, ..., N \\
t_i &= s_i - s_{i-1} \quad i = 1, 2, ..., N \text{ with } s_0 = 0 \text{ and } s_N = T \\
x_i &= \frac{s_i}{T} \quad i = 1, 2, ..., N-1 \\
z_i &= \frac{x_i}{x_{i+1}} \quad i = 1, 2, ..., N-1 \text{ with } x_N = 1 \\
r_i &= z_i^i \quad i = 1, 2, ..., N-1,
\end{aligned} \tag{3.35}$$

and the integration of the Dirac's delta on energy conservation, the initial integral becomes

$$\Phi\left(M, m_1, m_2, ..., m_N\right) = \int_0^1 dr_1 dr_2 \cdots dr_{N-1} \Upsilon(r_1, r_2, ..., r_N), \tag{3.36}$$

with

$$\Upsilon(r_1, r_2, ..., r_N) = \frac{(4\pi)^N T^{3-2N}}{(N-1)!} \prod_{i=1}^{N} p_i E_i W\left(p_1, p_2, ..., p_N\right). \tag{3.37}$$

Chapter 4

Numerical results

In the present chapter the results obtained with MCSTHAR++ for LEP experimental setup and for a center of mass energy equal to 91.2 GeV will be presented and discussed. Even if a full tuning of the hadronization module and a study of the influence of the main generator free parameter setup on the hadronization model prediction is needed, the accurate and rigorous tuning procedure will be left for a future work while in what follows a preliminary study on MCSTHAR++ performances will be presented, together with a discussion on the full set of parameters which will be involved in the final tuning. All the MCSTHAR++ results presented in the next sections are obtained without the inclusion of the quantum statistics and the interactions previously described.

4.1 Analysis

As it has been discussed in Sec. (3.3), a set of functions and classes has been developed in order to analyze the results obtained during the simulations, building the set of considered observables and the corresponding distributions, and comparing them with the available experimental data. For the present work the analysis of the following observables have been implemented[1]:

- Event shape: trust (T), thrust major (M), thrust minor (m), oblateness (O), sphericity (S), planarity (P), aplanarity (A), C-parameter (C), D-parameter (D), heavy hemisphere mass (M_h), light hemisphere mass (M_l), difference of hemisphere masses (M_d), wide hemisphere broadening (B_{max}), narrow hemisphere broadening (B_{min}), total hemisphere broadening (B_{sum}), difference of hemisphere broadenings (B_d), transverse momentum (in) with respect to thrust axis (P_t^T), transverse momentum (out) with respect to thrust axis (p_t^T), transverse momentum (in) with respect to sphericity axis (P_t^S), transverse momentum (out) with respect

[1] See the Appendix for the definitions of the considered quantities

to thrust axis (p_t^S), rapidity with respect to thrust axis (y^T), rapidity with respect to sphericity axis (y^S).

- Momentum and energy analysis for the following particles: $a_0^{\pm}$, η, η', ω, $\pi^{\pm}$, π^0, $\rho^{\pm}$, ρ^0, Σ^{*-}, Σ^{*+}, Ξ^+, Ξ^{*0}, $K^{\pm}$, K^{*0}, K^0, p, Δ^{++}, D^*, D^0, f_2, f_0, ϕ.
- Charged particle multiplicity.
- Mean multiplicities of 48 hadronic species plus charged particle number and photon number.

During the event generation the above observables are computed and compared with the experimental data. For each of them a χ^2 value is then calculated, in order to estimate the discrepancy between data and theoretical predictions. For a histogram the χ^2 value is computed as the sum on the channels of the discrepancy between the theoretical prediction y_t^i and the corresponding experimental data y_e^i normalized using the theoretical and experimental errors σ_t^i and σ_e^i:

$$\chi^2 = \sum_{i=1}^{N} \frac{\left(y_t^i - y_e^i\right)^2}{\sigma_t^{i\,2} + \sigma_e^{i\,2}}, \tag{4.1}$$

where N is the number of channels of the considered histogram. For the particle multiplicities the corresponding quantity is computed in a similar way summing over the list of considered particle instead of summing on the channels. In the next pages also the reduced χ^2 will be used: it must be noted that in the present case this quantity is just a measure of the discrepancy between theoretical and experimental results and not a real reduced χ^2, being calculated as χ^2/ν where ν is the number of channels of the considered histogram or the number of particles included in the analysis while, in the calculation of the real reduced χ^2, ν would be defined taking into account also the number of free parameters.

Even if no results coming from the implementation of `MCSTHAR++` in `Herwig++` will be presented here, it is worth to note that the above functions and classes do not need to be used in this case, since `Herwig++` provides by itself the code needed to analyze an analogous set of observables.

4.2 Light quark hadronization

The first study performed to check `MCSTHAR++` reliability and the theoretical predictions of the Statistical Hadronization Model, numerically implemented as described in the previous chapter, is focused on the hadronization of light quarks only [39]. Therefore, the results presented here have been obtained excluding from the set of used hadrons both charmed and bottomed particles and considering only the elementary collisions $e^+e^- \to u\bar{u}, d\bar{d}, s\bar{s}$. Even if among the LEP measurements only a small number of observables restricted to

light flavor exists, some comparisons are possible: in particular the observables studied here are the mean multiplicities of a subset of hadrons, the mean number of charged particles, the charged particle scaled momentum

$$x_p = \frac{2 \mid \mathbf{p} \mid}{\sqrt{s}} \tag{4.2}$$

and its logarithm

$$\xi_p = \log\left(\frac{1}{x_p}\right), \tag{4.3}$$

where $\mathbf{p}$ is the 3-momentum of the considered particle and $\sqrt{s}$ the collision center of mass energy.

The results reported in Tab. (4.1) and Fig. (4.1) and (4.2) show a comparison among LEP data (OPAL [40] and DELPHI [41] experiments) at 91.2 GeV center of mass energy, `MCSTHAR++` predictions when interfaced to `HERWIG6.510` as described in the previous chapter and a standard `HERWIG6.510` release. As it has been discussed, no tuning at all has been performed on `MCSTHAR++`: the results reported here have been obtained with a reasonable choice of the free parameters of the hadronization model, namely

$$\gamma_S = 0.65$$

and

$$\rho = 0.35\ GeV/fm^3,$$

and with no modification of `HERWIG`'s parameters except for the `QDIQK` $= 2m_s$ condition discussed in Sec. (3.3). The cluster mass cutoff M_C described in Sec. (3.2.1) has been set equal to 1.8 GeV for the following reason: first of all it must be noted that a selection has been introduced on the set of used hadrons, since the hadron spectrum is experimentally well known only for mass values smaller than about 1.8 GeV. Therefore the non charmed and non bottomed hadrons with a mass greater than the above value have been excluded from the simulations of the present work. Moreover, following Hagedorn's original hypothesis, the clusters should be considered as standard resonances and therefore their mass and charge configuration should correspond to observed particles, which are characterized by a discrete mass spectrum, a condition which can not be respected by the cluster mass spectrum.

As discussed in [39], even if a full tuning of the model is mandatory the preliminary results reported in this section show the good behavior of `MCSTHAR++` on the restricted set of observables chosen to study the hadronization of light quarks. The performances of the developed code will be investigated in more detail in the following section discussing the results obtained for the full hadronization process, which includes also the heavy quarks, and on a larger set of observables.

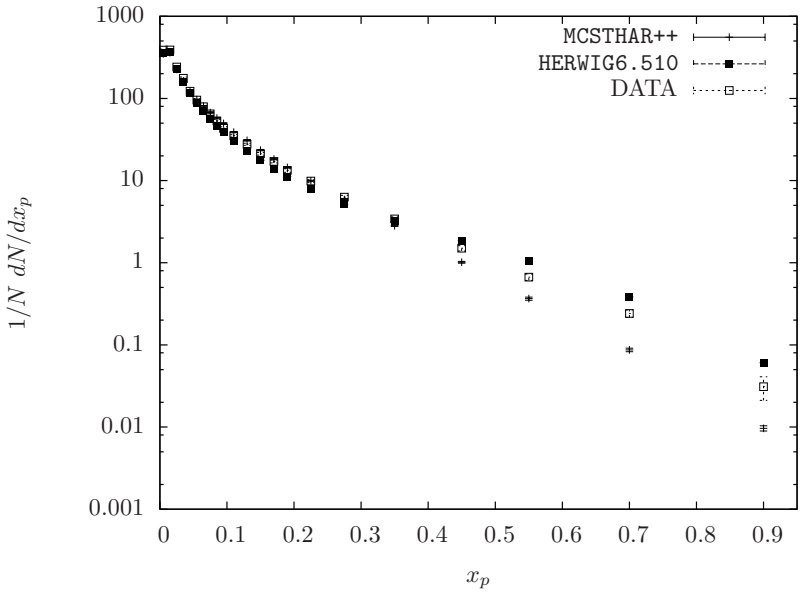

Figure 4.1: Charged particle scaled momentum x_p distribution: comparison among `MCSTHAR++`, `HERWIG6.510` and OPAL data [40] at 91.2 GeV center of mass energy.

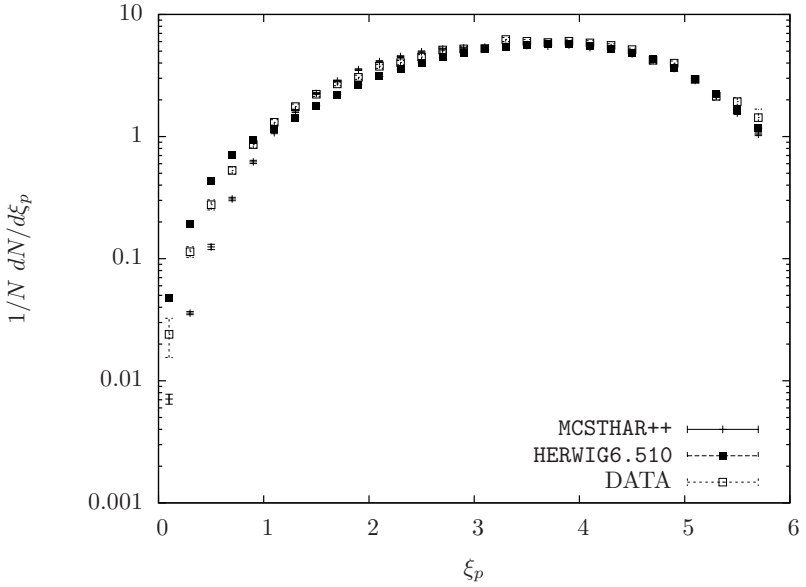

Figure 4.2: Charged particle ξ_p distribution: comparison among `MCSTHAR++`, `HERWIG6.510` and OPAL data [40] at 91.2 GeV center of mass energy.

4.3 Tuning strategy

As discussed in Chapter 3, the hadronization model implemented in `MCSTHAR++` requires two phenomenological parameters, γ_S and ρ, plus an additional parameter,

	N_{ch}	$N_{\pi^\pm}$	$N_{K^\pm}$	$N_{p,\bar{p}}$
MCSTHAR++	19.53 ± 0.14	16.64 ± 0.11	1.65 ± 0.04	0.98 ± 0.07
HERWIG6.510	18.601 ± 0.006	15.022 ± 0.006	1.628 ± 0.002	1.736 ± 0.002
DELPHI	19.94 ± 0.34	16.84 ± 0.87	2.02 ± 0.07	1.07 ± 0.05

Table 4.1: Mean values of charged particles, charged pions, charged kaons and (anti)protons multiplicities for the hadronization of light quarks only: comparison among MCSTHAR++, HERWIG6.510 and DELPHI data [41] at 91.2 GeV center of mass energy.

the cluster mass cut M_C, which however is more related to the interfacing of MCSTHAR++ to HERWIG6.510 (and Herwig++) than to the hadronization model itself. Moreover, the hadronization process is strongly influenced by the preceding collision steps, in particular by the QCD shower process and the cluster formation: these processes are performed, in the present work, by a sequence of HERWIG's routines whose algorithms depend on a set of free parameters which should be included in the tuning of the code. In particular, these parameters are:

- the effective d and u quark masses RMASS(1) and RMASS(2);
- the gluon effective mass RMASS(13);
- the quark and gluon virtuality cuts VQCUT and VGCUT;
- the QCD energy scale QCDLAM.

More in detail, as discussed in [8], the parton shower process is stopped when the virtuality reaches a cutoff value Q_c given by

$$Q_c = m + Q_0, \tag{4.4}$$

where m is the parton effective mass, given by the corresponding RMASS parameter, and Q_0 is set by the quark and gluon virtuality cutoff parameters VQCUT and VGCUT. Being involved in the definition of the virtuality condition which stops the shower algorithm and in the calculation of the Sudakov form factor which, again, is used in the shower process, the above parameters determine the phase space distribution of the clusters and their composition.

The full tuning procedure of the introduced hadronization model should therefore take into account also this set of parameters. A possible strategy to obtain the best fit of the model on the experimental data, avoiding to work on a large set of degrees of freedom, would be to obtain a preliminary tuning on the pre-hadronization parameters studying the performances of the main generator, in this case HERWIG6.510, on a set of observables not depending on the hadronization results: a possibility would be, for example, to consider the jet observables, which are more related to cluster phase space distribution and

almost independent of the particles produced during the hadronization of the clusters themselves. After the completion of this preliminary tuning, the final one can be obtained considering a set of hadronization dependent observables, such as the single particle mean productions, dealing with a smaller set of parameters, namely the one strictly belonging to the hadronization model.

In the next section the results obtained in a set of runs with different MCSTHAR++ parameter configurations will be presented and discussed, showing the dependencies of the considered observables on the free parameters of the model.

4.4 Full hadronization analysis

As discussed in the previous sections, a final tuning of MCSTHAR++ is yet to be performed. Nevertheless a set of explorative runs, with various free parameter configurations, has been collected in order to discriminate at least approximatively which configuration provides a better agreement between theoretical predictions and experimental data. For each run the χ^2 has been computed independently for the event shape, single particle and multiplicity distributions listed in Sec. (4.1) in order to evaluate the capacity of the code to reproduce each different set of observables. For this set of runs the only parameters which have been varied are the MCSTHAR++'s free parameters γ_S, ρ and M_C, while the free parameters of HERWIG6.510 described in the previous section have been set to their default values. Each run is given by about 10^8 $e^+e^- \to Z^0/\gamma \to q\bar{q}$ collisions, with $q = u, d, s, c, b$. The experimental data used for the comparison come from the measurements of the LEP experiments ALEPH, DELPHI and OPAL, again for a center of mass energy of 91.2 GeV.

The first study performed on the χ^2 function is focused on its dependence on the M_C and ρ parameters, while the γ_S parameter has been fixed equal to 0.65: the obtained results are shown in Tab. (4.2).

Unfortunately, the obtained results did not show unambiguously which parameter configuration is able to give the better agreement between theoretical predictions and data. In particular, the setup $M_C = 1.6\ GeV$ and $\rho = 0.35\ GeV/fm^3$, which provides the smaller χ^2_{red} for the single particle distributions, is not the best one if the event shape distributions are considered, since in this case the better setup would be $M_C = 1.6\ GeV$ and $\rho = 0.45\ GeV/fm^3$. This parameter configuration is the one, among the considered set, which gives also the smaller total χ^2 value. Moreover the configuration which shows the best agreement for the particle multiplicity predictions, given by $M_C = 1.4\ GeV$ and $\rho = 0.45\ GeV/fm^3$, is also the one which gives the worst overall agreement with the experimental data. Some extra runs have been considered to investigate the behavior of the discrepancy as a function of the γ_S parameter, for the configurations showing the minimum χ^2 value. The results obtained moving this parameter are shown in Tab. (4.3), where it can be seen that for both the above configurations the γ_s value which gives the

$M_C(GeV)$	$\rho(GeV/fm^3)$	χ^2_{red} (ES)	χ^2_{red} (SP)	χ^2_{red} (PM)	χ^2_{red}
1.4	0.25	12.43	6.93	16.52	10.04
1.4	0.35	16.45	7.35	18.01	12.24
1.4	0.45	36.00	21.29	6.50	27.57
1.6	0.25	21.38	7.85	21.49	15.00
1.6	0.35	14.59	6.46	16.04	10.83
1.6	0.45	9.95	7.48	18.15	9.20
1.8	0.25	31.34	8.04	17.23	19.63
1.8	0.35	20.23	7.26	19.30	14.06
1.8	0.45	17.66	8.75	10.18	13.08

Table 4.2: Reduced χ^2 values for event shape (ES) and single particle (SP) distributions and for mean particle multiplicities (PM). The value of γ_S is set to 0.65. The corresponding number of degrees of freedom are 425, 420 and 41 respectively. The total reduced χ^2 value, for 890 degrees of freedom, is reported in the last column.

best agreement between theoretical predictions and experimental data is 0.65, namely the one considered in Tab. (4.2).

γ_S	$\rho(GeV/fm^3)$	χ^2_{red} (ES)	χ^2_{red} (SP)	χ^2_{red} (PM)	χ^2_{red}
0.60	0.35	16.41	6.55	18.44	11.86
0.65	0.35	14.59	6.46	16.04	10.83
0.70	0.35	31.01	12.90	8.72	21.34
0.55	0.45	11.25	6.94	25.63	9.94
0.60	0.45	10.86	6.55	23.25	9.45
0.65	0.45	9.95	7.48	18.15	9.20
0.675	0.45	11.85	5.88	20.17	9.45
0.70	0.45	18.92	6.15	14.41	12.67

Table 4.3: Reduced χ^2 values for event shape (ES) and single particle (SP) distributions and for mean particle multiplicities (PM). The value of M_C is set to 1.6 GeV.

In conclusion, the above analysis shows that the parameter setup able to give the best overall reproduction of the experimental data is $M_C = 1.6\ GeV$, $\rho = 0.45\ GeV/fm^3$ and $\gamma_S = 0.65$. The following plots and tables, which show in detail the comparison among `MCSTHAR++` predictions, `HERWIG6.510` predictions and LEP data, have been obtained with the previous parameter configuration. The definitions of the considered event shape observables can be found in the appendix, while for the single particle energy and momentum

distributions the analyzed observables are the scaled momentum

$$x_p = \frac{2 \mid \mathbf{p} \mid}{\sqrt{s}},$$

its logarithm

$$\xi_p = \log\left(\frac{1}{x_p}\right),$$

and the scaled energy

$$x_E = \frac{2E}{\sqrt{s}},$$

where $\mathbf{p}$ and E are respectively the 3-momentum and the energy of the considered particle and $\sqrt{s}$ the collision center of mass energy. The results obtained for the various sets of observables will be now discussed.

Event shape: the comparison between `MCSTHAR++` and LEP experimental data shows a quite good agreement for the whole set of considered observables, even if in some cases an higher statistics would be needed to completely understand the behavior of the new hadronization code, in particular for some points in the thrust minor (Fig. (4.5)), aplanarity (Fig. (4.14)), D-parameter (Fig. (4.17)) and M_d (Fig. (4.20)) distributions. In other cases, for example for the transverse momentum and rapidity distributions of Figs. (4.6)-(4.8) and (4.10)-(4.12) and for the planarity distribution (Fig. (4.13)), the agreement between theoretical predictions and data is appreciable, in particular for the points located in the maximum zone of the distributions. While for some of these observables, namely the transverse momentum observables, `MCSTHAR++` fails to reproduce the distribution tail behavior of the experimental data which is correctly predicted by `HERWIG6.510`.

Single particle: also in this case a good agreement between `MCSTHAR++` predictions and LEP data is present for a large set of the considered single particle observables, in particular for $\pi^{\pm}$ momentum distribution (Fig. (4.24)), π^0, ω, $\rho^{\pm}$, $a_0^{\pm}$, η and η' scaled energy and momentum distributions (Figs. (4.27)-(4.32) and (4.37)-(4.42)) as well as for $\Sigma^{*\pm}$, ρ^0 scaled energy distributions (Figs. (4.45)-(4.47)) and for f_2 scaled momentum distribution (Fig. (4.52)), with a better agreement near the maximum of the plotted distributions. On the other hand, a wrong behavior of the theoretical predictions can be seen in the D^0 and D^* scaled energy distributions (Figs. (4.48)-(4.49)): in these cases also `HERWIG`'s predictions show a disagreement with the experimental data, however the cluster model seems to be able to reproduce the general behavior of these data better than `MCSTHAR++`.

Charged particle multiplicity: in this case the agreement between the

theoretical predictions of the microcanonical model and the experimental data is almost perfect, with the exception of a low statistics point with a large error, compatible with the experimental data, which would need higher statistics to confirm the goodness of the corresponding prediction. It is worth noting that for this distribution, in particular looking at the distribution tails, the predictions of `MCSTHAR++` show a better agreement with the experimental data with respect to `HERWIG6.510`'s results.

Particle multiplicities: the comparison on the mean particle multiplicities (Tabs. (4.4) and (4.5)), for this preliminary tuning, shows a better agreement with experimental data for `MCSTHAR++` predictions, with respect of `HERWIG6.510` results, in the 70% of the considered multiplicities. Moreover the discrepancies of the new hadronization module results with respect to LEP data are smaller than 3σ in the 72% of the reported measurements, a percentage which becomes 100% if only the charmed and bottomed hadrons are considered.

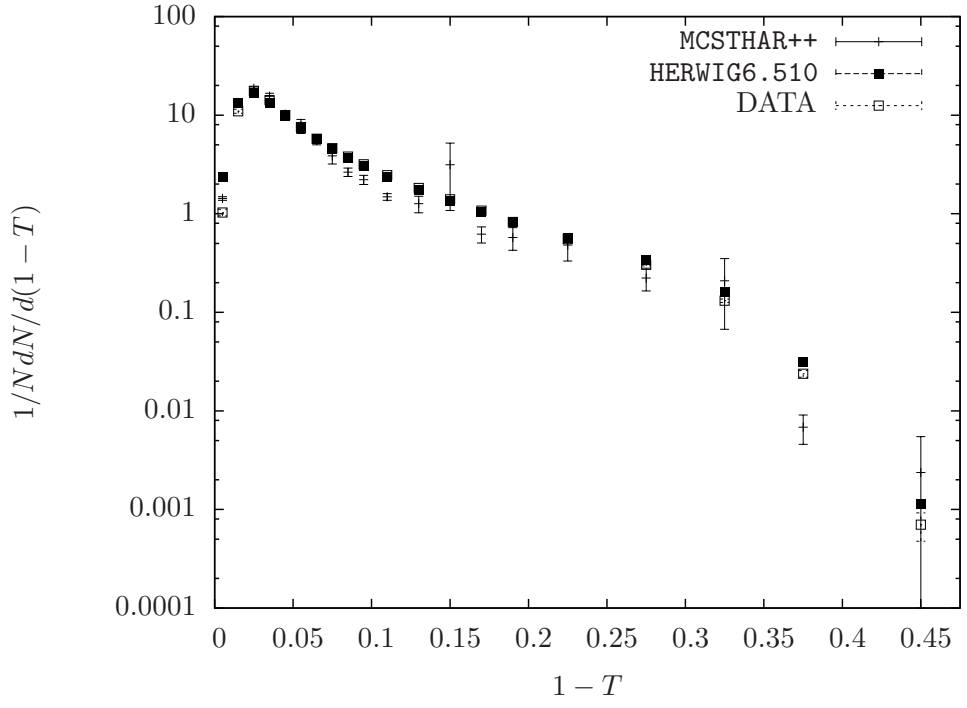

Figure 4.3: Thrust (T) distribution: comparison among `MCSTHAR++`, `HERWIG6.510` and DELPHI data [42] at 91.2 GeV center of mass energy.

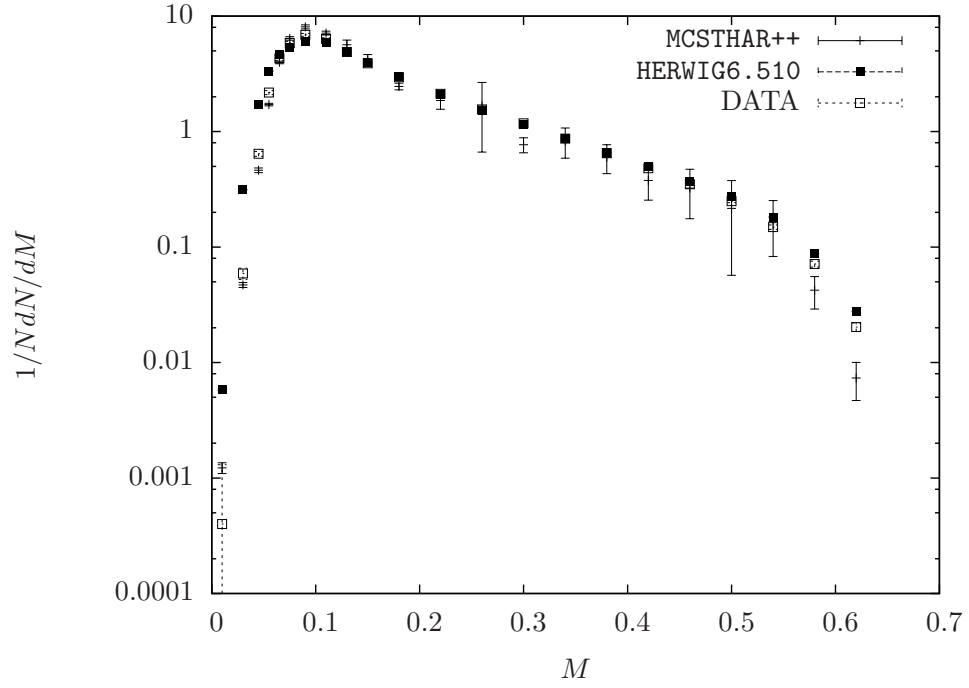

Figure 4.4: Thrust major (M) distribution: comparison among `MCSTHAR++`, `HERWIG6.510` and DELPHI data [42] at 91.2 GeV center of mass energy.

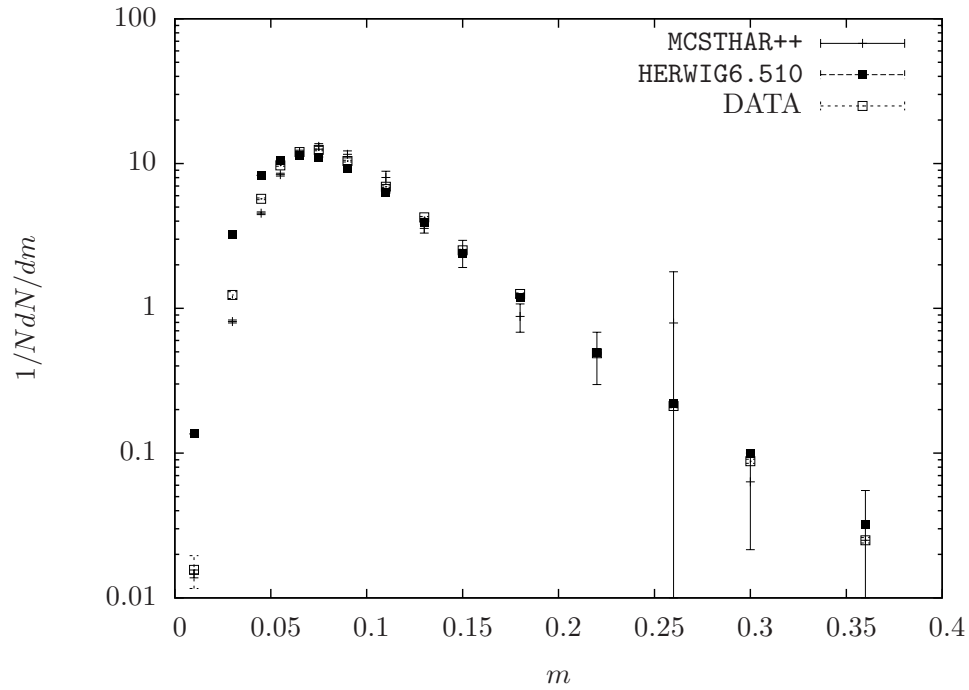

Figure 4.5: Thrust minor (m) distribution: comparison among `MCSTHAR++`, `HERWIG6.510` and DELPHI data [42] at 91.2 GeV center of mass energy.

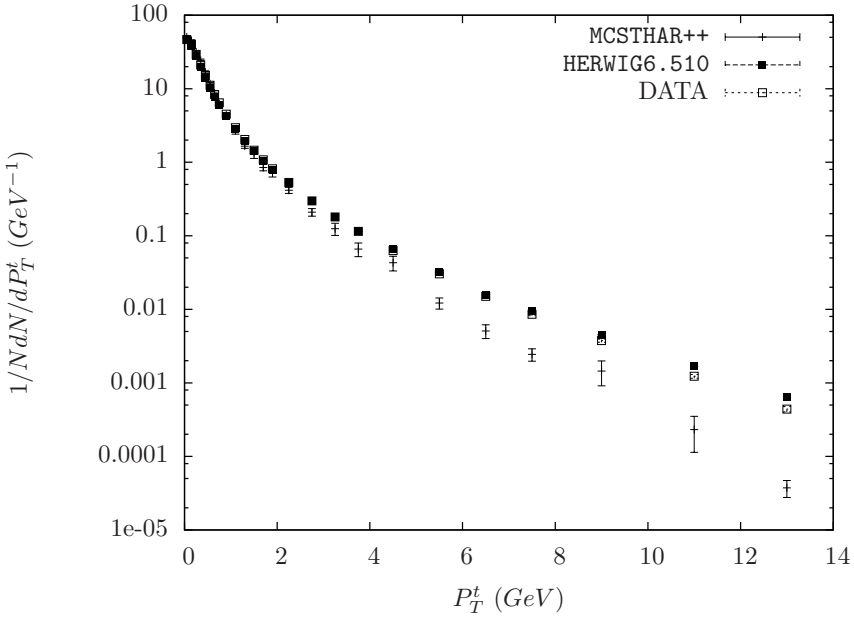

Figure 4.6: Transverse momentum (in) with respect to thrust axis (P_t^T) distribution: comparison among `MCSTHAR++`, `HERWIG6.510` and DELPHI data [42] at 91.2 GeV center of mass energy.

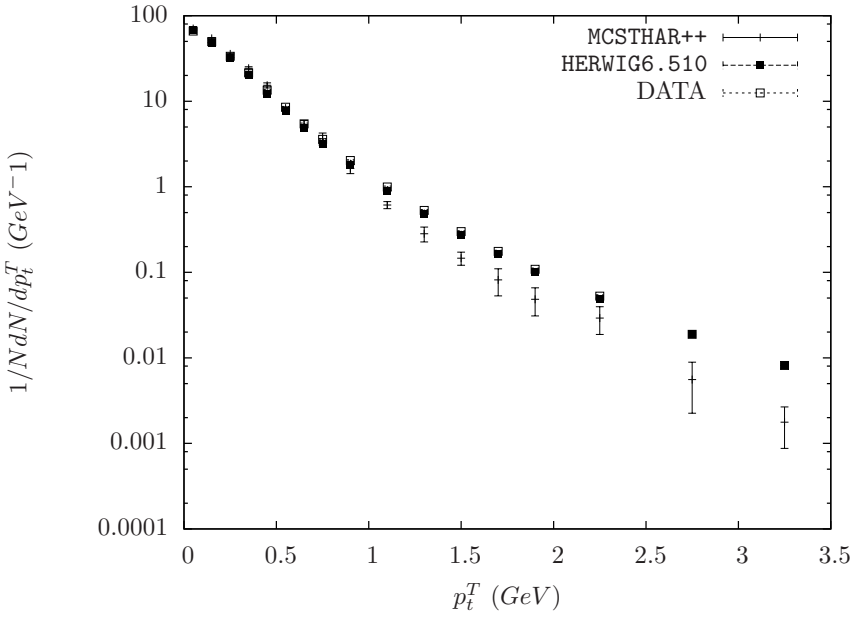

Figure 4.7: Transverse momentum (out) with respect to thrust axis (p_t^T) distribution: comparison among `MCSTHAR++`, `HERWIG6.510` and DELPHI data [42] at 91.2 GeV center of mass energy.

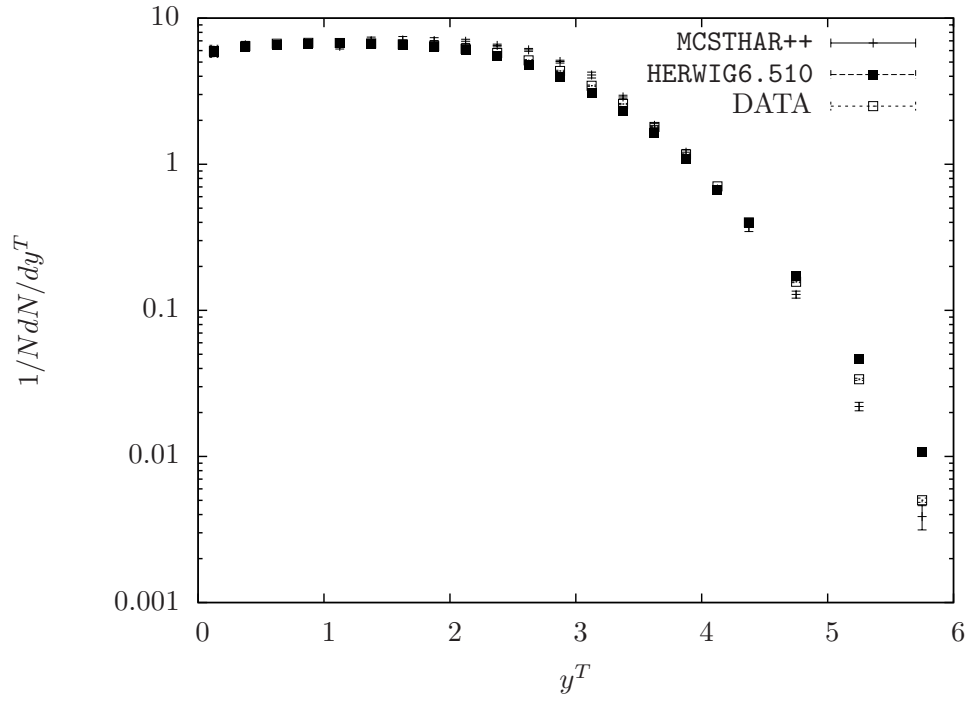

Figure 4.8: Rapidity with respect to thrust axis (y^T) distribution: comparison among `MCSTHAR++`, `HERWIG6.510` and DELPHI data [42] at 91.2 GeV center of mass energy.

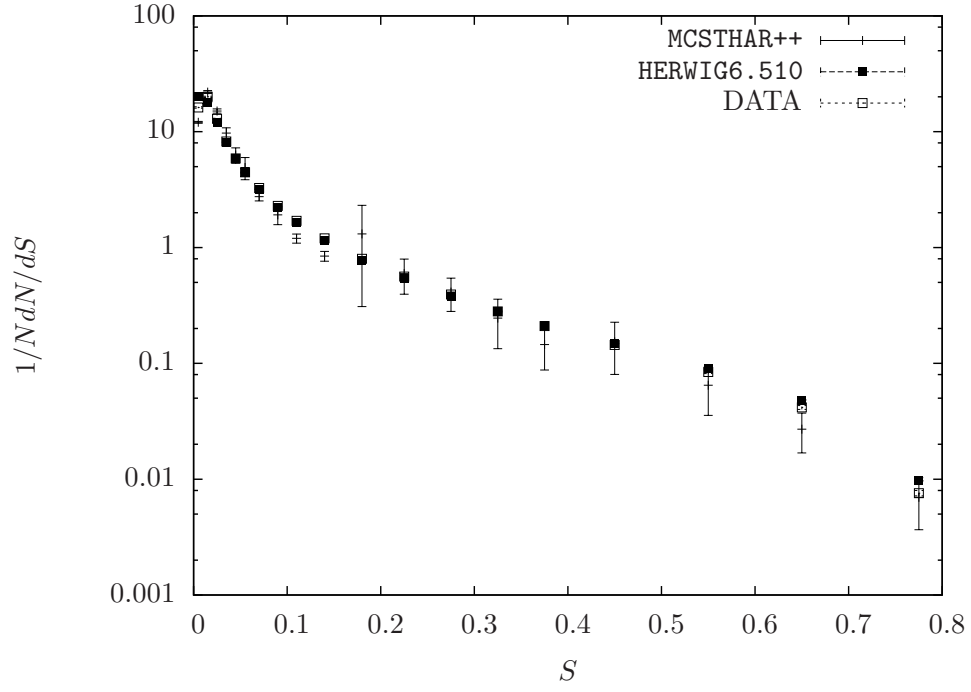

Figure 4.9: Sphericity (S) distribution: comparison among `MCSTHAR++`, `HERWIG6.510` and DELPHI data [42] at 91.2 GeV center of mass energy.

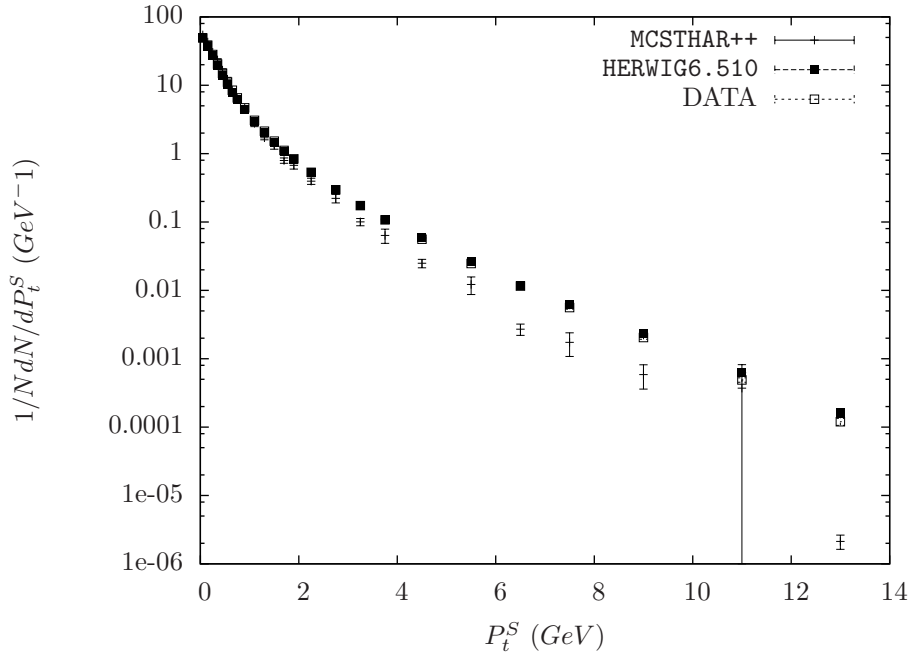

Figure 4.10: Transverse momentum (in) with respect to sphericity axis (P_t^S) distribution: comparison among `MCSTHAR++`, `HERWIG6.510` and DELPHI data [42] at 91.2 GeV center of mass energy.

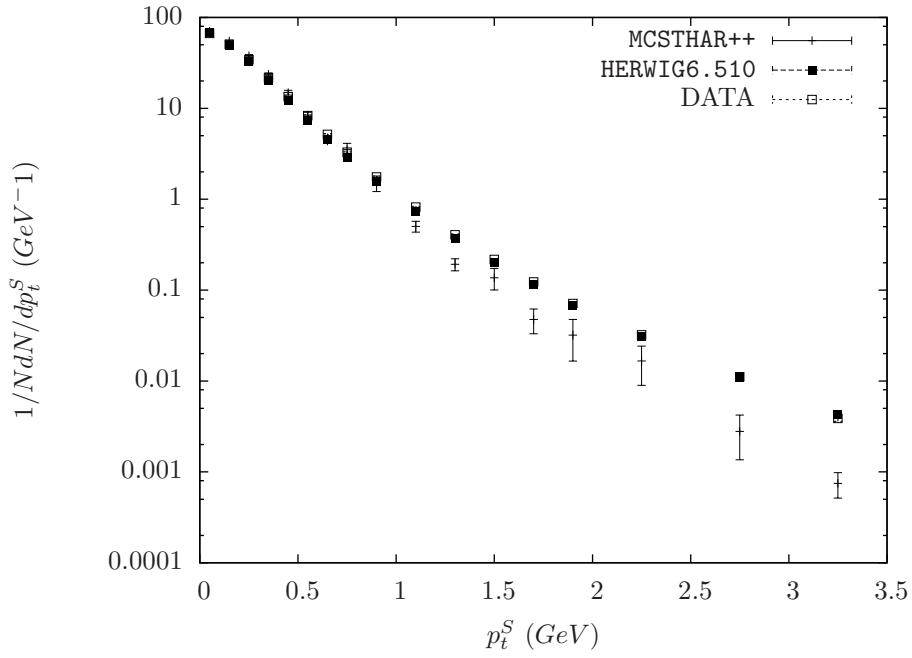

Figure 4.11: Transverse momentum (out) with respect to sphericity axis (p_t^S) distribution: comparison among `MCSTHAR++`, `HERWIG6.510` and DELPHI data [42] at 91.2 GeV center of mass energy.

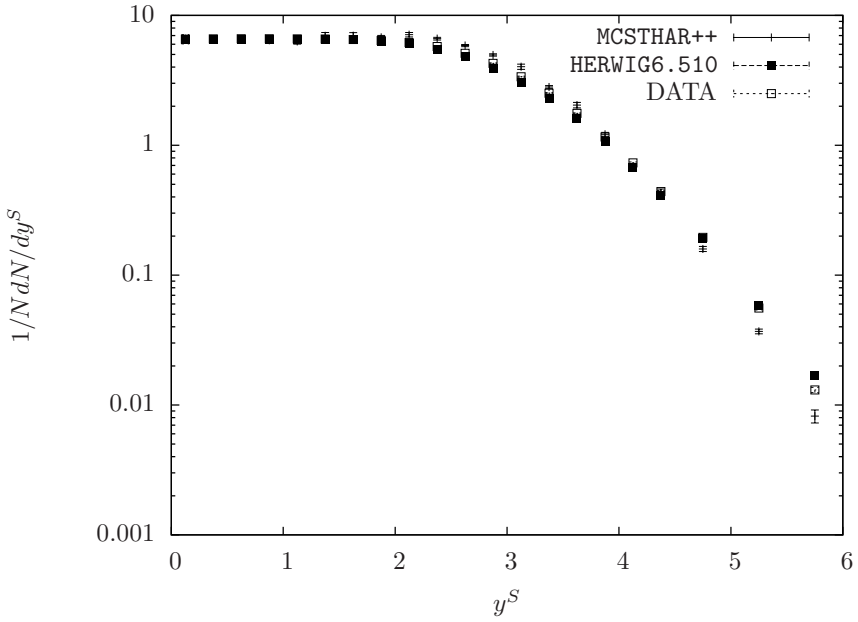

Figure 4.12: Rapidity with respect to sphericity axis (y^S) distribution: comparison among `MCSTHAR++`, `HERWIG6.510` and DELPHI data [42] at 91.2 GeV center of mass energy.

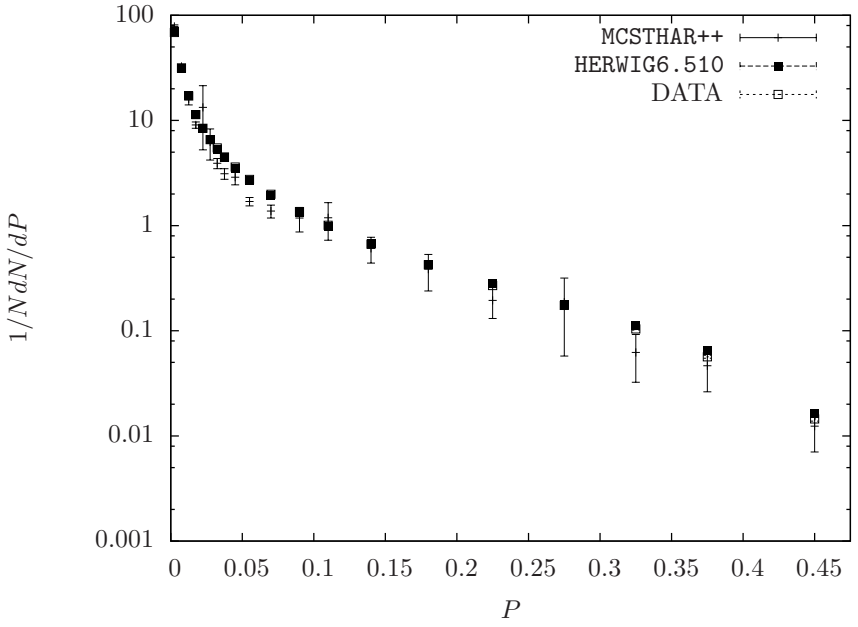

Figure 4.13: Planarity (P) distribution: comparison among `MCSTHAR++`, `HERWIG6.510` and DELPHI data [42] at 91.2 GeV center of mass energy.

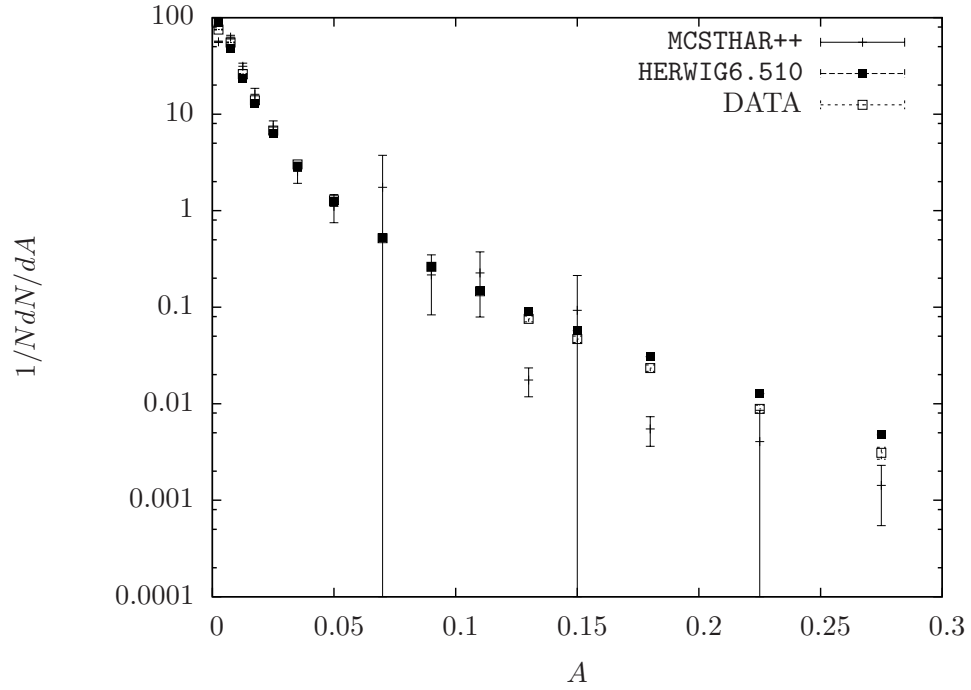

Figure 4.14: Aplanarity (A) distribution: comparison among `MCSTHAR++`, `HERWIG6.510` and DELPHI data [42] at 91.2 GeV center of mass energy.

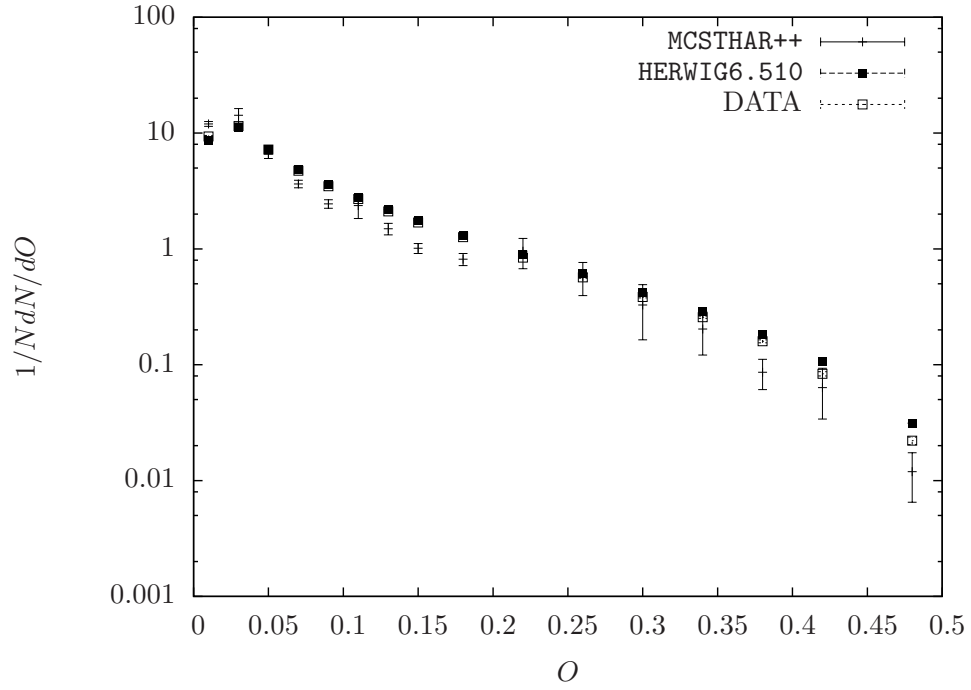

Figure 4.15: Oblateness (O) distribution: comparison among `MCSTHAR++`, `HERWIG6.510` and DELPHI data [42] at 91.2 GeV center of mass energy.

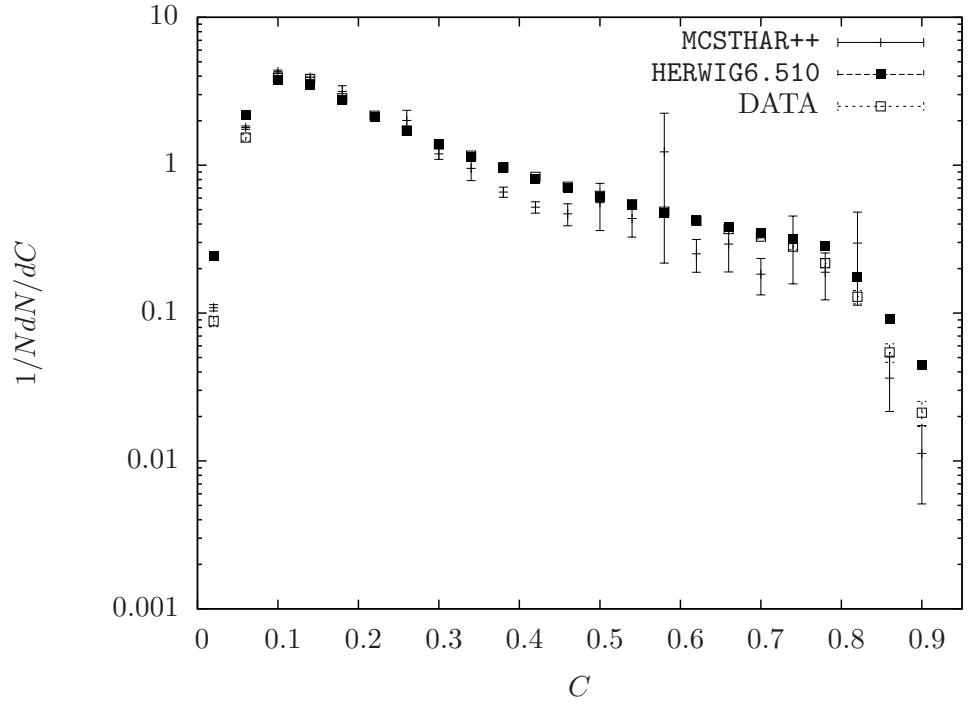

Figure 4.16: C-parameter (C) distribution: comparison among `MCSTHAR++`, `HERWIG6.510` and DELPHI data [42] at 91.2 GeV center of mass energy.

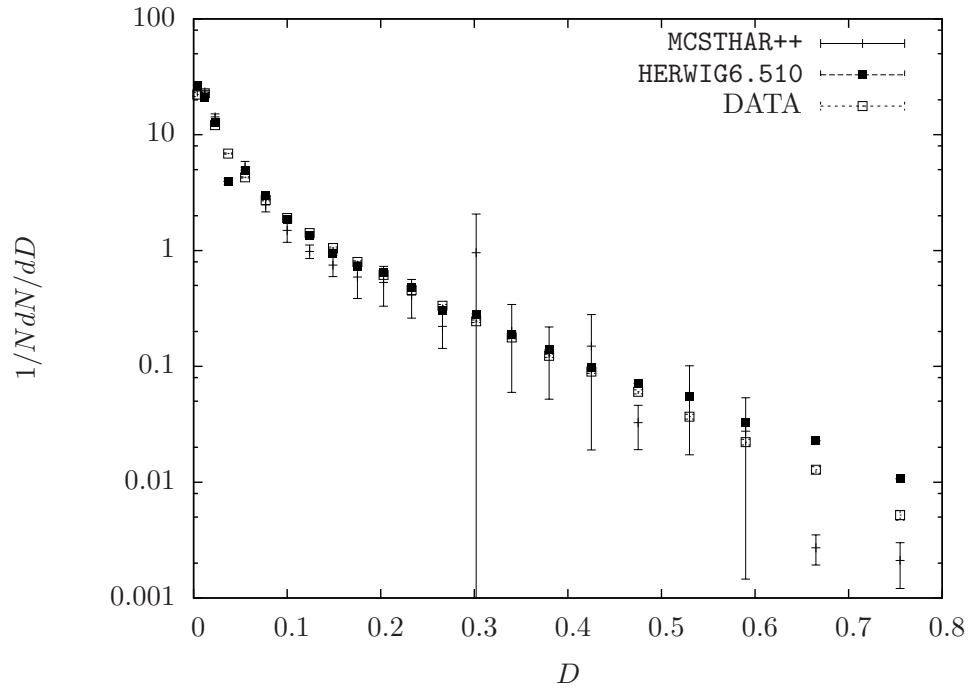

Figure 4.17: D-parameter (D) distribution: comparison among `MCSTHAR++`, `HERWIG6.510` and DELPHI data [42] at 91.2 GeV center of mass energy.

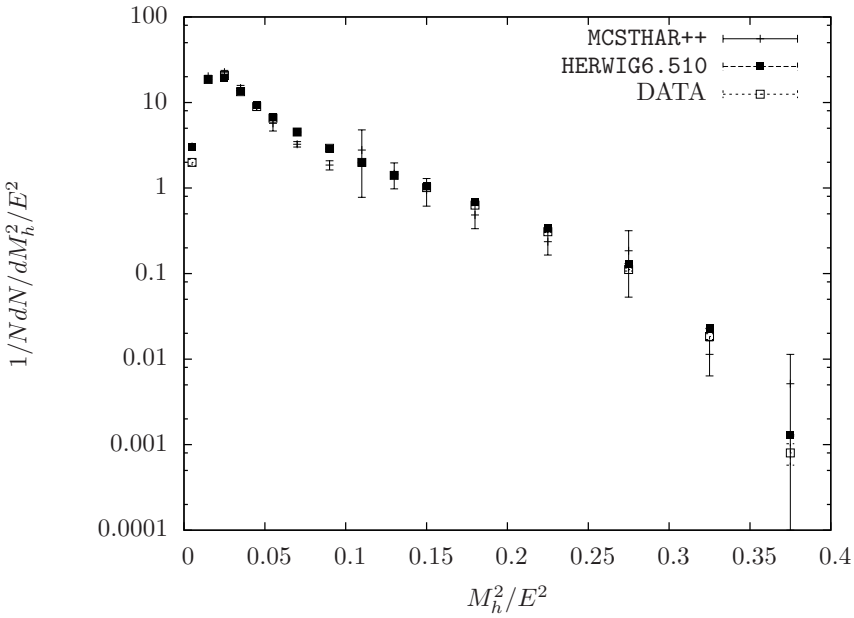

Figure 4.18: Heavy hemisphere mass (M_h) distribution: comparison among `MCSTHAR++`, `HERWIG6.510` and DELPHI data [42] at 91.2 GeV center of mass energy.

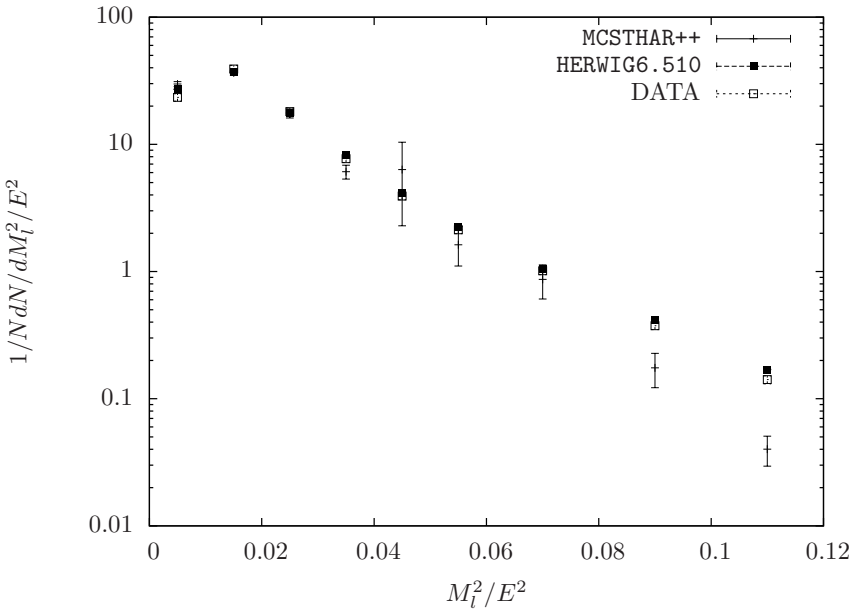

Figure 4.19: Light hemisphere mass (M_l) distribution: comparison among `MCSTHAR++`, `HERWIG6.510` and DELPHI data [42] at 91.2 GeV center of mass energy.

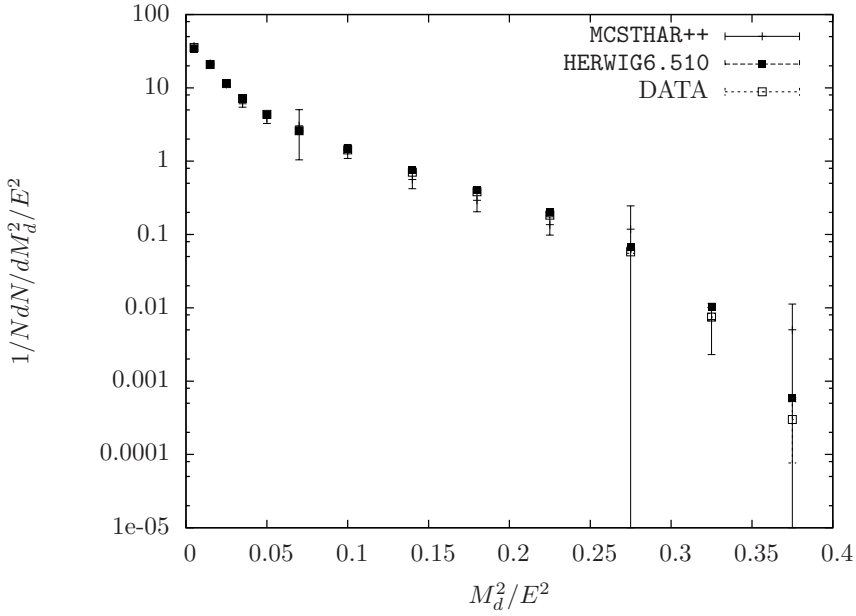

Figure 4.20: Difference of hemisphere masses (M_d) distribution: comparison among `MCSTHAR++`, `HERWIG6.510` and DELPHI data [42] at 91.2 GeV center of mass energy.

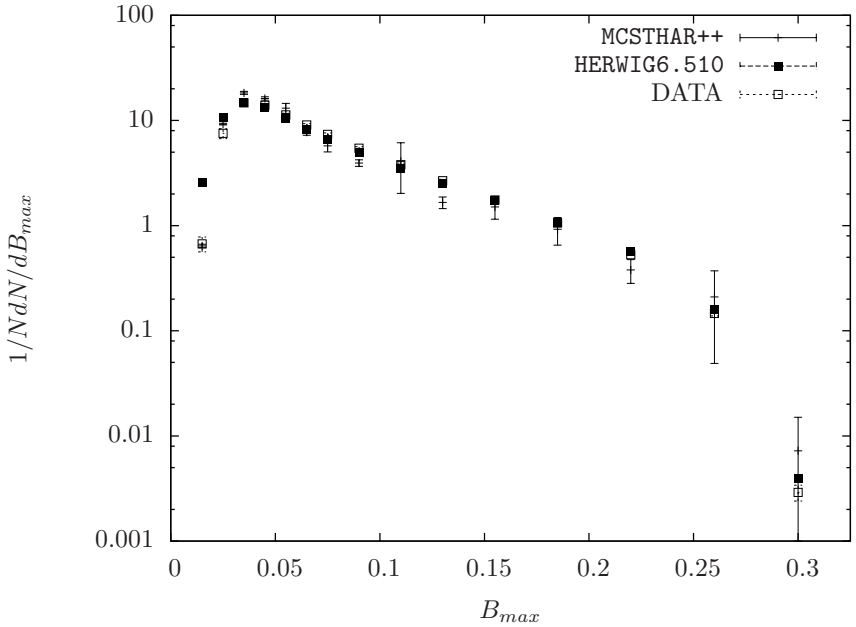

Figure 4.21: Wide hemisphere broadenind (B_{max}) distribution: comparison among `MCSTHAR++`, `HERWIG6.510` and DELPHI data [42] at 91.2 GeV center of mass energy.

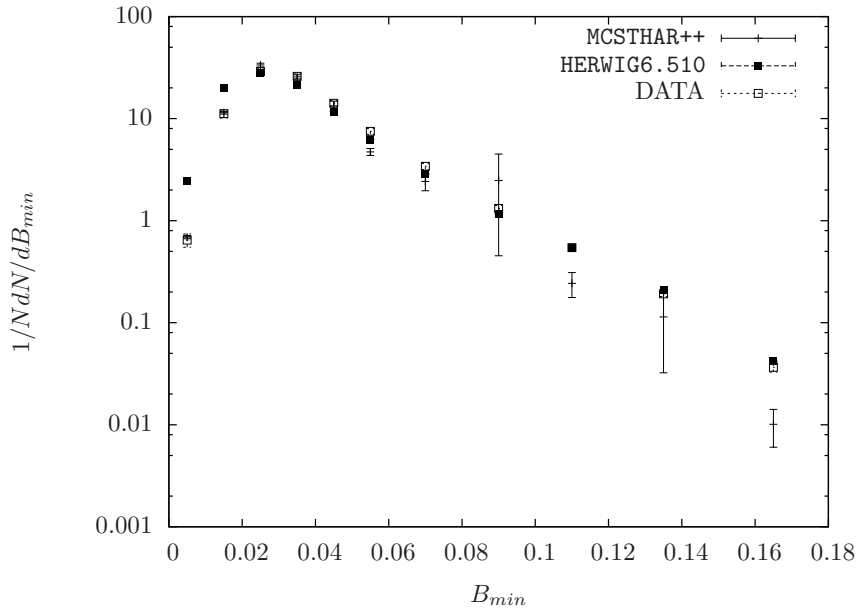

Figure 4.22: Narrow hemisphere broadenind (B_{max}) distribution: comparison among `MCSTHAR++`, `HERWIG6.510` and DELPHI data [42] at 91.2 GeV center of mass energy.

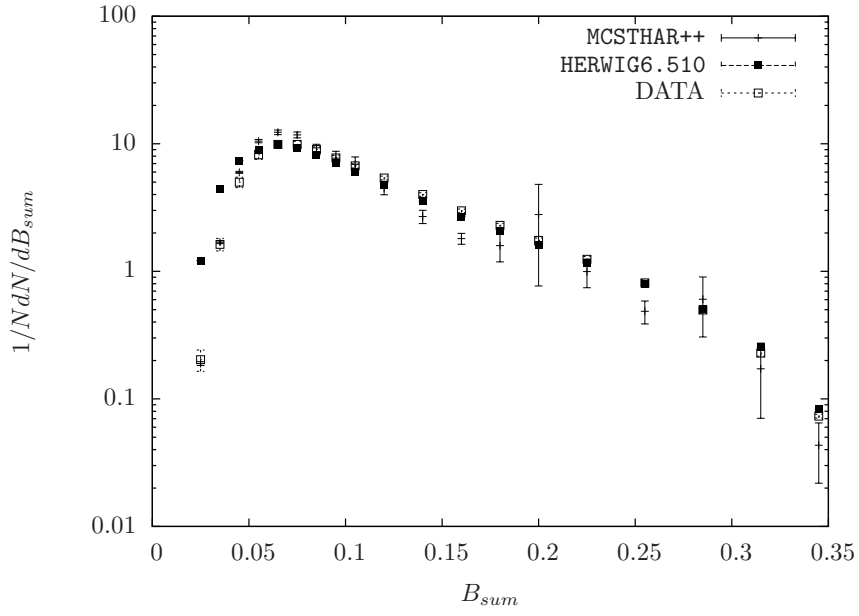

Figure 4.23: Sum of hemisphere broadenings (B_{sum}) distribution: comparison among `MCSTHAR++`, `HERWIG6.510` and DELPHI data [42] at 91.2 GeV center of mass energy.

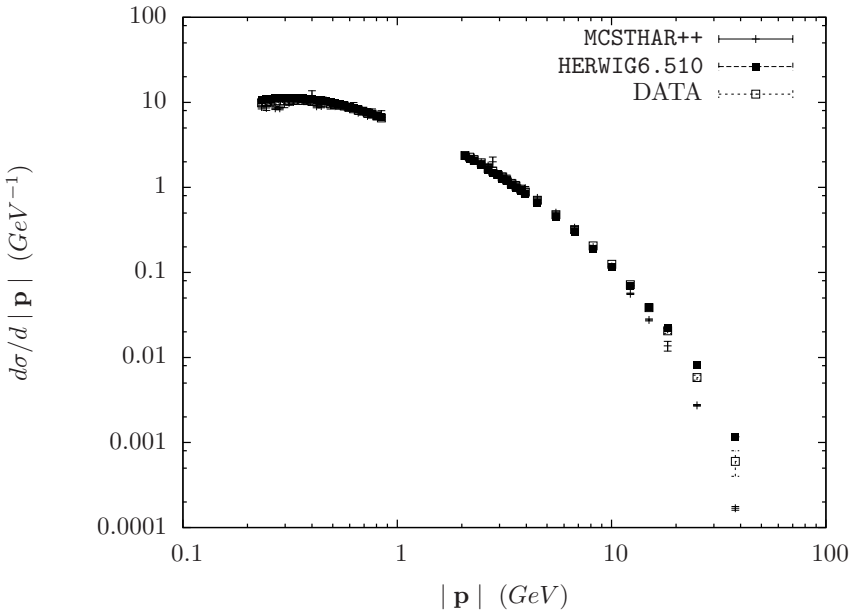

Figure 4.24: Charged pion momentum ($|\,\mathbf{p}\,|$) distribution: comparison among `MCSTHAR++`, `HERWIG6.510` and OPAL data [43] at 91.2 GeV center of mass energy.

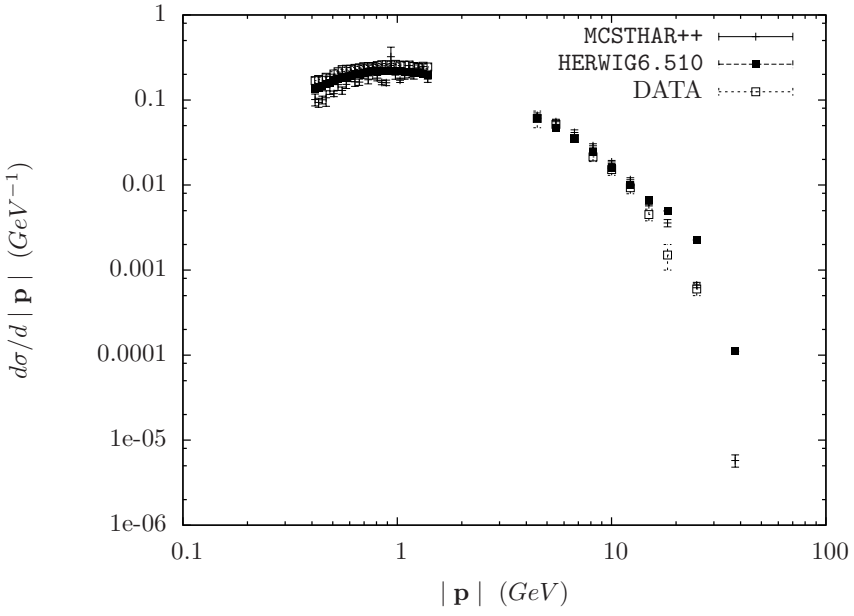

Figure 4.25: Proton momentum ($|\;\mathbf{p}\;|$) distribution: comparison among `MCSTHAR++`, `HERWIG6.510` and OPAL data [43] at 91.2 GeV center of mass energy.

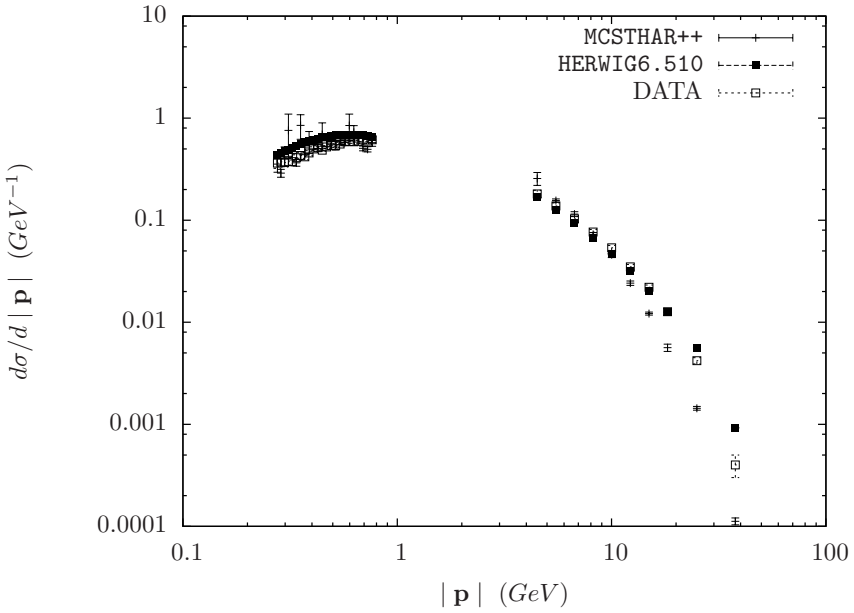

Figure 4.26: Charged kaon momentum (| **p** |) distribution: comparison among `MCSTHAR++`, `HERWIG6.510` and OPAL data [43] at 91.2 GeV center of mass energy.

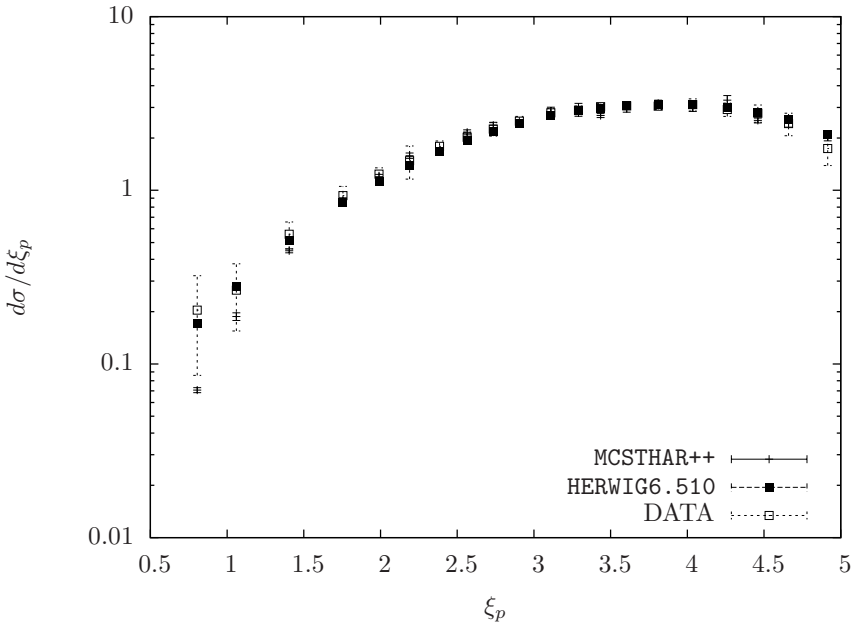

Figure 4.27: π^0 scaled momentum (ξ_p) distribution: comparison among `MCSTHAR++`, `HERWIG6.510` and OPAL data [49] at 91.2 GeV center of mass energy.

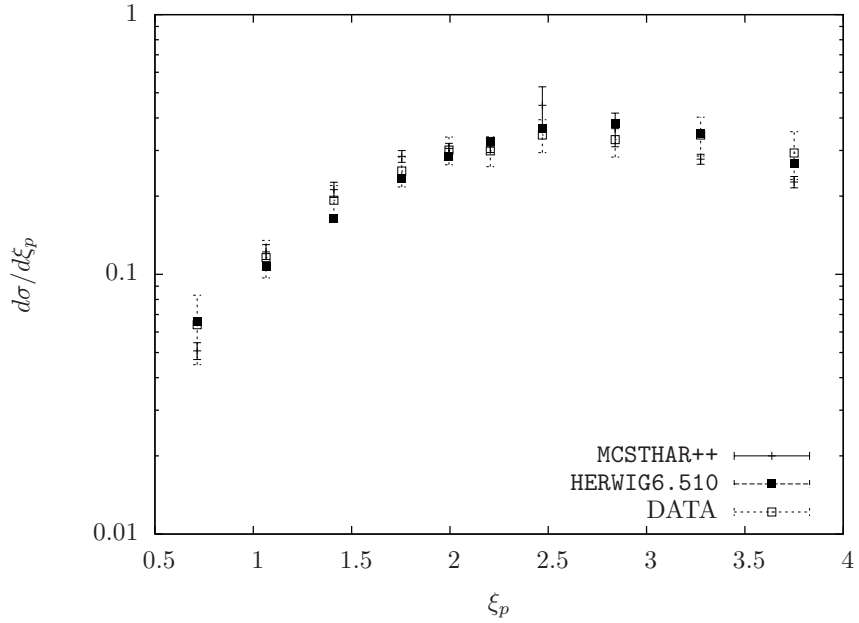

Figure 4.28: ω scaled momentum (ξ_p) distribution: comparison among `MCSTHAR++`, `HERWIG6.510` and OPAL data [49] at 91.2 GeV center of mass energy.

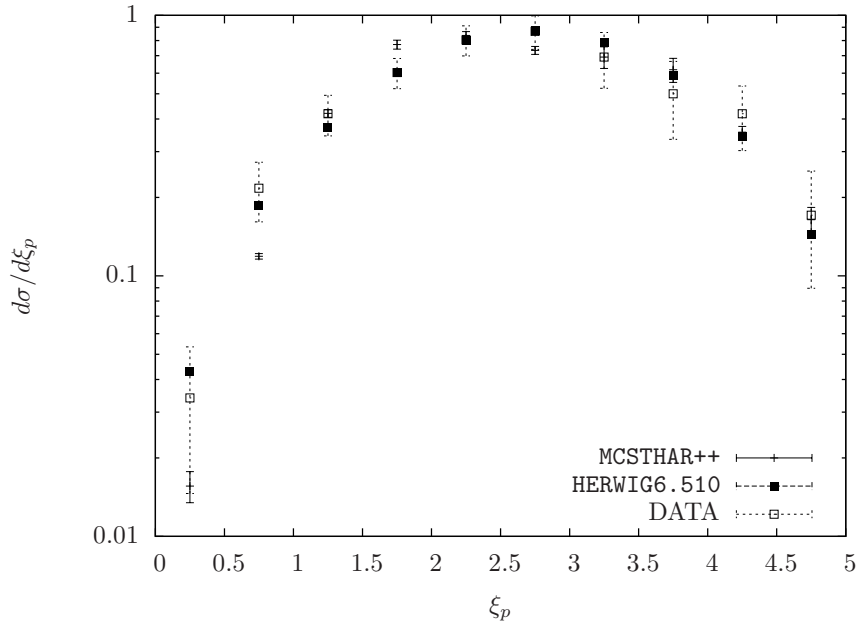

Figure 4.29: $\rho^{\pm}$ scaled momentum (ξ_p) distribution: comparison among `MCSTHAR++`, `HERWIG6.510` and OPAL data [49] at 91.2 GeV center of mass energy.

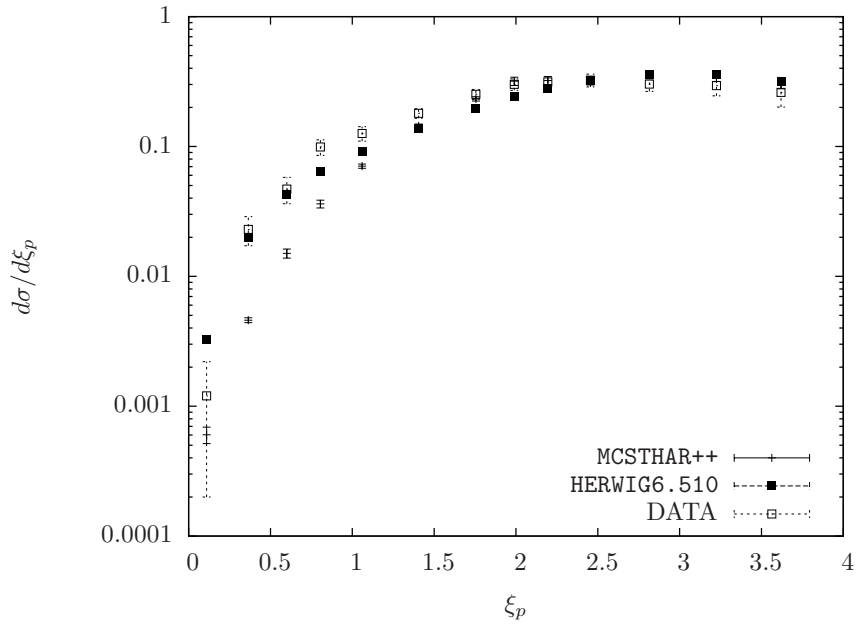

Figure 4.30: η scaled momentum (ξ_p) distribution: comparison among `MCSTHAR++`, `HERWIG6.510` and OPAL data [49] at 91.2 GeV center of mass energy.

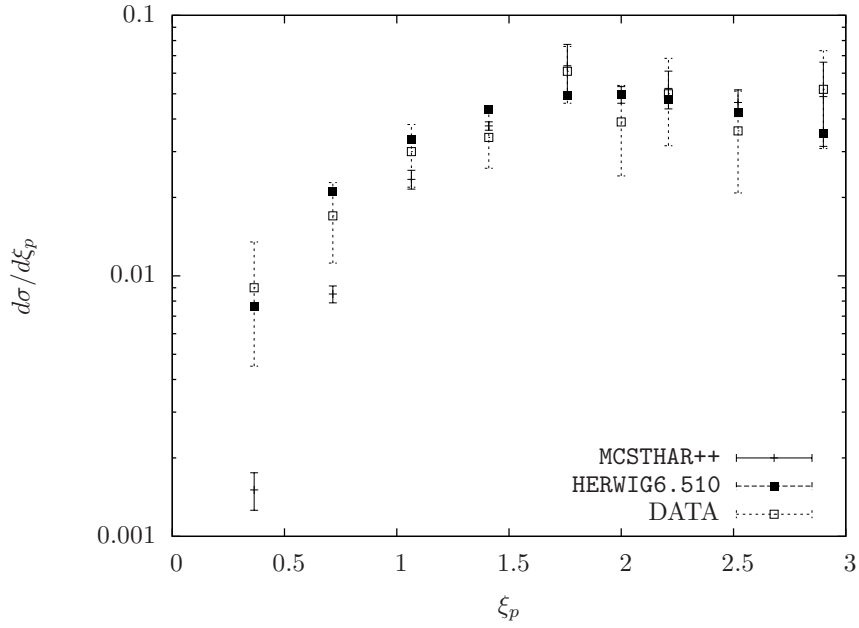

Figure 4.31: η' scaled momentum (ξ_p) distribution: comparison among `MCSTHAR++`, `HERWIG6.510` and OPAL data [49] at 91.2 GeV center of mass energy.

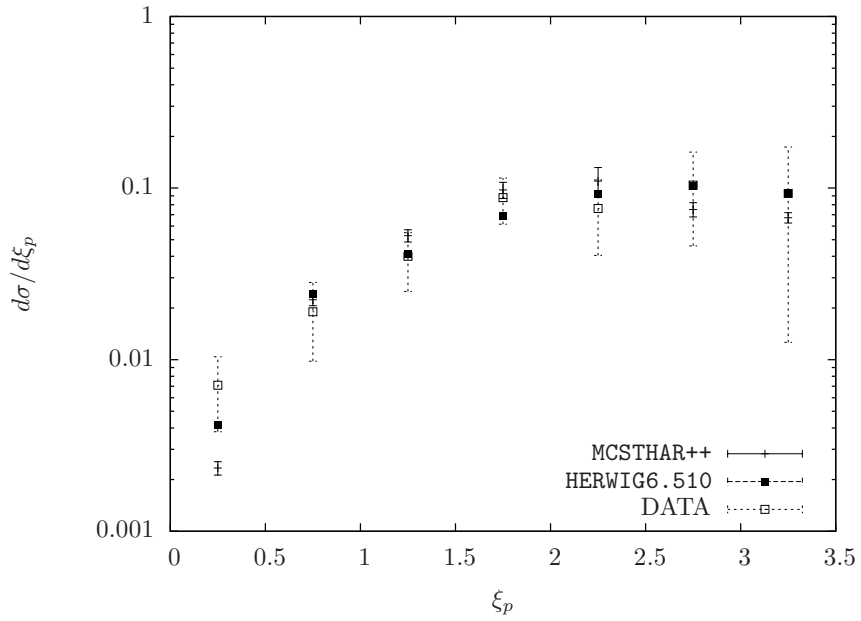

Figure 4.32: $a_0^{\pm}$ scaled momentum (ξ_p) distribution: comparison among `MCSTHAR++`, `HERWIG6.510` and OPAL data [49] at 91.2 GeV center of mass energy.

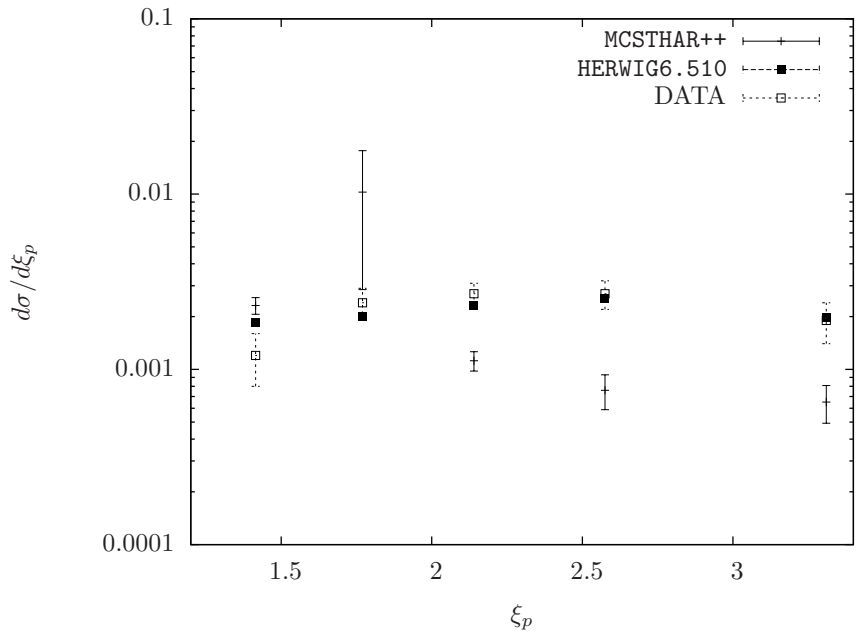

Figure 4.33: Ξ^{*0} scaled momentum (ξ_p) distribution: comparison among `MCSTHAR++`, `HERWIG6.510` and OPAL data [45] at 91.2 GeV center of mass energy.

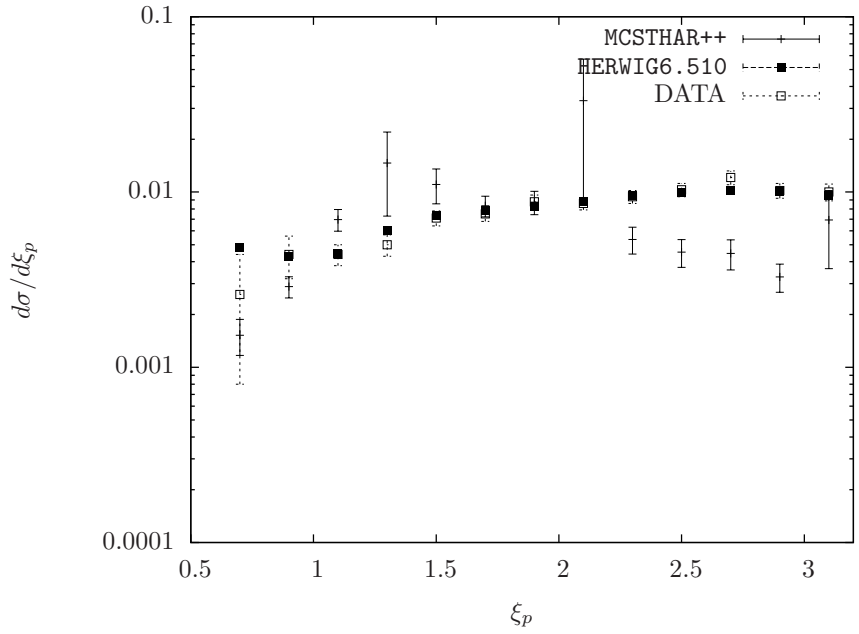

Figure 4.34: Ξ^- scaled momentum (ξ_p) distribution: comparison among `MCSTHAR++`, `HERWIG6.510` and OPAL data [45] at 91.2 GeV center of mass energy.

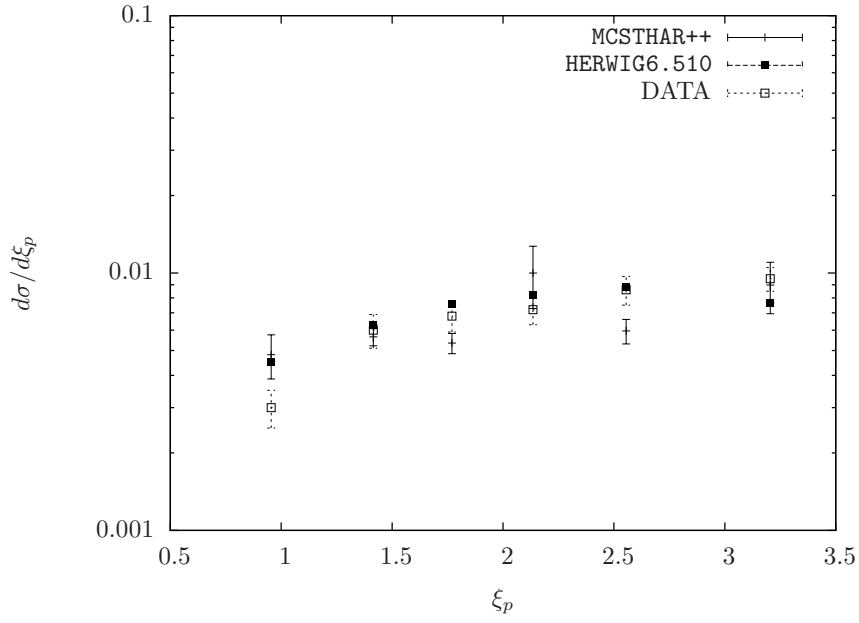

Figure 4.35: Σ^{*+} scaled momentum (ξ_p) distribution: comparison among `MCSTHAR++`, `HERWIG6.510` and OPAL data [45] at 91.2 GeV center of mass energy.

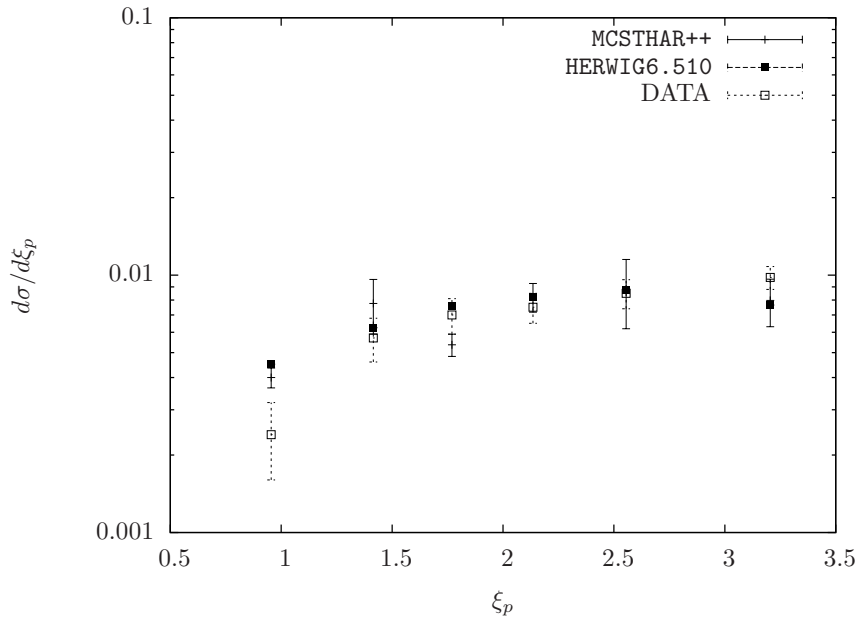

Figure 4.36: Σ^{*-} scaled momentum (ξ_p) distribution: comparison among `MCSTHAR++`, `HERWIG6.510` and OPAL data [45] at 91.2 GeV center of mass energy.

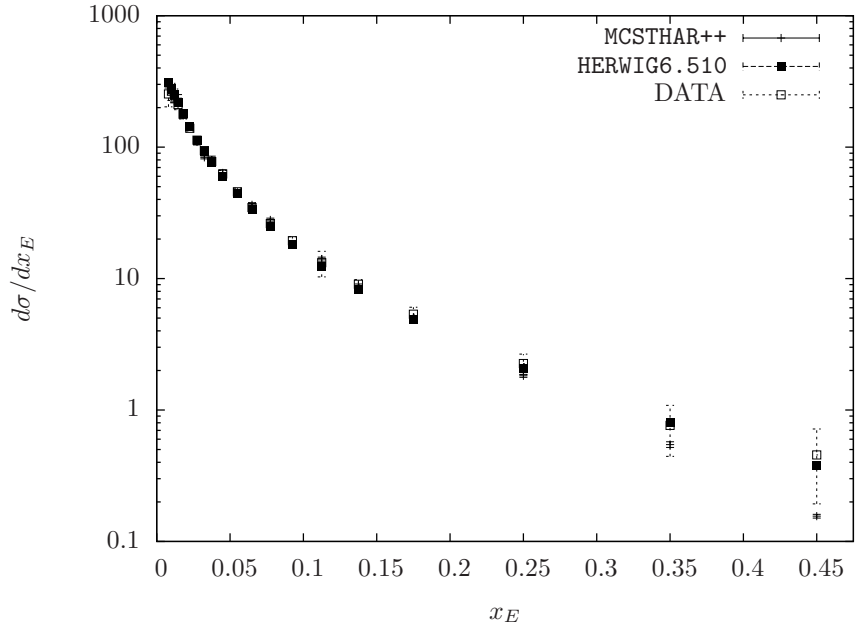

Figure 4.37: π^0 scaled energy (x_E) distribution: comparison among `MCSTHAR++`, `HERWIG6.510` and OPAL data [49] at 91.2 GeV center of mass energy.

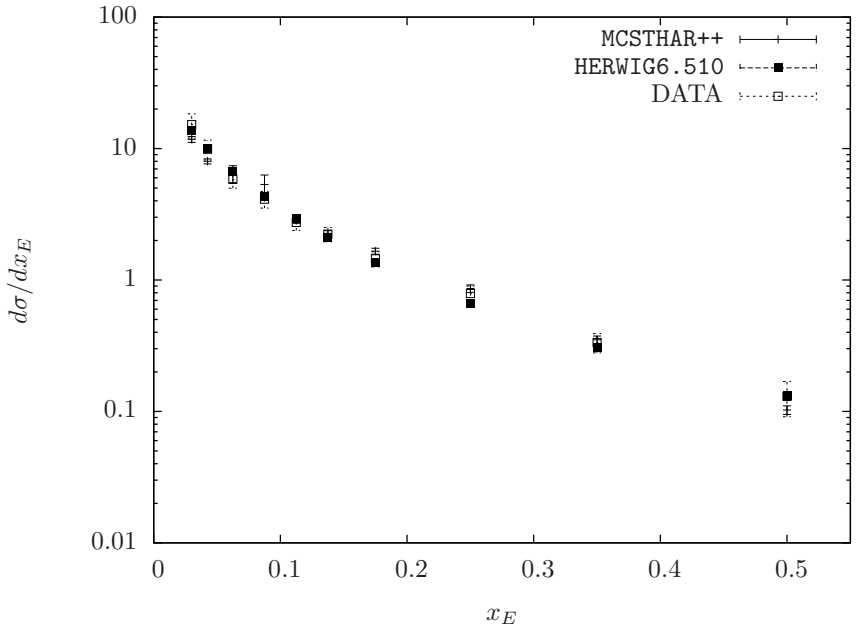

Figure 4.38: ω scaled energy (x_E) distribution: comparison among `MCSTHAR++`, `HERWIG6.510` and OPAL data [49] at 91.2 GeV center of mass energy.

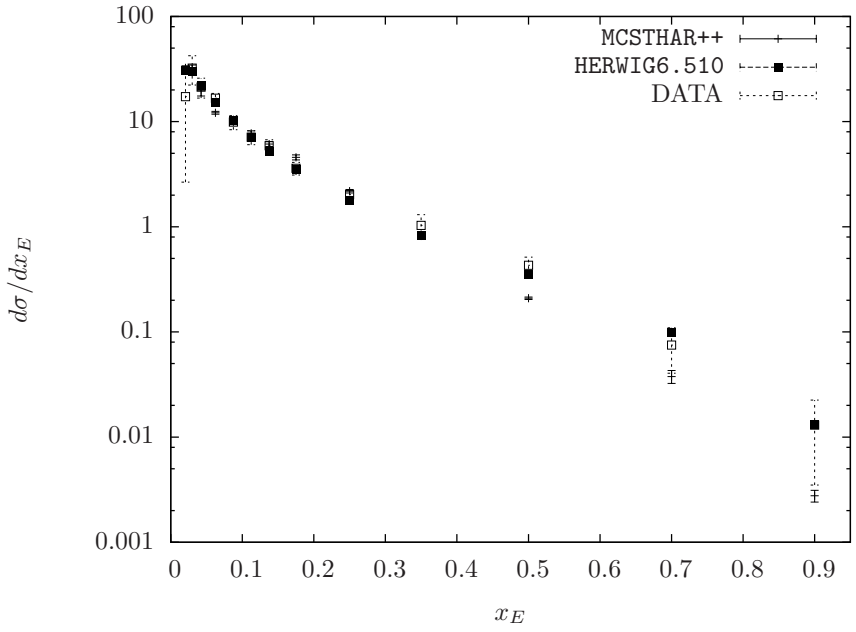

Figure 4.39: $\rho^{\pm}$ scaled energy (x_E) distribution: comparison among `MCSTHAR++`, `HERWIG6.510` and OPAL data [49] at 91.2 GeV center of mass energy.

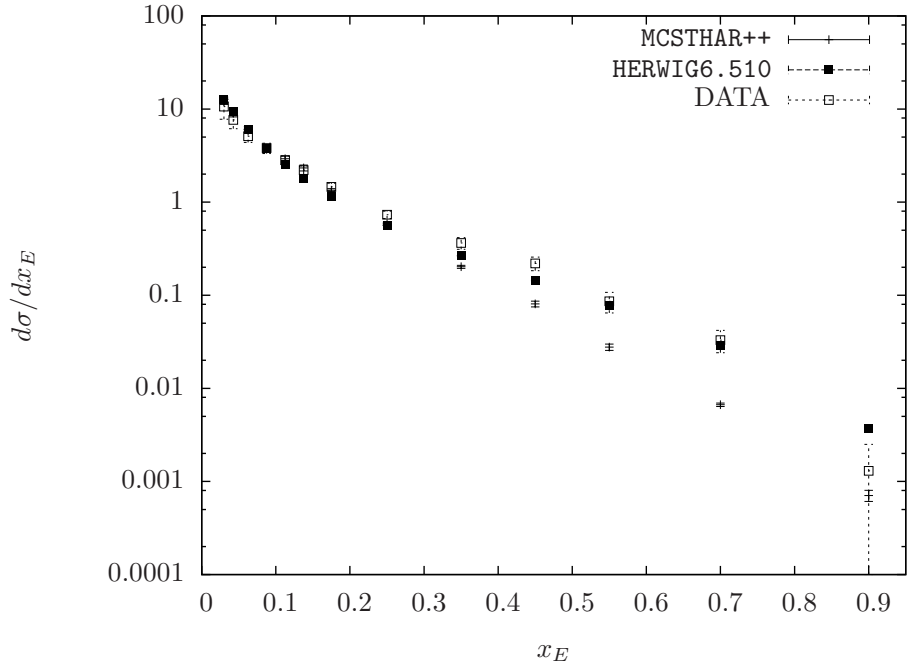

Figure 4.40: η scaled energy (x_E) distribution: comparison among `MCSTHAR++`, `HERWIG6.510` and OPAL data [49] at 91.2 GeV center of mass energy.

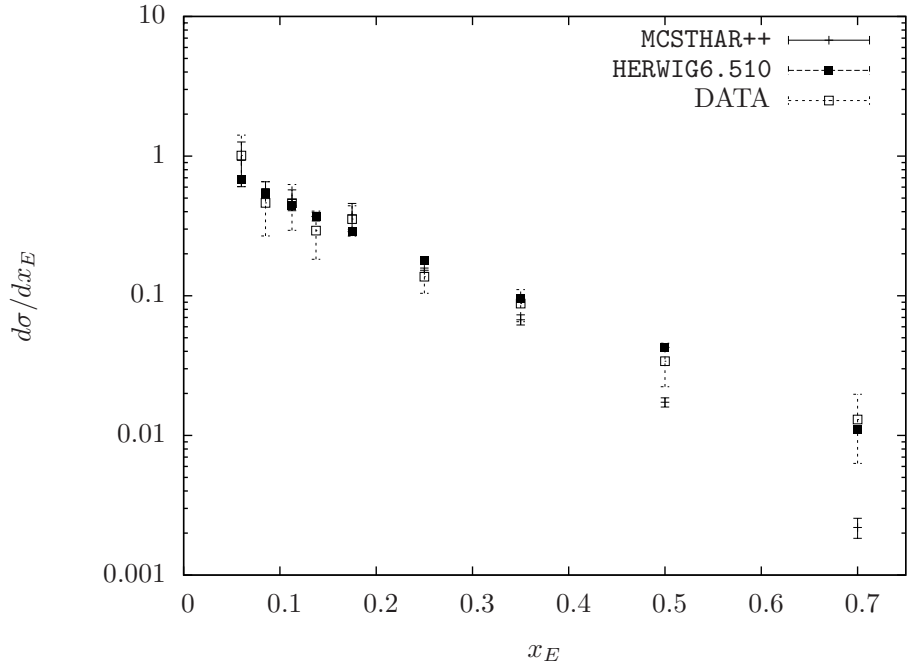

Figure 4.41: η' scaled energy x_E distribution: comparison among `MCSTHAR++`, `HERWIG6.510` and OPAL data [49] at 91.2 GeV center of mass energy.

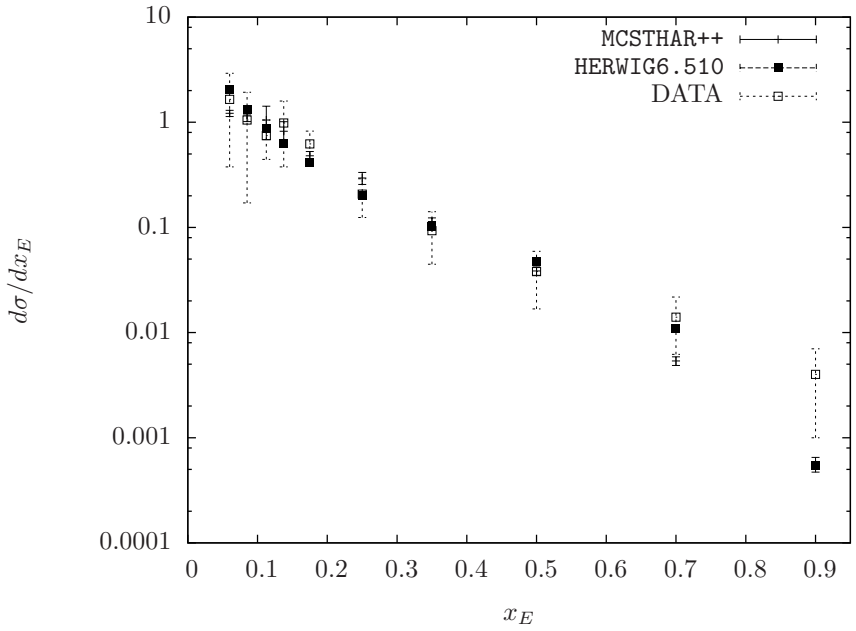

Figure 4.42: $a_0^{\pm}$ scaled energy (x_E) distribution: comparison among `MCSTHAR++`, `HERWIG6.510` and OPAL data [49] at 91.2 GeV center of mass energy.

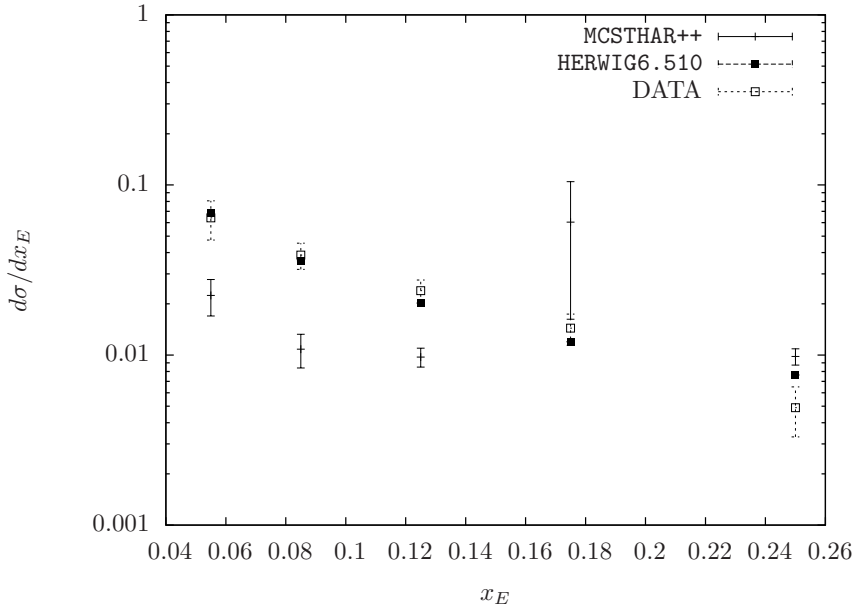

Figure 4.43: Ξ^{*0} scaled energy (x_E) distribution: comparison among `MCSTHAR++`, `HERWIG6.510` and OPAL data [45] at 91.2 GeV center of mass energy.

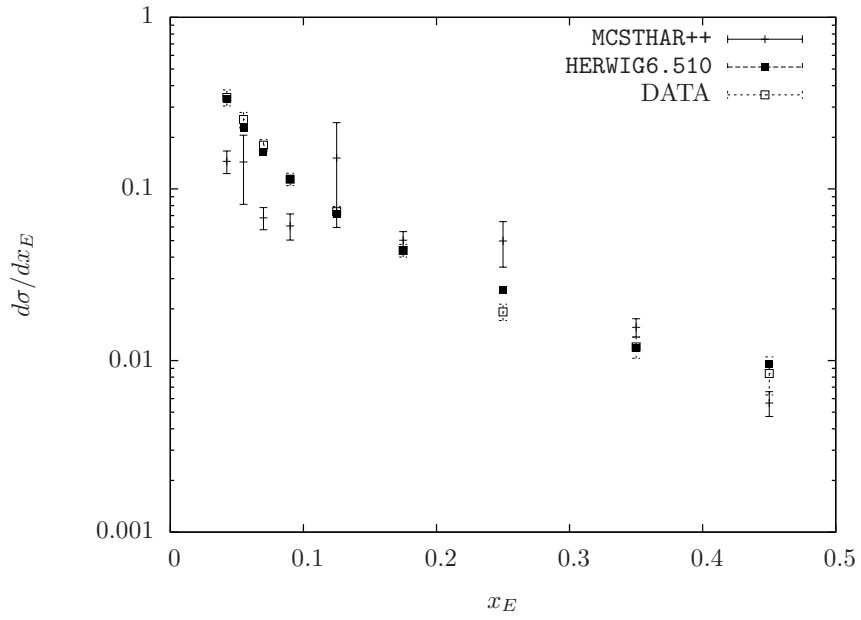

Figure 4.44: Ξ^- scaled energy (x_E) distribution: comparison among `MCSTHAR++`, `HERWIG6.510` and OPAL data [45] at 91.2 GeV center of mass energy.

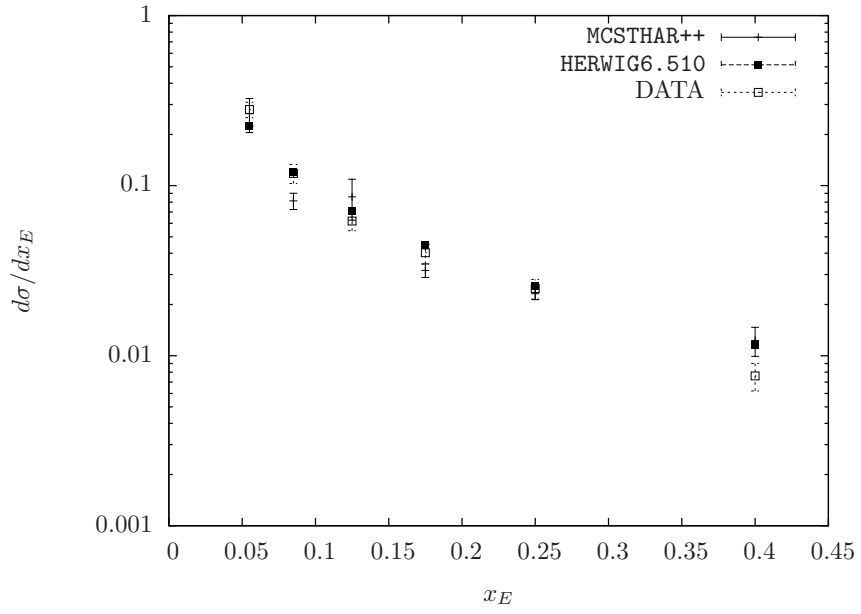

Figure 4.45: Σ^{*+} scaled energy (x_E) distribution: comparison among `MCSTHAR++`, `HERWIG6.510` and OPAL data [45] at 91.2 GeV center of mass energy.

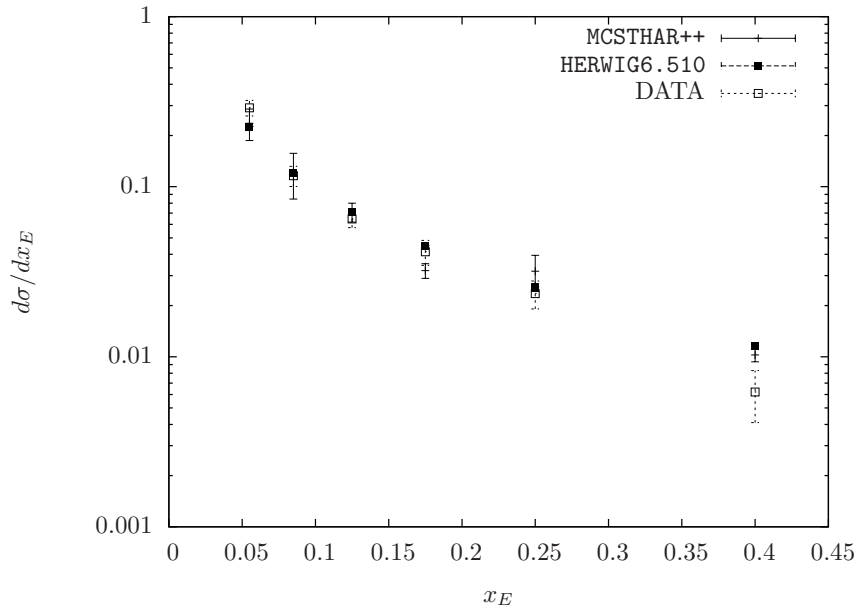

Figure 4.46: Σ^{*-} scaled energy (x_E) distribution: comparison among `MCSTHAR++`, `HERWIG6.510` and OPAL data [45] at 91.2 GeV center of mass energy.

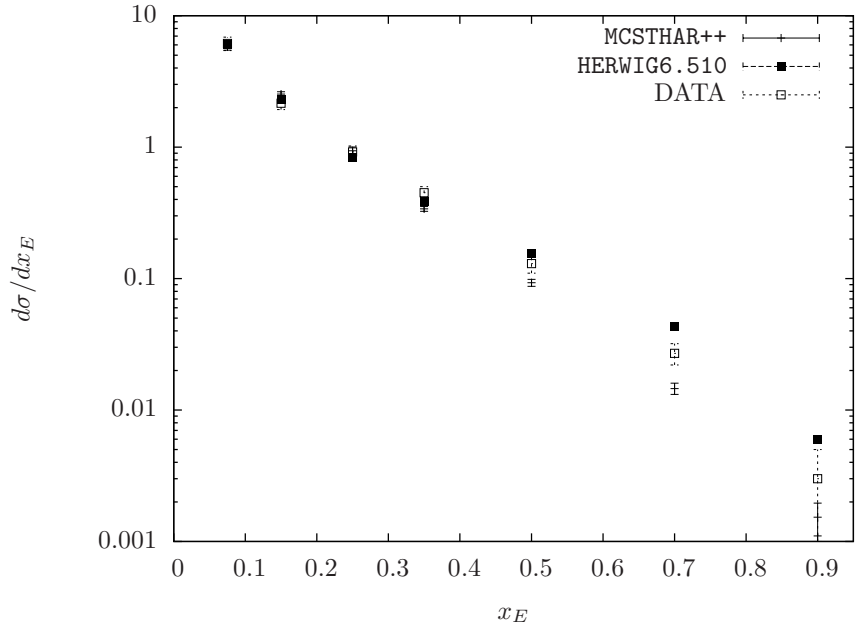

Figure 4.47: ρ^0 scaled energy (x_E) distribution: comparison among `MCSTHAR++`, `HERWIG6.510` and DELPHI data [51] at 91.2 GeV center of mass energy.

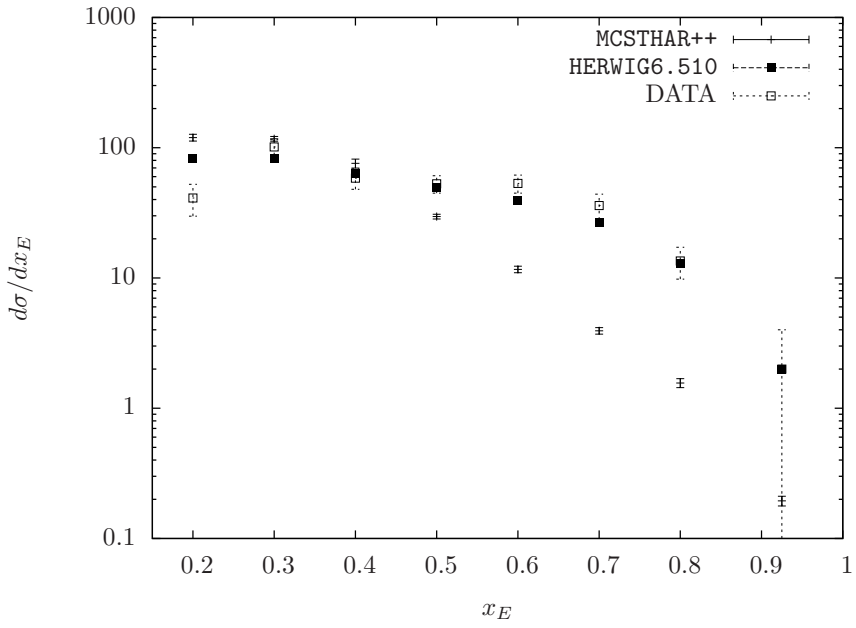

Figure 4.48: D^0 scaled energy (x_E) distribution: comparison among `MCSTHAR++`, `HERWIG6.510` and DELPHI data [52] at 91.2 GeV center of mass energy.

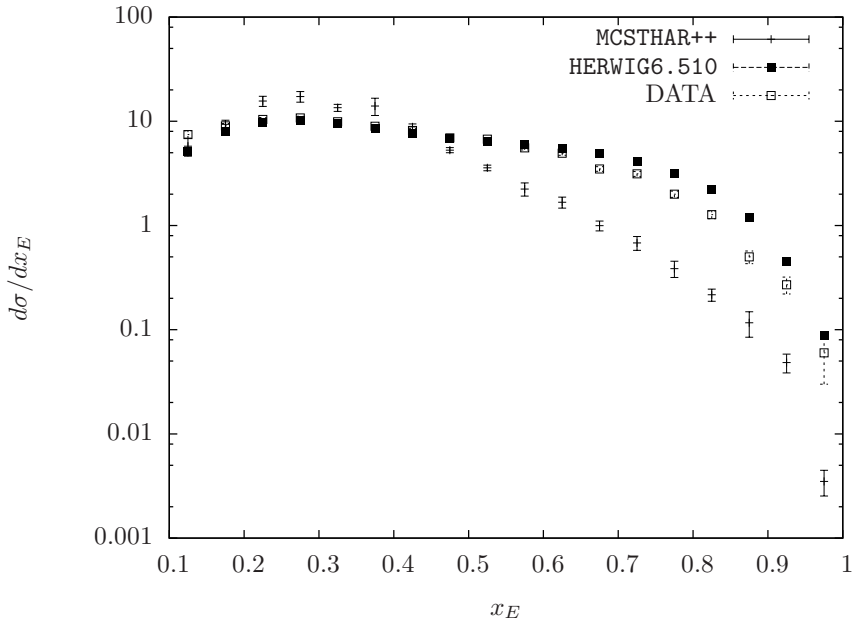

Figure 4.49: D^* scaled energy (x_E) distribution: comparison among `MCSTHAR++`, `HERWIG6.510` and DELPHI data [53] at 91.2 GeV center of mass energy.

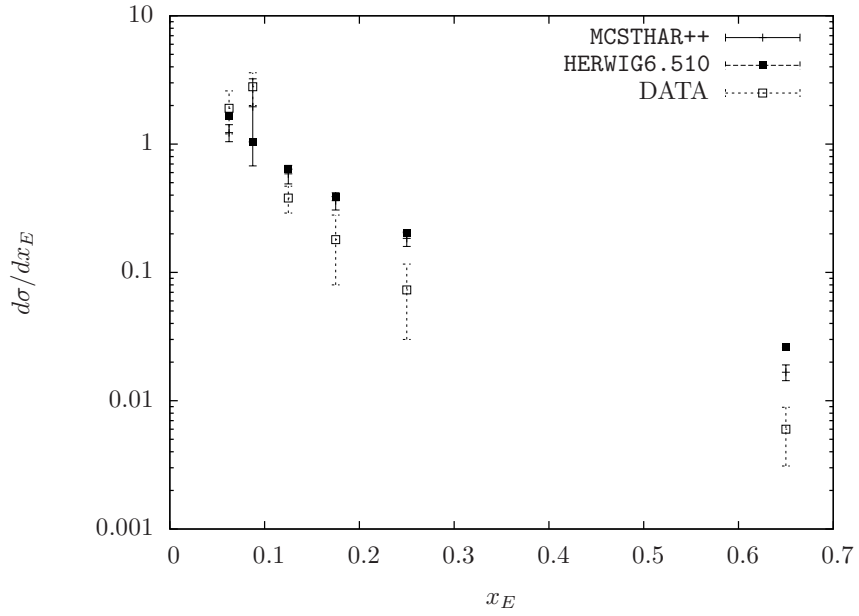

Figure 4.50: Δ^{++} scaled energy (x_E) distribution: comparison among `MCSTHAR++`, `HERWIG6.510` and OPAL data [44] at 91.2 GeV center of mass energy.

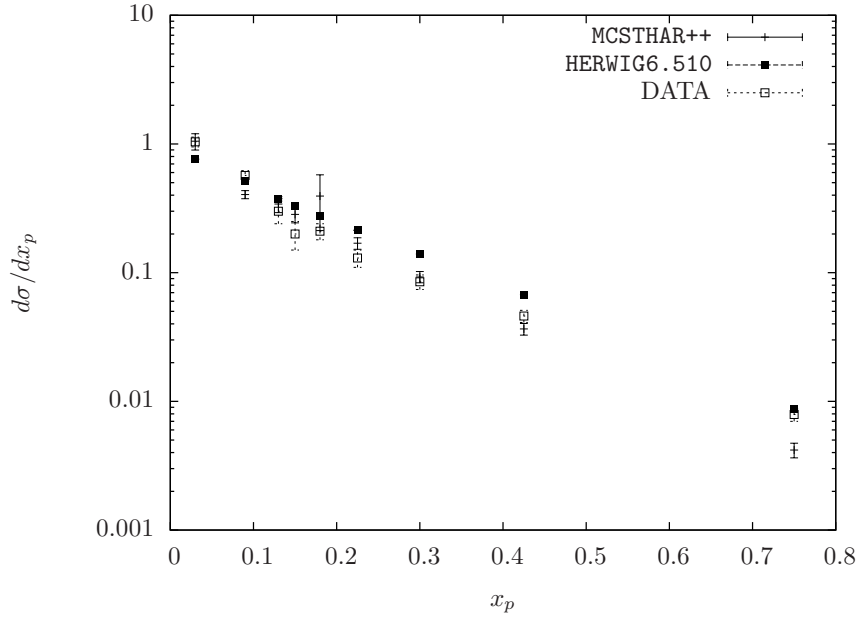

Figure 4.51: $f_0(980)$ scaled momentum x_p distribution: comparison among `MCSTHAR++`, `HERWIG6.510` and OPAL data [46] at 91.2 GeV center of mass energy.

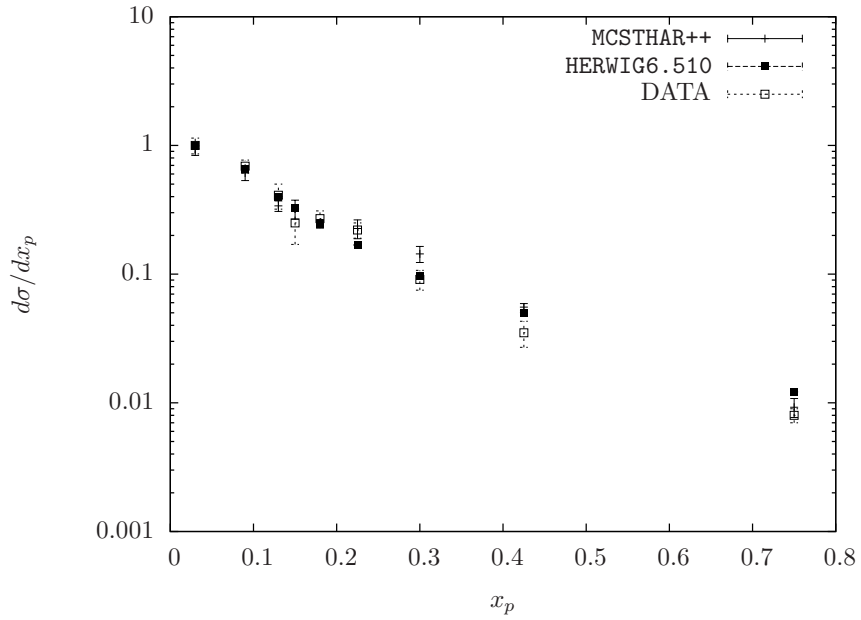

Figure 4.52: f_2 scaled momentum (x_p) distribution: comparison among `MCSTHAR++`, `HERWIG6.510` and OPAL data [46] at 91.2 GeV center of mass energy.

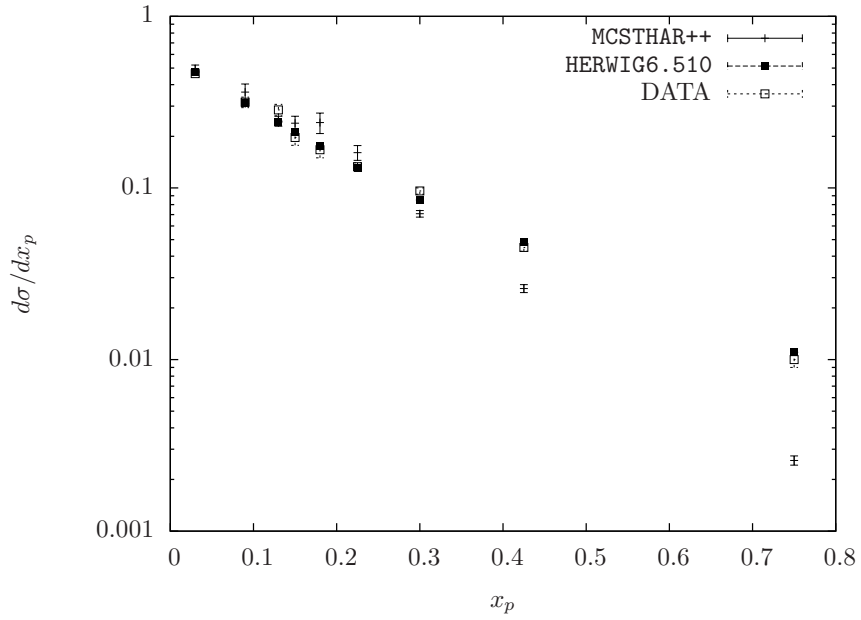

Figure 4.53: ϕ scaled momentum (x_p) distribution: comparison among `MCSTHAR++`, `HERWIG6.510` and OPAL data [46] at 91.2 GeV center of mass energy.

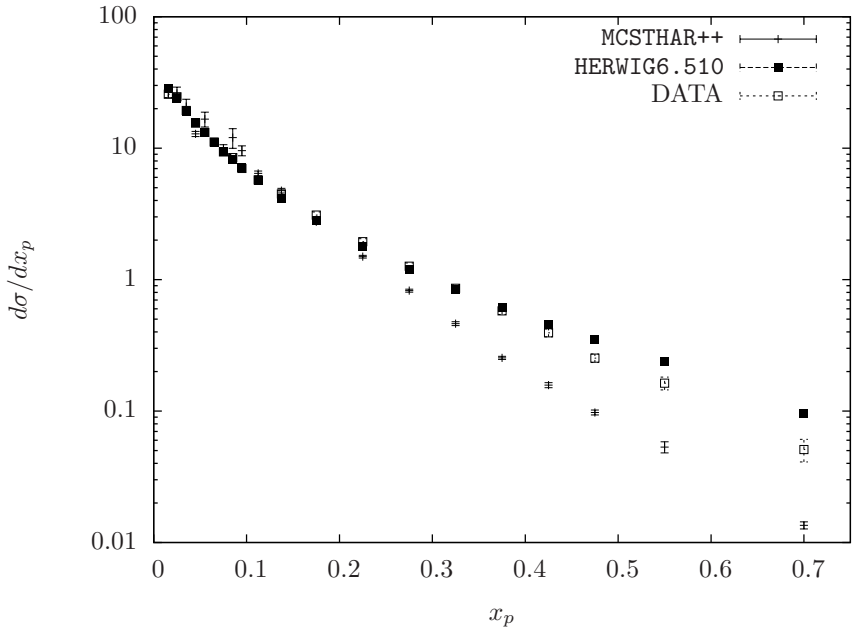

Figure 4.54: K^0 scaled momentum (x_p) distribution: comparison among `MCSTHAR++`, `HERWIG6.510` and OPAL data [48] at 91.2 GeV center of mass energy.

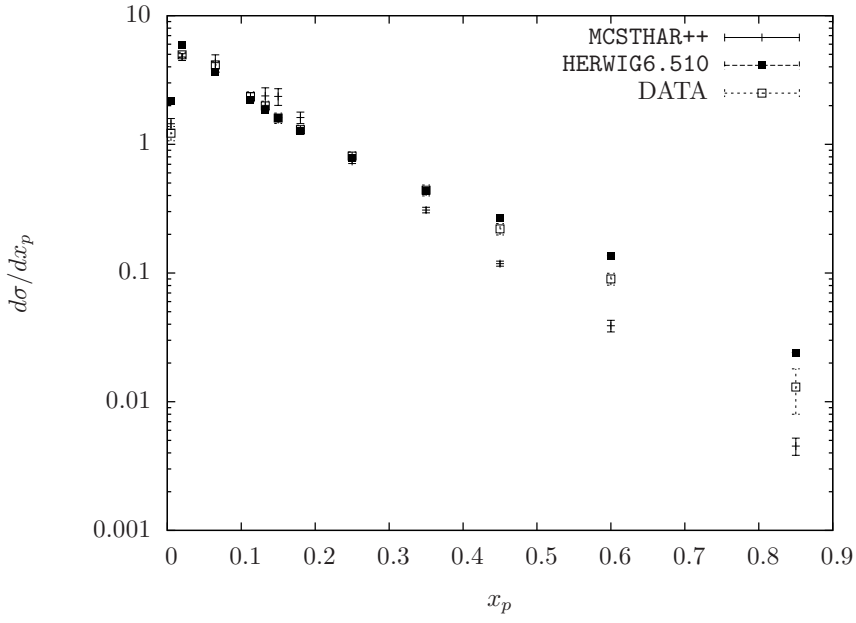

Figure 4.55: K^{*0} scaled momentum (x_p) distribution: comparison among `MCSTHAR++`, `HERWIG6.510` and OPAL data [47] at 91.2 GeV center of mass energy.

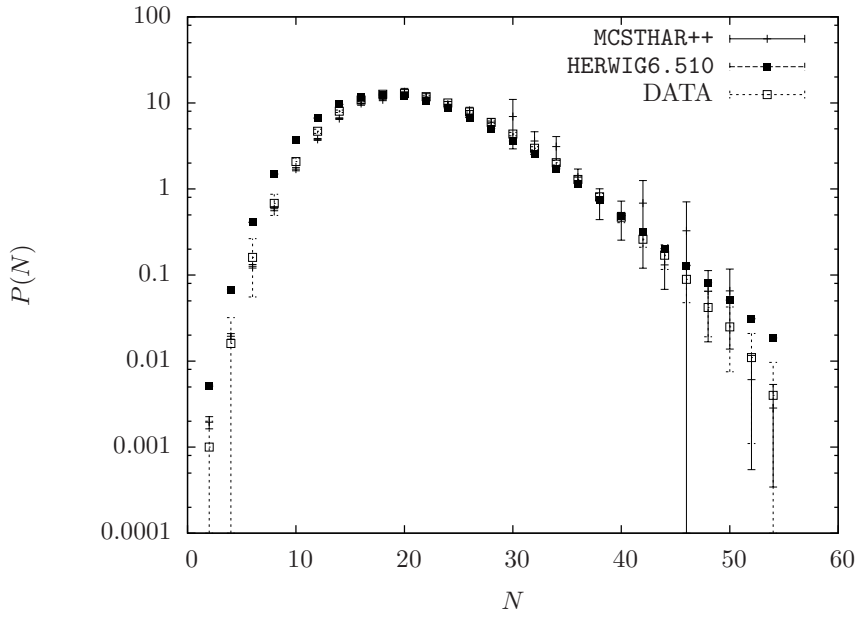

Figure 4.56: Charged particle number (N) distribution: comparison among `MCSTHAR++`, `HERWIG6.510` and OPAL data [50] at 91.2 GeV center of mass energy.

	MCSTHAR++	HERWIG6.510	LEP data	$\Delta_{\text{MCSTHAR++}}$
Charged	22.34 ± 0.27	20.45	20.76 ± 0.16	5.00
γ	23.64 ± 0.33	20.11	20.97 ± 1.17	2.20
π^0	10.98 ± 0.13	9.56	9.61 ± 0.29	4.33
π^+	9.33 ± 0.15	8.16	8.50 ± 0.10	4.55
η	1.18 ± 0.04	0.63	1.059 ± 0.086	1.26
ρ^+	1.16 ± 0.03	0.97	1.20 ± 0.22	-0.18
ρ^0	1.42 ± 0.04	1.00	1.40 ± 0.13	0.13
ω	1.29 ± 0.03	0.97	1.024 ± 0.059	4.10
η'	0.13 ± 0.01	0.10	0.166 ± 0.047	-0.61
$f_0(980)$	0.12 ± 0.01	0.010	0.1555 ± 0.0085	-2.43
a_0^+	0.12 ± 0.01	0.01	0.135 ± 0.054	-0.26
ϕ	0.167 ± 0.007	0.1278	0.0977 ± 0.0058	7.16
f_2	0.17 ± 0.01	0.169	0.188 ± 0.020	-0.74
f_{L1}	0.081 ± 0.005	0.072	0.165 ± 0.051	-1.63
f_2'	0.019 ± 0.002	0.012	0.0120 ± 0.0058	1.19
K^+	1.11 ± 0.02	1.05	1.127 ± 0.026	-0.31
K^0	1.07 ± 0.11	0.942	1.0376 ± 0.0096	0.30
K^{*+}	0.34 ± 0.04	0.273	0.357 ± 0.022	-0.37
K^{*0}	0.33 ± 0.02	0.274	0.370 ± 0.013	-1.92
K_2^{*0}	0.031 ± 0.004	0.0361	0.036 ± 0.012	-0.38
p	0.45 ± 0.02	0.762	0.519 ± 0.018	-2.79
Δ^{++}	0.069 ± 0.003	0.148	0.044 ± 0.017	1.47
Λ	0.128 ± 0.004	0.322	0.1943 ± 0.0038	-11.43
Σ^+	0.0253 ± 0.0009	0.0667	0.0535 ± 0.0052	-5.35
Σ^-	0.0233 ± 0.0007	0.0548	0.0410 ± 0.0037	-4.68
Σ^0	0.034 ± 0.001	0.0450	0.0389 ± 0.0041	-1.23
Σ^{*+}	0.0176 ± 0.0006	0.0551	0.0118 ± 0.0011	4.62
Σ^{*-}	0.0156 ± 0.0005	0.0519	0.0240 ± 0.0024	-3.43
Ξ^-	0.0040 ± 0.0001	0.0391	0.01319 ± 0.00050	-17.7
Ξ^{*0}	$(2.12 \pm 0.07) \times 10^{-3}$	1.84×10^{-2}	$(2.89 \pm 0.50) \times 10^{-3}$	-1.53
Ω	$(1.09 \pm 0.04) \times 10^{-4}$	4.94×10^{-3}	$(6.2 \pm 1.0) \times 10^{-4}$	-5.11
n	0.51 ± 0.01	0.683	0.991 ± 0.054	-8.49

Table 4.4: Mean value of charged particles, photon and hadron multiplicity: comparison among MCSTHAR++, HERWIG6.510 and LEP data [35][54] at 91.2 GeV center of mass energy. The last column contains the discrepancy, measured in standard deviations, for MCSTHAR++ with respect to experimental data.

	MCSTHAR++	HERWIG6.510	LEP data	$\Delta_{\text{MCSTHAR++}}$
D^+	0.22 ± 0.01	0.287	0.238 ± 0.024	0.53
D^0	0.54 ± 0.04	0.577	0.559 ± 0.022	0.33
D_{s}	0.110 ± 0.009	0.112	0.116 ± 0.036	0.18
D^{*+}	0.19 ± 0.01	0.207	0.2377 ± 0.0098	-2.40
D^{*0}	0.23 ± 0.01	0.210	0.218 ± 0.071	0.11
D_1^0	0.015 ± 0.001	0.022	0.0173 ± 0.0039	-0.46
D_2^{*0}	0.033 ± 0.003	0.030	0.0484 ± 0.008	-1.85
D_{s}^*	0.072 ± 0.005	0.036	0.069 ± 0.026	0.12
D_{s1}	0.0053 ± 0.0004	0.0044	0.0106 ± 0.0025	-2.11
D_{s2}^*	0.0039 ± 0.0003	0.0059	0.0140 ± 0.0062	-1.65
Λ_{c}	0.13 ± 0.01	0.036	0.079 ± 0.022	2.19

Table 4.5: Mean values of charmed hadron multiplicities: comparison among MCSTHAR++, HERWIG6.510 and LEP data [54] at 91.2 GeV center of mass energy. The last column contains the discrepancy, measured in standard deviations for MCSTHAR++ with respect to experimental data.

	MCSTHAR++	HERWIG6.510	LEP data	$\Delta_{\text{MCSTHAR++}}$
$(B^0 + B^+)/2$	0.411 ± 0.005	0.4474 ± 0.0005	0.399 ± 0.011	1.03
B_{s}	0.105 ± 0.001	0.107 ± 0.001	0.098 ± 0.012	0.61
B^*/B_{uds}	0.69 ± 0.01	0.426 ± 0.002	0.749 ± 0.040	-1.50
B^{**}	0.183 ± 0.002	0.144 ± 0.001	0.180 ± 0.025	0.11
$(B_2^* + B_1)$	0.121 ± 0.001	0.094 ± 0.001	0.09 ± 0.018	1.73
B_{s2}^*	0.00776 ± 0.00009	0	0.0093 ± 0.0024	-0.64
b-baryon	0.110 ± 0.001	0	0.103 ± 0.018	0.37

Table 4.6: Mean values of bottomed hadron multiplicities: comparison among MCSTHAR++, HERWIG6.510 and LEP data [54] at 91.2 GeV center of mass energy. The last column contains the discrepancy, measured in standard deviations for MCSTHAR++ with respect to experimental data.

Conclusions and outlook

The present thesis is an extended report of the research project focused on the development of the Monte Carlo code MCSTHAR++ and on the study of the Microcanonical Statistical Model ability to reproduce the experimental data when used in a numerical simulation describing the full dynamics of a high energy collision. In fact the two topics are strongly related to each other since, to perform a complete and exhaustive analysis of the theoretical predictions of the hadronization model in the above extended framework, a microcanonical hadronization module which could be interfaced to the existing general purpose Monte Carlo event generators is needed and, at the same time, a detailed comparison of the theoretical predictions with the experimental data is a fundamental step towards the fine tuning and preparation of the first release of MCSTHAR++.

The general framework of the present project has been set in the first chapter, with the description of the hadronization problem and with a discussion on the available phenomenological models used to describe the hadronization process itself. The Statistical Hadronization Model, in its microcanonical formulation, has been introduced in the second chapter, where a complete derivation of the transition probabilities which characterize the model itself and which represent the fundamental quantities needed to simulate the hadronzation process has been presented. Moreover, the most important features of the considered model have been discussed, in particular the possibility to include in the theoretical predictions the effects coming from the quantum statistics, due to the presence of identical particles, and from the interactions among the produced hadrons. Another fundamental feature of the microcanonical model implemented in MCSTHAR++ is the number of free parameters needed by the model itself, represented by the strangeness suppression parameter γ_S and by the energy density of the clusters ρ. The number of parameters needed by a phenomenological model is obviously related to the predictivity level of the model itself: considering as benchmark the number of adjustable parameters characterizing the hadronization models presented in the first chapter, which is 7 for the cluster model used by HERWIG6.510, the minimum number for the considered cases, the small number of parameters needed by the microcanonical model, together with its "advanced" features and its independent approach to the hadronization process, is the fundamental motivation for the introduction of this hadronization model in the Monte Carlo event generators and therefore

for the development of MCSTHAR++.

The implementation of the microcanonical model in MCSTHAR++ has been discussed in the third chapter, with a detailed explanation of the algorithms used in the various steps of the simulation: particular attention has been given to the description of the procedure adopted for the calculation of the microcanonical partition function, needed to correctly normalize the event weight, as discussed in the previous chapters, but also very demanding to be computed.

One of the major drawbacks in dealing with a phenomenological model is the need for a tuning of the model itself, which consists in looking for the configuration of the free parameters which gives the better agreement between theoretical predictions and the considered experimental data. In general, and this is the case of the Monte Carlo event generators, this operation is quite expensive from a computational point of view and for this reasons it is yet to be performed on MCSTHAR++. Nevertheless, a preliminary and approximated tuning has been obtained, as described in Chapter 4, with a comparison among MCSTHAR++ theoretical predictions, HERWIG6.510 results and LEP data at 91.2 GeV center of mass energy for a quite large set of observables, showing the good performances of the new hadronization code. The quantum statistics and interaction contributions previously cited have not been included in this first run of the hadronization code, since they give a relevant reduction of the speed of the event generation and, more important, they make hard to produce the set of partition functions needed by the code.

The inclusion of these important features, together with a final and rigorous tuning of the new hadronization module, will be the next steps of the present project, with the final objective to build a complete and public release of MCSTHAR++.

Appendices

Event shape observable definitions

In the present appendix the definitions of the event shape observales considered in Sec. (4.1) for the analysis of the theoretical predictions obtained with `MCSTHAR++` will be given [55].

Thrust related oservables

- The thrust T value is defined as

$$T = \max_{\vec{n}} \frac{\sum_{i=1}^{N} \mid \vec{p}_i \cdot \vec{n} \mid}{\sum_{i=1}^{N} \mid \vec{p}_i \mid},$$

  where $\vec{n}$ is a unit vector along the thrust axis and N the number of particles.

- Thust major M and minor m are similarly defined, replacing $\vec{n}$ with $\vec{n}_M$ perpendicular to $\vec{n}$ and with $\vec{n}_m = \vec{n}_M \times \vec{n}$ respectively.

- The rapidity with respect to thrust axis y^T is defined as

$$y^T = \frac{1}{2} \cdot \log \frac{E + p_T}{E - p_T},$$

  where p_T is the particle momentum parallel to the trust axis.

- Oblateness O is given by $O = M - m$.

- The in and out components of the transverse momentum with respect to thrust axis, P_t^T and p_t^T, are defined as $P_t^T = p \cdot \vec{n}_M$ and $p_t^T = p \cdot \vec{n}_m$.

Sphericity related oservables

- Considering the quadratic momentum tensor

$$M^{\alpha\beta} = \sum_{i=1}^{N} p_i^\alpha p_i^\beta \quad (\alpha, \beta = 1, 2, 3)\,,$$

after the ordering and normalization of the corresponding eigenvalues λ_i in order to have

$$\lambda_1 \geq \lambda_2 \geq \lambda_3 \quad \text{and} \quad \lambda_1 + \lambda_2 + \lambda_3 = 1,$$

the sphericity S, aplanarity A and planarity P are defined as

$$S = \frac{3}{2}(\lambda_2 + \lambda_3), \quad A = \frac{3}{2}\lambda_3 \quad \text{and} \quad P = \frac{2}{3}(S - 2A)$$

respectively.

- The rapidity with respect to sphericity axis y^S is defined as

$$y^S = \frac{1}{2} \cdot \log \frac{E + p_S}{E - p_S},$$

where p_S is the particle momentum parallel to the sphericity axis.

- The in and out components of the transverse momentum with respect to sphericity axis, P_t^S and p_t^S, are defined similarly to the P_t^T and p_t^T transverse momentum, using the eigenvectors of the quadratic momentum tensor instead of the $\vec{n}_M$ and $\vec{n}_m$ versors.

C and D parameters

- Considering the linear momentum tensor

$$\Theta^{\alpha\beta} = \frac{1}{\sum_{i=1}^{N} |\vec{p}_i|} \sum_{i=1}^{N} \frac{p_i^\alpha p_i^\beta}{|\vec{p}_i|},$$

the C and D parameters are defined starting from its eigenvalues λ_i in the following way:

$$C = 3(\lambda_1\lambda_2 + \lambda_2\lambda_3 + \lambda_3\lambda_1) \quad \text{and} \quad D = 27\lambda_1\lambda_2\lambda_3.$$

Hemisphere masses

- To calculate the hemisphere masses, the particles are separated in the two hemispheres identified by the plane perpendicular to the thrust axis. After this particle identification the heavy hemisphere mass M_h is defined as

$$M_h = max\left(\left(\sum_{\vec{p}_i \cdot \vec{n} > 0} \vec{p}_i\right)^2, \left(\sum_{\vec{p}_i \cdot \vec{n} < 0} \vec{p}_i\right)^2\right),$$

where $\vec{n}$ is a unit vector along the thrust axis. The light hemisphere mass M_l is defined as in the previous equation with the maximum replaced by the minimum. The difference of hemisphere masses is defined as $M_d = M_h - M_l$.

Hemisphere broadenings

- Considering the event hemispheres, defined in the previous item, the particle momenta transverse to the thrust axis are summed and normalized as follow to define the quantities B_+ and B_-:

$$B_{\pm} = \frac{\sum\limits_{\pm\vec{p}_i\cdot\vec{n}>0} \mid \vec{p}_i \times \vec{n} \mid}{2\sum\limits_i \mid \vec{p}_i \mid}.$$

  The hemisphere broadening observables are then defined as $B_{max} = max\,(B_+, B_-)$, $B_{min} = min\,(B_+, B_-)$, $B_{sum} = B_+ + B_-$ and $B_d = \mid B_+ - B_- \mid$.

Bibliography

[1] J.C. Collins, D.E. Soper and G. Sterman, Adv. Ser. Direct. High Energy Phys. **5** (1988) 1.

[2] D. Amati and G. Veneziano, Phys. Lett. B **83** (1979) 87.

[3] R.D. Field and R.P. Feynman, Nucl Phys. B **136** (1978) 1.

[4] B.R. Webber, Nucl. Phys. B **238** (1984) 492;
G. Marchesini and B.R. Webber, Nucl. Phys. B **310** (1988) 461.

[5] B. Andersson, G. Gustafson, G. Ingelman and T. Sjöstrand, Phys. Rep. **97** (1983) 31.

[6] B. Andersson, G. Gustafson and T. Sjöstrand, Physica Scripta 32 (1985) 574.

[7] J.C. Winter, F. Krauss and G. Soff, Eur. Phys. J. C **36** (2004) 381.

[8] G. Corcella, I.G. Knowles, G. Marchesini, S. Moretti, K. Odagiri, P. Richardson, M.H. Seymour and B.R. Webber, JHEP **0101** (2001) 010.

[9] M. Bahr, S. Gieseke, M. A. Gigg, D. Grellscheid, K. Hamilton, O. Latunde-Dada, S. Platzer, P. Richardson, M. H. Seymour, A. Sherstnev, J. Tully and B. R. Webber, Eur. Phys. J. C **58** (2008) 639.

[10] T. Sjöstrand, S. Mrenna and P.Z. Skands, JHEP **0606** (2006) 026.

[11] T. Sjöstrand, S. Mrenna and P.Z. Skands, Comp. Phys. Commun. **178** (2008) 852.

[12] V.N. Gribov and L.N. Lipatov, Sov. J. Nucl. Phys. **15** (1972) 438;
G. Altarelli and G. Parisi, Nucl. Phys. B **126** (1977) 298;
Yu. L. Dokshitzer, Sov. Phys. JETP **46** (1977) 641.

[13] A. Buckley, H. Hoeth, H. Lacker, H. Schulz, J. E. von Seggern, Eur. Phys. J. C **65** (2010) 331.

[14] R.J. Hemingway, OPAL Techical Note TN652 (2000).

[15] T. Gleisberg, S. Hoche, F. Krauss, M. Schonherr, S. Schumann and F. Siegert, J. Winter, JHEP **0902** (2009) 007.

[16] T. Gleisberg, S. Höche, F. Krauss, M. Schonherr, S. Schumann, F. Siegert, J. Winter, `SHERPA` manual, `http://www.hepforge.org/archive/sherpa/howto-1.1.1.pdf`

[17] G. Torrieri, S. Steinke, W. Broniowski, W. Florkowski, J. Letessier and J. Rafelski, Comput. Phys. Commun. **167** (2005) 229;
G. Torrieri, S. Jeon, J. Letessier and J. Rafelski, Comput. Phys. Commun. **175** (2006) 635.

[18] S. Wheaton, J. Cleymans and M. Hauer, Comput. Phys. Commun. **180** (2009) 84.

[19] A. Kisiel, T. Taluc, W. Broniowski and W. Florkowski, Comput. Phys. Commun. **174** (2006) 669.

[20] S. Bethke, Prog. Part. Nucl. Phys. **58** (2007) 351.

[21] E. Fermi, Progr. Theor. Phys. **5** (1950) 570.

[22] R. Hagedorn, Nuovo Cim. Suppl. **3** (1965) 147.

[23] E. Schnedermann, J. Sollfrank and U. W. Heinz, Phys. Rev. C **48** (1993) 2462;
J. Cleymans, D. Elliott, H. Satz and R.L. Thews, Z. Phys. C **74** (1997) 319.

[24] J. Cleymans, H. Satz and Z. Phys. C **57** (1993) 135;
P. Braun-Munzinger, J. Stachel, J. P. Wessels and N. Xu, Phys. Lett. B **365** (1996) 1;
F. Becattini, M. Gazdzicki and J. Sollfrank, Eur. Phys. J. C **5** (1998) 143;
P. Braun-Munzinger, D. Magestro, K. Redlich and J. Stachel, Phys. Lett. B **518** (2001) 41;
A. Baran, W. Broniowski and W. Florkowski, Acta Phys. Polon. B **35** (2004) 779;
J. Cleymans, B. Kampfer, M. Kaneta, S. Wheaton and N. Xu, Phys. Rev. C **71** (2005) 054901;
F. Becattini, M. Gazdzicki, A. Keranen, J. Manninen and R. Stock, Phys. Rev. C **69** (2004) 024905.

[25] F. Becattini, *An introduction to the Statistical Hadronization Model*, The statistical model of hadron formation and the nature of the QCD hadronization process, ECT* Trento, Italy, 1-5 Sep 2008.

[26] V.V. Begun, L. Ferroni, M. I. Gorenstein, M. Gazdzicki, F. Becattini, J. Phys. G **32** (2006) 1003.

[27] F. Becattini and L. Ferroni, Eur. Phys. J. C **35** (2004) 243.

[28] F. Becattini and L. Ferroni, Eur. Phys. J. C **38** (2004) 225.

[29] F. Becattini, Z. Phys. C **69** (1996) 485.

[30] F. Becattini, Proc. of XXXIII Eloisatron Workshop on Universality Features of Multihadron Production and the Leading Effect, Erice, Italy, 19-25 Oct 1996.

[31] F. Becattini and U. Heinz, Z. Phys. C **76** (1997) 269.

[32] F. Becattini and G. Passaleva, Eur. Phys. J. C **23** (2002) 551.

[33] R. Dashen, S. Ma and H. Bernstein, Phys. Rev. **187** (1969) 345.

[34] N. Metropolis, A.W. Rosenbluth, M.N. Rosenbluth, A.H. Teller and E. Teller, J. Chem. Phys. 21 (6) (1953) 1087.

[35] W.M. Yao *et al.* (Particle Data Group), J. Phys. G **33** (2006) 1.

[36] L. Lönnblad, Nucl. Instrum. Methods A **246** (2006) 559.

[37] F. Cerulus and R. Hagedorn, Suppl. N. Cim. IX, serie X, **2** (1958) 646; Suppl. N. Cim. IX, serie X, **2** (1958) 659.

[38] K. Werner and J. Aichelin, Phys. Rev. C **52** (1995) 1584.

[39] C. Bignamini, F. Becattini and F. Piccinini, Proc. of IFAE 2010, Roma, Italy, 7-9 Apr 2010.

[40] K. Ackerstaff *et al.*, Eur. Phys. J. C **7** (1999) 369.

[41] P. Abreu *et al.*, Eur. Phys. J. C **5** (1998) 585.

[42] P. Abreu *et al.*, Z. Phys. C **73** (1996) 11 .

[43] R. Akers *et al.*, Z. Phys. C **63** (1994) 181.

[44] G. Alexander *et al.*, Phys. Lett. B **358** (1995) 162.

[45] G. Alexander *et al.*, Z. Phys. C **73** (1997) 569.

[46] K. Ackerstaff *et al.*, Eur. Phys. J. C **4** (1998) 19.

[47] K. Ackerstaff *et al.*, Phys. Lett. B **412** (1997) 210.

[48] G. Abbiendi *et al.*, Eur. Phys. J. C **17** (2000) 373.

[49] K. Ackerstaff *et al.*, Eur. Phys. J. C **5** (1998) 411.

[50] P.D. Acton *et al.*, Z. Phys. C **53** (1992) 539.

[51] P. Abreu *et al.*, Phys. Lett. B **449** (1999) 364.

[52] P. Abreu *et al.*, Z. Phys. C **59** (1993) 533.

[53] R. Barate *et al.*, Eur. Phys. J. C **16** (2000) 597.

[54] F. Becattini, P. Castorina, J. Manninen and H. Satz, Eur. Phys. J. C **56** (2008) 493.

[55] P. Abreu *et al.*, Z. Phys. C **73** (1996) 11.

Acknowledgements

The present PhD thesis is a condensed description of the research work I carried out during the last three years, a beautiful and gratifying experience for which I want to thank some important people.

The first one is Fulvio Piccinini, my supervisor during these years: there is no way I could really repay your support, constantly present since the first day of this collaboration. It has been a pleasure to work with you and a excellent growth opportunity from many points of view.

I have also to thank Guido Montagna and Oreste Nicrosini, for having given me the possibility to work in the Pavia High Energy Physics group and to collaborate with the group research activities in parallel to my main project.

Many thanks also to Carlo Carloni Calame for providing part of the routines of event shapes and for fruitful collaboration and to Giulia Zanderighi for providing part of the event analysis routines.

A big thank you goes to Francesco Becattini, the original inspirer of this project together with Fulvio Piccinini, for the support and the opportunity to work on it. Thanks also to Lorenzo Ferroni for his help in various occasions.

Since January 2009 and for six months I have been in Karlsruhe (Germany) thanks to a MCNet scholarship: for this important and formative experience I am grateful to all the network members and in particular to Stephan Gieseke, my supervisor in Karlsruhe.

I am also grateful to Antonio Polosa for having read this thesis and for the opportunity to present my work at IFAE2010 conference in Rome.

My PhD years have been not only gratifying but also infinitely funny and for this I have to thank my Physics Department colleagues and, more important, friends Giovanni Balossini, Luca Barzè, Giacomo Bormetti, Valentina Cazzola and Danilo Delpini. A special thank you goes to my friend and officemate Giacomo Livan.

I also wish to thank all the italians I met in Karlsruhe, who made my german experience more relaxing and funny.

A huge hug and an even bigger thank you goes to Sara, for always supporting me in my projects and for having shown me a magic way of looking at life.

A big thanks goes to my family, for having supported me during these years, giving me the possibility to follow my interests, and for always helping me to do my best.

Christopher Bignamini